

FANCA MAINTAINS GENOMIC STABILITY THROUGH REGULATING BUBR1  
ACETYLATION

Zahi Abass Abdul Sater

Submitted to the faculty of the University Graduate School  
in partial fulfillment of the requirements  
for the degree  
Doctor of Philosophy  
in the Department of Biochemistry and Molecular Biology  
Indiana University

August 2017

Accepted by the Graduate Faculty of Indiana University, in partial fulfillment of the requirements for the degree of Doctor of Philosophy.

---

Grzegorz Nalepa, M.D., Ph.D., Chair

Doctoral Committee

---

Wade Clapp, M.D.

June 22, 2017

---

Mark Goebel, Ph.D.

---

Ronald Wek, Ph.D.

## ACKNOWLEDGEMENTS

First, I would like to thank my mentor, Grzegorz Nalepa, for his guidance and support throughout the last four years. He has been a tremendous mentor and has helped me grow as a person and a scientist. His passion and dedication for science will always be an inspiration for me. I am also very thankful to my committee members, Drs. Wade Clapp, Mark Goebel, and Ron Wek for their support and scientific input. They were always there when I needed guidance.

I also want to thank the Nalepa team: Donna for being my lab buddy and great friend, Elizabeth for being an older sister, Zejin for all the help and support, Ying for her beautiful and happy soul, and Richa for her friendship inside and outside the lab.

I dedicate this work to my friends and family, especially to my parents Abass and Itaf. Without them, life has no taste or meaning.

Zahi Abass Abdul Sater

## FANCA MAINTAINS GENOMIC STABILITY THROUGH REGULATING BUBR1 ACETYLATION

Fanconi Anemia (FA), a chromosomal instability syndrome, is characterized by bone marrow failure, genetic malformations, and predisposition to malignancies like acute myeloid leukemia (AML) and solid tumors. FA is caused by germline bi-allelic mutations in one of 21 known FA pathway genes and somatic mutations in FA genes are also found in a variety of sporadic cancers. Recently, numerous reports have discovered that the protective function of the FA pathway extends beyond its canonical role in regulation of DNA repair in interphase. In particular, the FA pathway has been shown to function in essential mitotic processes including spindle assembly checkpoint (SAC), cytokinesis, and centrosome maintenance.

Understanding of the mechanistic origins of genomic instability leading to carcinogenesis and bone marrow failure has important scientific and clinical implications. To this end, using a micronucleus assay, we showed that both interphase DNA damage and mitotic errors contribute to genomic instability in FA ex vivo and in vivo. Functional studies of primary FA patient cells coupled with super-resolution microscopy revealed that FANCA is important for centrosome

dependent spindle assembly supporting the protective role of FA pathway in mitotic processes.

Furthermore, we dissected the interactions between the FA pathway and cellular kinase networks by employing a synthetic lethality sh-RNA screen targeting all human kinases. We mapped kinases that were synthetically lethal upon loss of FANCA, particularly those involved in highly conserved signal transduction pathways governing proliferation and cell cycle homeostasis. We mechanistically show that loss of FANCA, the most abundant FA subtype, results in premature degradation of the mitotic kinase BUBR1 and faster mitotic exit. We further demonstrate that FANCA is important for PCAF-dependent acetylation of BUBR1 to prevent its premature degradation.

Our results deepen our understanding of the molecular functions of the FA pathway in mitosis and uncover a mechanistic connection between FANCA and SAC phosphosignaling networks. These findings support the notion that further weakening the SAC through targeting kinases like BUBR1 in FA-deficient cancers may prove to be a rational therapeutic strategy.

Grzegorz Nalepa, M.D., Ph.D., Chair

## TABLE OF CONTENTS

List of Tables .....	ix
List of Figures .....	x
List of Abbreviations .....	xiv
Chapter one. Introduction .....	1
Clinical features of Fanconi anemia (FA) .....	1
Genetics of FA .....	3
FA and cancer .....	4
The Fanconi anemia pathway .....	5
FA pathway and mitosis .....	8
Fanconi anemia, complementation group A (FANCA) .....	11
The spindle assembly checkpoint .....	12
Chapter two. Materials and Methods .....	22
Cell culture .....	22
shRNA screen .....	23
Bioinformatics .....	23
shRNA transduction .....	24
siRNA transfection .....	24
Immunofluorescence and Microscopy .....	24
Live Imaging .....	26
Quantification of intensities on CENPA spots .....	27
Immunoblotting .....	27
CD34+ CFU assay .....	28

Co-Immunoprecipitation (Co-IP) .....	29
Flow cytometry.....	30
Cytokinesis-block micronucleus assays.....	30
Mitotic spindle assembly assay.....	31
S-phase quantification .....	31
Colony Forming Unit- Fibroblast (CFUF) assay and direct cell count assay.....	32
Small molecule inhibitors .....	32
Bioinformatics analysis of cancer-associated FA mutations .....	33
in vitro Kinase assay .....	33
Antibodies .....	34
Chapter three. Interphase and mitotic errors result in genomic instability in FA.....	
Introduction .....	38
Results.....	41
Discussion .....	80
Chapter four. FANCA maintains the SAC through regulating BUBR1 acetylation .....	
Introduction .....	89
Results.....	91
Discussion .....	133
Chapter five. Conclusions and future directions .....	134
References .....	136

## Curriculum Vitae



## LIST OF TABLES

Table 1. Summary of known Fanconi anemia genes .....	17
Table 2. Fanconi anemia genes are associated with cancers in non-FA patients .....	19
Table 3. A list of FANCA interacting proteins.....	21

## LIST OF FIGURES

Figure 1. Fanconi anemia: a complex genetic disorder with developmental abnormalities .....	16
Figure 2. Functional domains in FANCA protein.....	20
Figure 3. Functional rescue of FANCA isogenic gene defect in primary patient fibroblasts .....	36
Figure 4. Chromosomal instability and abnormal mitoses during hematopoiesis in human FANCA <sup>-/-</sup> patients.....	43
Figure 5. FANCA maintains genomic integrity during interphase and mitosis in primary human CD34 <sup>+</sup> cells .....	47
Figure 6. Schematic representing micronucleus assay .....	49
Figure 7. Micronucleation upon loss of FA signaling results from a combination of interphase and mitotic errors.....	50
Figure 8. Loss of FANCA disrupts spindle microtubule assembly at prometaphase centrosomes .....	53
Figure 9. FANCA shuttles to the pericentriolar material during mitosis.....	55
Figure 10. Endogenous FANCA colocalizes with pericentrin and $\gamma$ -tubulin during metaphase .....	57
Figure 11. Profile of FANCA and pericentrin localization profile throughout the cell cycle.....	58
Figure 12. FANCA localizes to the mother centriole during interphase .....	60
Figure 13. SAC escape assay schematic .....	62
Figure 14. FANCA <sup>-/-</sup> cells escape from taxol-induced SAC arrest .....	63

Figure 15. <i>FANCA</i> <sup>-/-</sup> primary patient cells harboring different FANCA mutations are hypersensitive to taxol and MMC.....	66
Figure 16. Taxol dose-response curves of <i>FANCA</i> <sup>-/-</sup> and isogenic gene-corrected cells .....	67
Figure 17. Validation of taxol hypersensitivity in additional FANCA patient fibroblast cell lines .....	69
Figure 18. Rescue of mitomycin C (MMC) hypersensitivity by FANCA gene correction in primary <i>FANCA</i> <sup>-/-</sup> patient cells.....	71
Figure 19. Baseline cell cycle evaluation in <i>FANCA</i> <sup>-/-</sup> fibroblasts and FANCA-corrected isogenic cells .....	75
Figure 20. <i>FANCA</i> <sup>-/-</sup> cells exposed to genotoxic stressors develop genomic instability through a combination of interphase and mitotic checkpoint abnormalities .....	77
Figure 21. Continued DNA replication in multi-nucleated <i>FANCA</i> <sup>-/-</sup> and gene-corrected cells .....	79
Figure 22. Somatic mutations of FANCA in human malignancies .....	87
Figure 23. Loss of FANCA results in escape from SAC .....	93
Figure 24. Decreased CDC20 and CCNB1 levels upon loss of FANCA.....	94
Figure 25. <i>FANCA</i> <sup>-/-</sup> cells exit mitosis faster compared to <i>FANCA</i> <sup>+</sup> cells .....	95
Figure 26. Design of Kinome-wide screen using shRNAs .....	96
Figure 27. Kinome-wide shRNA screen hits heat map .....	97
Figure 28. Genes in mitotic pathways that are essential for survival of <i>FANCA</i> <sup>-/-</sup> primary patient fibroblasts .....	99

Figure 29. <i>FANCA</i> <sup>-/-</sup> fibroblasts are hypersensitive to inhibition of kinases involved in DNA damage and cell cycle pathways using clinical grade small molecule inhibitors.....	100
Figure 30. shRNA-mediated silencing of SAC protein kinases, BUB1 and BUBR1, confers lethality of <i>FANCA</i> <sup>-/-</sup> MNHN fibroblasts. ....	102
Figure 31. <i>FANCA</i> localizes to the kinetochore and interacts with SAC protein kinase, BUB1 .....	107
Figure 32. Confirmation of <i>FANCA</i> :BUB1 co-localization .....	108
Figure 33. Phosphorylation of BUB1 substrates upon loss of <i>FANCA</i> remains unchanged .....	109
Figure 34. Pattern of localization of <i>FANCA</i> during the cell cycle stages .....	111
Figure 35. Expression of <i>FANCA</i> protein is increased in early mitotic stages.....	112
Figure 36. Taxol and Nocodazole are drugs that modulate .....	113
Figure 37. Pattern of <i>FANCA</i> localization in nocodazole vs taxol treated cells .....	114
Figure 38. <i>FANCA</i> interacts with SAC protein kinase, BUB1, in a cell cycle and microtubule-dependent manner.....	115
Figure 39. Inter-centromeric localization of BUB1 with Aurora Kinase B (AURKB) following treatment with Nocadozole.....	117
Figure 40. <i>FANCA</i> interaction with BUB1 in the presence of microtubule-altering agents .....	118
Figure 41. <i>FANCA</i> interacts with BUBR1 .....	121

Figure 42. Decreased BUBR1 stability upon loss of FANCA.....	122
Figure 43. FANCA <sup>-/-</sup> cells exhibit faster BUBR1 degradation.....	124
Figure 44. FANCA is essential for BRCA2 mediated BUBR1 acetylation.....	125
Figure 45. Levels of acetylated BUBR1 protein is decreased upon loss of FANCA in unsynchronized cells .....	126
Figure 46. Diminished localization of PCAF in FANCA <sup>-/-</sup> MNHN fibroblast kinetochores .....	128
Figure 47. PCAF recruitment is reduced upon loss of FANCA .....	129
Figure 48. Diminished localization of FANCD1 in FANCA <sup>-/-</sup> MNHN fibroblast kinetochores.....	130
Figure 49. Diminished FANCD1 localization is observed upon knockdown of FANCA .....	131
Figure 50. FANCA maintains the SAC through a mechanism involving acetylation of BUBR1 protein.....	132

## LIST OF ABBREVIATIONS

8-OHG	8-Hydroxy-Guanosine
8-oxo-dg	8-Oxo-2'-deoxyguanosine
AML	acute myeloid leukemia
APC/C	Anaphase Promoting Complex/Cyclosome
APH	aphidicolin
ATR	Ataxia Telangiectasia And Rad3-Related Protein
AURKB	Aurora Kinase B
BACH1	BTB Domain And CNC Homolog 1
BLM	Bloom Syndrome RecQ Like Helicase
BMF	bone marrow failure
BRCA	Breast And Ovarian Cancer Susceptibility Protein
BRG1	Brahma-Related Gene 1
BRIP1	BRCA1 Interacting Protein C-Terminal Helicase 1
BS	Bloom Syndrome
BSA	bovine serum albumin
BTBD12	budding uninhibited by benzimidazole 1
BUB	Budding Uninhibited By Benzimidazoles
BUBR1	Budding Uninhibited By Benzimidazoles 1 Homolog Beta
CCNB1	Cyclin B1
CD34	cluster of differentiation (designation) 34
Cdc20	cell division cycle 20
CDC27	Cell Division Cycle 27

CDK	Cyclin Dependent Kinase
CENP-	Centromere-associated protein
CFUF	Colony Forming Unit- Fibroblast
CHK1	Checkpoint Kinase
CHX	Cycloheximide
CIN	chromosomal instability
COSMIC	Catalogue Of Somatic Mutations In Cancer
DDR	DNA damage response
DEB	diepoxy butane
DMEM	Dulbecco's modified Eagle medium
DMSO	dimethyl sulfoxide
DNA	Deoxyribonucleic acid
ECL	enhanced chemiluminescence
FA	Fanconi anemia
FAAP	Fanconi anaemia-associated protein
FANC	Fanconi anemia, complementation group
FIS	Functional Impact Score
GFP	green fluorescent protein
H2A	Histone 2A
HES1	Hes Family BHLH Transcription Factor 1
HNSCC	Head and neck squamous cell carcinoma
HSC	hematopoietic stem cell
HU	Hydroxyurea

ICL	interstrand crosslink
IKK2	IKB Kinase-2
IKK2	IKB Kinase-2
IP	Immunoprecipitation
KMN	KNL-1/Mis12 complex/Ndc80
KNL1	Kinetochores Scaffold 1
MAD	mitotic arrest deficient
MAD2L2	Mitotic Arrest Deficient 2-Like Protein 2
MCC	Mitotic Checkpoint Complex
MDS	myelodysplastic syndrome
MMC	mitomycin C
MOI	multiplicity of infection
M-PER	Mammalian Protein Extraction Reagent
NEB	Nuclear envelope breakdown
NEK2	never-in-mitosis-gene-a related kinase 2
NES	nuclear export signal
NLS	nuclear localization signal
PAGE	polyacrylamide gel electrophoresis
PARP	Poly(ADP-Ribose) Polymerase
PBS	Phosphate buffer saline
PCM	pericentriolar material
PFA	Paraformaldehyde
pH3	phospho-histone H3



PLK1	polo-like kinase 1
RAD51	human homolog C of yeast Rad51
RBC	red blood cell
RNA	Ribonucleic acid
ROS	Reactive oxygen species
SAC	Spindle assembly checkpoint
SCC	squamous cell carcinoma
SDS	sodium dodecyl sulfate
SEM	Standard error of the mean
ShRNA	Short hairpin RNA
siRNA	Small interfering RNA
SNX5	sorting nexin-5
S-phase	synthesis phase
Ub	Ubiquitin
UBE2T	Ubiquitin Conjugating Enzyme E2 T
UFB	Ultra-fine bridge
USP	Ubiquitin specific peptidase
WB	Western blot

## CHAPTER ONE

### INTRODUCTION

#### **Clinical features of Fanconi anemia (FA)**

Fanconi anemia (FA) is an inherited chromosomal instability disorder characterized by congenital defects, bone marrow failure, cellular hypersensitivity to DNA cross-linkers, and increased risk of malignancies. FA is relatively uncommon with an incidence rate of 1 in 360,000 live births and a carrier frequency of 1 in 181 in North America. However, the prevalence and carrier frequency of this disease varies in different geographical areas. Increased carrier frequency is seen in geo-specific populations like Ashkenazi Jews, Afrikaners, and Spanish Gypsies (Mamrak, Shimamura, & Howlett, 2016; Philip S Rosenberg, Tamary, & Alter, 2011).

Congenital defects are present in most FA patients and they include malformations of the upper and lower limbs, fused vertebrae, hypopigmentation, microcephaly, short stature, and hypogonadism (**Figure 1A and B**) (D'Andrea & Grompe, 2003; Giampietro et al., 1993; Joenje & Patel, 2001; Young & Alter, 1994). Fanconi anemia, as the name suggests, also involves hematological defects. At birth, blood count is normal but macrocytosis (large erythrocytes) is not uncommon. This is typically followed by thrombocytopenia (low platelet count), neutropenia, and pancytopenia (low blood cell count) by the second

decade of life (Young & Alter, 1994). By the age of forty, 98% of FA patients would have developed myelodysplastic syndrome (MDS), acute myeloid leukemia (AML), or bone marrow failure (BMF). The age of onset of BMF, while highly variable, is 7.6 years on average (Shimamura & Alter, 2010).

Diagnosis of FA entails a cytogenetic test of patient lymphocytes to quantify chromosome breakage and radial forms after treatment with DNA damaging agents like Mitomycin C (MMC) or Di-epoxy butane (DEB). If the lymphocyte breakage test is inconclusive, a similar test is done on a different cell type, such as skin fibroblasts (Auerbach, 2009). Upon discovery of DEB/MMC-induced chromosome breakage, the affected FA gene is identified through FA gene-sequencing panels. Whole-exome sequencing (WES) may be needed for patients with a positive breakage test and no mutations within known FA genes, although sequencing may be non-revealing if the disease is caused by deep intronic mutations or copy number variation.

Management of FA in patients is improving alongside our understanding of the etiology of the disease. FA patients are routinely monitored for cytopenia, BMF and leukemic transformation. Some forms of treatments, including androgens, corticosteroids, or hematopoietic growth factors, are available to stimulate hematopoietic functions in FA patients (D'Andrea, 2010). The best long term option is hematopoietic stem cell (HSC) transplantation, which is contingent on finding a compatible donor (Gluckman et al., 1995; Gluckman et al., 1989; Green

& Kupfer, 2009). HSC is ideally performed before the onset of AML/MDS and Fludarabine is used to reduce the incidence of graft failure (MacMillan et al., 2015; MacMillan & Wagner, 2010).

## **Genetics of FA**

Early on, it was hypothesized that FA is caused by a single gene defect due to relatively uniform phenotype. Genetic heterogeneity in FA was first proposed in 1976 and later confirmed in 1980 through complementation analysis (Schroeder, Tilgen, Kruger, & Vogel, 1976; Zakrzewski & Sperling, 1980). Complementation analysis is carried out by fusing different FA cells, which are then checked for the ability of the fused cells to correct the FA cellular phenotype. The ability of fused cells to complement the cross-linker sensitivity conveys different complementation groups. Now, with the help of complementation cloning, protein association, and positional cloning and sequencing, we know that FA can be caused by bi-allelic mutation in one of 21 different genes (**Table 1**). Mutations in *FANCO*, *FANCS*, and *FANCR* (*RAD51*) do not result in classical FA phenotype, such as bone marrow failure. Thus, these are considered to be FA-like genes. Fanconi anemia genes are inherited in an autosomal recessive fashion. *FANCR* (*RAD51*) and *FANCB* are exceptions since they are inherited in an autosomal dominant and X-linked fashion respectively (Ameziane et al., 2015; Dong et al., 2015; Meetei et al., 2004).

## **FA and cancer**

As mentioned previously, FA patients have high proclivity towards developing malignancies, especially AML. The relative risk of developing AML is increased more than 500 folds in FA-patients (Alter et al., 2010; P. S. Rosenberg, Alter, & Ebell, 2008). In addition to hematological malignancies, FA patients have increased susceptibility to solid tumors like squamous cell carcinoma (SCC) as well as adenomas and carcinomas of the liver.

Alter et al. reviewed more than 2000 FA cases (1927-2012) and reported the following figures of cancer incidence: Leukemia (188 cases, 8.5%) of which 84% were AML, solid tumors (286 cases, 13%) of which 25% were head and neck squamous cell carcinoma (HNSCC) and 9.1% were liver carcinomas (Alter & Clinician, 2014). In a more geographically restricted study reviewing data of 180 FA patients from the Italian Fanconi Anemia Registry (1994-2014), Risitano et al. reported that FA patients developed a variety of cancers: MDS/AML (13 patients, 8%) and solid tumors (27 patients, 11%) (Risitano et al., 2016).

Of equal importance, FA genes are frequently mutated in non-FA human cancers including breast, ovarian, and pancreatic cancers in non-FA patients (Hahn et al., 2003; Hwang et al., 2003; Knudson, 1971; Rahman et al., 2007). This includes acquired mutations and epigenetic silencing of FA genes (Hess et al., 2008; Shen et al., 2015; Xie et al., 2000), including *FANCA* inactivation in AML (M.

Tischkowitz et al., 2003; M. D. Tischkowitz et al., 2004). Analysis of 68 DNA sequence datasets reveals that FA genes are mutated in a plethora of human cancers in non-FA patients. For example, FA genes are mutated in 4.3% of AMLs (188 cases), 36.1% of breast carcinoma (962 cases), and 50.6% of lung squamous cell carcinoma (178 cases) among others (Shen et al., 2015).

Furthermore, somatic *BRCA2* (*FANCD1*) mutations vastly increase the risk of developing breast and ovarian cancers (**Table 2**). An expanded list of FA genes and their association to cancer in non-FA patients is found in Table 2. These studies may provide a basis for future targeted therapies since loss of FA renders cancers susceptible to inhibition of selected signaling pathways that cross-talk with FA network.

### **The Fanconi anemia pathway**

The protein products of the FA genes work together in a common pathway termed the Fanconi anemia (FA) pathway. The FA pathway, also known as FA/BRCA pathway, functions as a tumor suppressor pathway that guards the genome against genomic instability. The most studied role of this pathway is in regulating DNA repair of inter-strand crosslinks (ICLs) during interphase. Thus, FA-deficient cells are hypersensitive to DNA crosslinking agents like Mitomycin C (MMC), Diepoxybutane (DEB), and Cyclophosphamide (Taniguchi & Dandrea, 2002). The FA pathway is also activated by other DNA damaging agents, such as ionizing radiation (IR) and ultraviolet radiation (UV) (Casado, Nunez, Segovia, Ruiz de Almodovar, & Bueren, 2005; Dunn, Potter, Rees, & Runger, 2006).

During the S-phase of the cell cycle, endogenously or exogenously induced DNA cross-links results in replication stall to allow for DNA repair mechanisms, which include FA signaling, to operate. First, FANCM recognizes the DNA crosslinks through its helicase activity and subsequently recruits the FA core complex. Eight FA proteins (FANC -A, -B, -C, -E, -F, -G, -L, -M) and five FA associated proteins (FAAP100, FAAP20, FAAP24, HES1, MHF1, and MHF) make up the FA core complex (Dong et al., 2015). This complex, through the activity of the E3 ubiquitin (ub) ligase, FANCL, and the ubiquitin conjugating enzyme, FANCT (UBE2T), monoubiquitinates and activates FANCD2-FANCI heterodimer (also termed ID complex). The ID complex then recruits downstream effector proteins, including FANCO (DNA endonuclease), FANCP (scaffolding protein), FANCV (translesion synthesis factor), and the recombination proteins FANCD1 (BRCA2), FANCI, FANCN, FANCO, FANCR, FANCS (BRCA1), and FANCU. This results in a cascade of events culminating in DNA repair through homologous recombination, in which FA proteins are involved (Palovcak, Liu, Yuan, & Zhang, 2017). Inactivating the FA pathway is accomplished by deubiquitinating FANCD/FANCI, a process regulated by USP1 (ubiquitin-specific peptidase 1) and UAF1 deubiquitinating complex (Nijman et al. 2005).

In addition to the canonical role in DNA repair, the FA pathway protects against another driver of genomic instability, namely oxidative stress. FANCD2 monoubiquitination and formation of di-sulfide bridges between FANCA and

FANCG is observed in presence of H<sub>2</sub>O<sub>2</sub>, an oxidative agent, reflecting activation of the pathway in oxidative conditions (S. J. Park et al., 2004). FA-deficient cells also exhibit changes in mitochondrial morphology affecting ATP synthesis and detoxification of Reactive oxygen species (ROS) (Kumari, Ya Jun, Huat Bay, & Lyakhovich, 2014). ROS can cause alterations to nucleotide bases, like 8-hydroxyguanine (8-OHG) or 8-oxo-2'-deoxyguanosine (8-oxo-dg). These alterations lead to chromosomal instability (CIN) through causing base mismatch, insertion, deletions, and chromosomal translocations (Wiseman & Halliwell, 1996). Importantly FA -deficient cells are hypersensitive to oxidative stress, evidenced by elevated 8-OHG, and increased apoptosis (Zunino, Degan, Vigo, & Abbondandolo, 2001).

Endogenous sources of oxidative stress, such as aldehydes, are also deleterious to DNA and are highly carcinogenic reactive molecules (O'Brien, Siraki, & Shangari, 2005). Endogenous aldehydes may be in the form of acetaldehyde produced from ethanol metabolism, and crotonaldehyde from lipid peroxidation (Voulgaridou, Anastopoulos, Franco, Panayiotidis, & Pappa, 2011). Multiple FA patient cells and those derived from *Fancd2* null mice are hypersensitive to aldehyde accumulation, which supports the implication of FA pathway in managing ICLs caused by aldehydes. Interestingly, disruption of aldehyde dehydrogenase (*Aldh2*) promoted perinatal lethality and marrow malfunction evolving into lymphoblastic leukemia in *Fancd2*<sup>-/-</sup> animals (Garaycochea et al., 2012; Langevin, Crossan, Rosado, Arends, & Patel, 2011).



## **FA pathway and mitosis**

The functions of the FA pathway are not exclusive to interphase as mounting evidence implicate multiple FA proteins in various mitotic processes. The FA pathway ensures faithful chromosome segregation, thus avoiding chromosomal instability (Nalepa & Clapp, 2014).

Rosselli et al. reported that the FA pathway monitors unrepaired DNA, namely fragile sites, which arise spontaneously or after drug treatment (like APH) (Naim & Rosselli, 2009a). Fragile sites are incompletely replicated DNA that persists into mitosis causing chromosomal alterations. Interestingly, FANCD2 foci at the fragile sites were elevated upon treatment with APH and increased micronucleation was observed upon loss of FA signaling. Furthermore, FANCD2 and FANCI localize to the extremities of ultrafine bridges (UFB), a special class of DNA bridges, which connect fragile sites between two sister chromatids (Chan, Palmai-Pallag, Ying, & Hickson, 2009; Naim & Rosselli, 2009a). FANCD2 and FANCI are important in recruiting BLM (Bloom syndrome protein) which mediates resolution of UFBs. BLM, a protein that belongs to the RecQ family of DNA helicases, is mutated in a rare autosomal recessive disorder termed Bloom Syndrome (BS). BS patients share a lot of features with FA patients including cancer predisposition, increased incidence of BMF, high CIN levels and hypersensitivity to ICL agents (Pichierri, Franchitto, & Rosselli, 2004). Of interest, FA-deficient cells exhibited increased chromosomal breakage at the fragile sites thus providing a functional link between UFBs and genomic instability (Howlett,

Taniguchi, Durkin, D'Andrea, & Glover, 2005). These studies argue for a functional role of the FA pathway in resolving interphase DNA damage persisting into mitosis, protecting the cell against chromosomal instability.

Centrosomes are essential for normal cellular division, and abnormal centrosome number is associated with CIN. Supernumerary centrosomes (>2 centrosomes per cell) are associated with merotelic kinetochore-microtubule attachment, whereby a single kinetochore is attached to the microtubules emanating from two poles, resulting in unfaithful chromosome segregation (Ganem, Godinho, & Pellman, 2009; Gregan, Polakova, Zhang, Tolic-Norrelykke, & Cimini, 2011). Multiple FA proteins localize to the centrosome and are important to maintain proper centrosome number (Kim et al., 2013; Nalepa & Clapp, 2014; Zou et al., 2013). Yet, very few studies functionally connect FA proteins to centrosome maintenance. Recently, FANCA was found to be phosphorylated by NEK2 (never-in-mitosis-gene-a relate kinase 2), a serine/threonine kinase implicated in centrosome maintenance, bipolar spindle assembly and proper chromosome segregation. This phosphorylation at residue T351 was found to be essential for normal centrosome number (Kim et al., 2013). Another study reported that another FA protein, FANCI, functions upstream of and interacts with the mitotic regulator, PLK1 (polo like kinase 1), to promote hydroxyurea (HU) and MMC induced centrosome amplification in U2-OS cells (Zou et al., 2013). The same group showed that both, FANCI and FANCD1 (BRCA1), are implicated in PLK1 dependent centrosome maintenance (Zou et al., 2014). In summary, our

understanding of the role of FA in centrosome replication and maintenance is advancing but still rudimentary.

During mitosis, the cell employs multiple mechanisms to ensure error-free progression of the cytoplasmic and nuclear division. One such mechanism is the spindle assembly checkpoint (SAC) which coordinates the events that inhibit anaphase onset until proper kinetochore-microtubule attachment are attained (Gollin, 2005). Weakened spindle checkpoint increases the risk of random chromosome segregation, aneuploidy, and cancer (Musacchio & Salmon, 2007). Multiple FA proteins localize to the mitotic spindle and are required for a robust SAC, evidenced by multinucleated cells after exposure to taxol, a mitotic poison that activates SAC through stabilizing microtubules. Importantly, the reintroduction of FA proteins restores mitotic arrest and SAC function (Nalepa et al., 2013). Further studies are needed to establish a mechanistic connection between the FA pathway and SAC.

FA proteins also participate in cytokinesis, the cytoplasmic division at the end of mitosis. Loss of FA signaling results in binucleated cells caused by failed cytokinesis. Specifically, *FANCD1 (BRCA2)* localizes to the central spindle and midbody as cells exit cell division. Loss of *FANCD1 (BRCA2)* resulted in delayed cytokinesis and binucleated cells, associated with mislocalization of myosin II, an essential protein for cleavage furrow formation (Vinciguerra, Godinho, Parmar, Pellman, & D'Andrea, 2010) (X. Wang & Dai, 2006).

## **Fanconi anemia, complementation group A (FANCA)**

*FANCA*, cloned in 1996, is the most prevalent complementation group in FA. Mutations in *FANCA* account for 65% of all FA cases (Solomon et al., 2015). Interestingly, more than 250 different *FANCA* mutations, including deletions, have been identified. Thus, *FANCA* is a hypermutable gene (Levran et al., 1997; Morgan, Tipping, Joenje, & Mathew, 1999). The *FANCA* gene, harboring 43 exons, encodes for a 1,455 amino acid long protein. FANCA protein harbors a nuclear localization signal (NLS), a partial leucine zipper, and a nuclear export signal (NES), which suggests that the protein localizes to the nucleus (**Figure 2**) (Ferrer et al., 2005; Naf, Kupfer, Suliman, Lambert, & D'Andrea, 1998). FANCA protein stability is dependent on its interaction with another FA protein, namely FANCG (Reuter, Herterich, Bernhard, Hoehn, & Gross, 2000).

The protein interactions of FANCA shed a light on its regulation and molecular functions within the cell. FANCA-interacting proteins include Sorting nexin-5 (SNX5), Brahma-Related Gene 1 (BRG1), IKB Kinase-2 (IKK2) (Reuter et al., 2000). The functional relevance of these interactions is detailed in **Table 3**. Importantly, FANCA has been shown to have FA core complex-independent functions in mitosis. The N-terminus of FANCA directly interacts with the C-terminus of CENP-E (Centromere-associated protein E). CENP-E acts as a motor protein that transports and aligns chromosomes and is thus important for proper chromosome segregation (Du, Chen, & Shen, 2009). CENP-E also interacts with the mitotic checkpoint complex kinase, BUBR1 (budding

uninhibited by benzimidazole-related 1), inducing its autophosphorylation which is essential for its SAC activity (Guo, Kim, Ahmad, Zhang, & Mao, 2012). The functional relevance of FANCA-CENP-E interaction is yet to be defined.

A *Fanca* knockout mice model has been generated and homozygote mice displayed FA-like features including facial malformations and hypogonadism, consistent with high levels of FANCA in testes and ovaries, but failed to replicate hematological defects. Homozygote females showed premature oocyte senescence, while male homozygotes increased apoptosis in germ cells and mis-paired meiotic chromosomes. This study hinted that FANCA may be important for reproductive function (Wong et al., 2003). Importantly, FANCA and other FA knockout mice fail to fully recapitulate the clinical phenotypes of FA, most notably developing anemia (M. Chen et al., 1996).

### **The spindle assembly checkpoint**

Mitotic division of cells is a highly complex and regulated process. It ensures that the duplicated genetic material in S-phase of the cell cycle is distributed evenly between two daughter cells. Mitosis is partitioned into six different phases: prophase, prometaphase, metaphase, anaphase, telophase, and cytokinesis. In prophase, chromosome condensation and polar centrosome migration occur followed by microtubule nucleation initiating the formation of the mitotic spindle. In prometaphase, the spindle microtubule performs a “seek and capture” to

connect to chromosomes through a specialized structure called the kinetochore. This is followed by metaphase, in which bipolar attachment of chromosomes occurs. Anaphase onset is marked upon loss of sister chromatid cohesion, resulting in chromatid separation. In telophase, chromosomes de-condense and nuclear envelope reforms, followed by cytokinesis, where cleavage furrow forms to split the cytoplasm and form two daughter cells (Imoto, Yoshida, Yagisawa, Kuroiwa, & Kuroiwa, 2011).

Proper chromosome segregation is a crucial step towards a successful mitosis. This complicated process is governed by a surveillance mechanism provided by the spindle assembly checkpoint (SAC), which monitors chromosome alignment and orientation as well as kinetochore attachment to the spindle microtubules (Naim & Rosselli, 2009b). Chromosome mis-segregation caused by a defective SAC could result in changes in oncogene or tumor suppressor gene expression leading to genomic instability, a hallmark of cancer (Kops, Foltz, & Cleveland, 2004).

The complex SAC signaling pathways are mediated by the kinetochore, a subcellular structure comprised of at least 80 proteins. The kinetochore is composed of two parts, the inner kinetochore, which is the stable structural part, and the outer kinetochore that is the site of microtubule binding and SAC activity (Cheeseman & Desai, 2008; Santaguida & Musacchio, 2009). Upon mitotic entry, unattached kinetochores activate the SAC resulting in recruitment of several SAC

proteins, like BUB1. BUB1 (budding uninhibited by benzimidazole 1) is a kinase recruited early on in prophase through the KNL1 (Kinetochore Scaffold 1), a member of the KMN network (Desai et al., 2003; Jablonski, Chan, Cooke, Earnshaw, & Yen, 1998) (Shepperd et al., 2012). BUB1 is essential for recruitment downstream SAC effectors, including MAD1 (mitotic arrest deficient 1) and members of the highly conserved mitotic checkpoint complex (MCC): MAD2 (mitotic arrest deficient 2), BUBR1 (budding uninhibited by benzimidazole-related 1), BUB3 (budding uninhibited by benzimidazole 3), and CDC20 (cell division cycle 20). The MCC prevents the activation of the anaphase promoting complex/cyclosome (APC/C) thus inhibiting anaphase onset (R.-H. Chen, Waters, Salmon, & Murray, 1996). Compared to MAD2 alone, the MCC exhibits more than 3000 fold higher inhibitory effect on APC/C (V. Sudakin, Chan, & Yen, 2001).

The APC/C is a multi-subunit E3 ubiquitin ligase that controls anaphase onset (Valery Sudakin et al., 1995). When APC/C is active, the master mitotic regulator CDK1 is inactivated and sister chromatid cohesion is lost. Specifically, APC/C through its ubiquitin ligase activity targets cyclin B1, the M-phase cyclin that binds CDK1, and securin, essential for sister chromatid cohesion, for proteasomal degradation signaling entry to anaphase (Hagting et al., 2002).

In this work, using a micronucleus assay, we tried to assess the contribution of mitotic errors to genomic instability in FA. We then sought to identify the nature of these mitotic aberrations (Chapter III). Some of the content in chapter III was originally published in *Experimental Hematology* (2015 Dec 31;43(12):1031-46). Furthermore, we used an unbiased shRNA screen to identify perturbed mitotic phosphosignaling pathway upon loss of FA. We focused on mechanistically understanding how loss of FANCA affects the mitotic functions of essential SAC kinases (Chapter IV). We hope that this work contributes to the basic understanding of the etiology of FA and lays down the base for future targeted therapies in FA-deficient cancers.



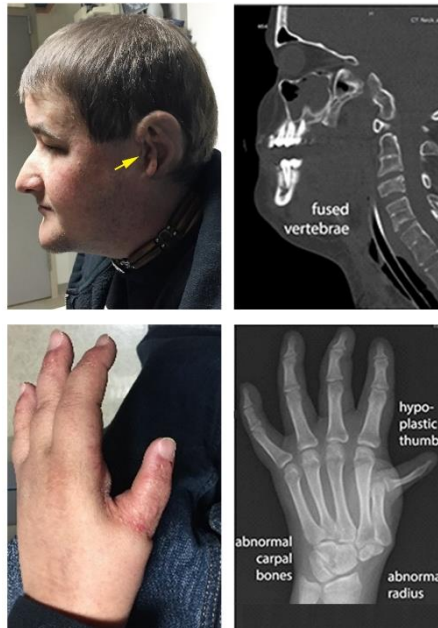


**Figure 1. Fanconi anemia: a complex genetic disorder with developmental abnormalities.** Thumb and radial abnormalities, vertebral fusion and external ear malformation in a *FANCC*<sup>-/-</sup> patient (images courtesy of G. Nalepa).

<b>FA gene name</b>	<b>Gene synonyms</b>	<b>Chromosome location</b>	<b>Protein size (aa)</b>
<i>FANCA</i>	<i>FAA, FACA, FANCH</i>	16q24.3	1455
<i>FANCB</i>	<i>FACB, FAAP95</i>	Xp22.31	859
<i>FANCC</i>	<i>FAC, FACC</i>	9q22.3	558
<i>FANCD1</i>	<i>FAD1, BRCC2, BRCA2</i>	13q12.13	3418
<i>FANCD2</i>	<i>FA-D2, FA4</i>	3p25.3	1451
<i>FANCE</i>	<i>FACE, FAE</i>	6p21.22	536
<i>FANCF</i>	<i>FAF</i>	11p15	374
<i>FANCG</i>	<i>FAG, XRCC9</i>	9p13	622
<i>FANCI</i>	<i>KIAA1794</i>	15q26.1	1328
<i>FANCI</i>	<i>BRIP1, BACH1, OF</i>	17q23.2	1249
<i>FANCL</i>	<i>FAAP43, PHF9, POG</i>	2p16.1	380
<i>FANCM</i>	<i>FAAP250, KIAA1596</i>	14q21.3	2048
<i>FANCN</i>	<i>PNCA3</i>	16p12	1186
<i>FANCO</i>	<i>ROVCA3, R51H3, RAD51L2</i>	17q23	376
<i>FANCP</i>	<i>BTBD12, MUS312</i>	16p13.3	1834
<i>FANCQ</i>	<i>RAD1, XPF, ERCC11</i>	16p13.12	916

<i>FANCR</i>	<i>BRCC5, RECA, RAD51A</i>	15q15.1	340
<i>FANCS</i>	<i>BRCA1, PNCA4, BRCC1</i>	17q21.31	1863
<i>FANCT</i>	<i>UBE2T, HSPC150</i>	1q32.1	197
<i>FANCU</i>	<i>XRCC2</i>	7q36.1	280
<i>FANCV</i>	<i>REV7, MAD2L2</i>	1p36.22	211

**Table 1. Summary of known Fanconi anemia genes.** Gene name, gene synonyms, chromosome locations, and protein sizes encoded by FA genes. The table is partially adopted from Table 1 in (Dong et al., 2015)

FA gene	Association with cancer	citation
<i>BRCA2</i> ( <i>FANCD1</i> )	Mutations result 82% Increased risk of breast cancer and 23% increased risk of ovarian cancer	(Hahn et al., 2003; Taniguchi et al., 2003)
<i>FANCF</i>	Hypermethylated promoter is found in 6.7% to 30% of testis, lung, ovarian and cervical cancer cell lines	(Marsit et al., 2004; Narayan et al., 2004)
<i>FANCA</i>	Reduced protein levels in sporadic AML	(M. D. Tischkowitz et al., 2004)
<i>FANCD2</i>	Reduced protein levels in breast cancer	(van der Groep et al., 2008)
<i>FANCL</i>	Reduced protein levels in lung cancer cells	(J. Zhang, Wang, Lin, Couch, & Fei, 2006)
<i>FANCO</i>	Mutations Increase risk of breast cancer	(Goldberg & Borgen, 2006)
<i>FANCC</i>	Mutations Increase risk of pancreatic cancer	(van der Heijden, Yeo, Hruban, & Kern, 2003)
<i>FANCG</i>	Mutations Increase risk of pancreatic cancer	(van der Heijden et al., 2003)

**Table 2. Fanconi anemia genes are associated with cancers in non-FA**

**patients.** Mutations in some FA genes increase the risk of developing different types of cancers in non-FA patients. Gene expression of FA genes is decreased in some types of cancers or cancer cell lines.

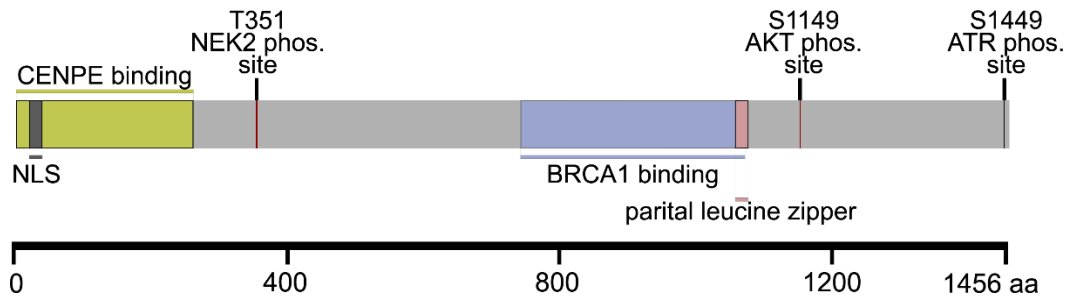


**Figure 2. Functional domains in FANCA protein.** These include a nuclear localization signal (NLS) (amino acids 18-29), a partial leucine zipper domain (amino acid residues 1069-1090), a BRCA1 binding domain, and a CENPE binding domain.

FANCA interacting protein	Functional relevance of interaction	citation
SNX5	Affects SNX5 trafficking with cell surface receptors	(Otsuki, Kajigaya, Ozawa, & Liu, 1999)
BRG1	Important for SWI/SNF recruitment to target genes	(Otsuki et al., 2001)
CENPE	May be important for maintenance of mitotic checkpoint signaling	(Du et al., 2009)
IKK2	May be important for recruitment of IKK2 in response to stress	(Liu, Otsuki, Young, & Mercurio, 2000)

**Table 3. A list of FANCA interacting proteins.** Interaction of FANCA with various proteins sheds a light on the cellular functions of this protein. This table lists FANCA interacting proteins, the functional relevance of the interaction, and the relevant citation.

## CHAPTER TWO

### MATERIALS AND METHODS

#### Cell culture

*FANCA*<sup>-/-</sup> primary patient fibroblasts (cell lines: MNHN, RA8851 and JRAST) were gifted from Dr. Helmut Hanenberg (Heinrich Heine University, Germany). MNHN cells harbor two *FANCA* mutations: c.3163C>T and c.4124-4125delCA. JRAST cells also harbor two *FANCA* mutations: p.Arg1055Trp and p.Thr1131Ala. *FANCA*-deficient lines have been described and the functional gene correction of all cell lines used in this work has been validated in G2/M MMC hypersensitivity assays (**Figure 3**). Patient fibroblasts, HeLa cells, and CENPA-GFP expressing HeLa cells were cultured in Dulbecco's modified Eagle medium (DMEM) containing 10% fetal bovine serum (FBS), 1% penicillin-streptomycin, 1% sodium pyruvate in 37°C 5% CO<sub>2</sub> in 5% O<sub>2</sub> incubator or normal O<sub>2</sub> incubators.

For RO-3306 synchronization, cells at 70% confluency were synchronized by adding 10µM RO-3306 and incubated in 37°C, 5% CO<sub>2</sub> and either 5% O<sub>2</sub> or normal incubators for 22 hours. Cells were then washed with PBS and released into growth media for the noted times. Alternatively, cells were PBS washed after RO-3306 synchronization and then released into 10µM MG132-containing growth media for 3 hours. Cells were then fixed accordingly for Immunofluorescence or protein extracted for IP or WB.

For cycloheximide treatment, cells at 80% confluency were treated with cycloheximide (CHX) to a final concentration of 20 µg/ml. Cells were treated simultaneously for different time points and then collected for western blot using protein extraction described below.

### **shRNA screen**

*FANCA* deficient patient fibroblasts (*FANCA*<sup>-/-</sup>) and their corrected counterparts (*FANCA*<sup>+</sup>) were plated (2 replicates/cell line) to 50% confluency in 15 cm plates (Falcon). The next day (day 1), cells were transduced per manufacturer's protocol with a viral library (MISSION® LentiExpress™ Human Kinases, Sigma Aldrich) that contains ~3200 lenti-viruses carrying sh-RNA sequences that target ~501 human kinase genes with a puromycin resistant backbone at a multiplicity of infection (MOI) of ~0.5. A non-transduced plate served as a negative control. On day 3, cells were selected with 1 µg/ml puromycin media for 5 days. Next, cells were pelleted and sent to Sigma for deep sequencing.

### **Bioinformatics**

The screen shRNA library consists of 4-10 shRNA clones targeting each kinase. Four raw copy numbers were determined for each clone representing 2 *FANCA*<sup>+</sup> replicates (a and b) and 2 *FANCA*<sup>-/-</sup> replicates (c and d). Four ratios were calculated from the raw data (a/c, a/d, b/c, and b/d). Kinases with at least one shRNA showing a 5-fold copy number fold change (increase or decrease)



between *FANCA*<sup>+</sup> and *FANCA*<sup>-/-</sup> cells in all four comparisons were considered significant. Raw data was also processed using the Panther gene classification database to confirm significant results.

### **shRNA transduction**

To generate stable shRNA-expressing *FANCA* gene-corrected and uncorrected fibroblasts, lentiviral particles were produced and transduced as described previously (Staser et al., 2013). Control shRNA, BUB1 (clone ID NM\_004336.x-1478s1c1, clone ID NM\_004336.x-2991s1c1, clone ID NM\_004336.3-520s21c1) and BUBR1 (clone ID NM\_001211.x-3346s1c1, clone ID NM\_001211.x-1705s1c1, clone ID NM\_001211.x-1560s1c1). Cells were transduced for 48 hours, selected with 1 µg/ml puromycin for 5 days, and then used for indicated experiments.

### **siRNA transfection**

Using siPORT NeoFX transfection reagent (Ambion), cells were reverse-transfected in 6-well plates (50,000 cells per well) or 10-cm plates (250,000 cells) with 25 nM siRNA on day 1, followed by forward-transfection with 25 nM siRNA on day 2. Cells were left to grow for 24-48 hours before harvesting for further experiments. List of siRNA purchased from Ambion: *FANCA* siRNA (s164), BUB1 siRNA (s2130, s2131, s2132), Negative control #2 (4390847).

## **Immunofluorescence and Microscopy**

Different methods (referred to as a, b, c, d and e) were used to perform Immunofluorescence: Cells were grown on ultrafine glass coverslips (Fisher) using the following methods: (a) fixed with 4% Paraformaldehyde (PFA) (Electron Microscopy Sciences) in PBS for 20 minutes, (b) pre-extracted with 0.2% TritonX-100 (Sigma Aldrich) for 30 seconds at room temperature and then fixed with 4% PFA for 20 minutes. Coverslips were then permeabilized and blocked with 0.2% triton in 5% BSA (Fisher Scientific) in PBS, (c) cells were pre-fixed with 4% PFA in PHEM buffer solution (50 mM Pipes, 25 mM Hepes, 10 mM EGTA, 8.5 mM MgSO<sub>4</sub>, pH 7.0) for 20 seconds, permeabilized with 0.5% TritonX-100 in PHEM buffer for 5 minutes, and then fixed in 4% PFA in PHEM for 20 minutes. Coverslips were then quenched with 25mM Glycine in PBS for 20 minutes and then blocked with 3% BSA in PBS-T (0.1% Tween in PBS) for 30 minutes, (d) fixed with 4% PFA for 15 minutes and then soaked in 50mM NH<sub>4</sub>Cl for 5 minutes, (e) pre-extracted with 0.1% triton for 2 minutes at room temperature, fixed with 4% PFA for 15 minutes, and then permeabilized with 0.5% triton in PBS for 15 minutes. Coverslips a, b and c were incubated in primary antibodies diluted in either 1% BSA in PBS or PBS overnight. Cells were then PBS washed and incubated in secondary antibodies diluted (1:2000) in 1% BSA in PBS or PBS for 1 hour. Coverslips d and e were blocked with 10% normal goat serum (NGS) (*Sigma Aldrich*) in 0.1% tween in PBS (PBST) for 1 hour and incubated overnight in primary antibodies diluted in blocking buffer. All coverslips were washed with PBS and incubated in secondary antibodies diluted in blocking buffer for 1 hour.

All coverslips were incubated in Hoechst-33342 (Life Technologies) diluted in PBS (1:10,000) for 10 min and then mounted using SlowFade Antifade (Life Technologies) or mounted directly (without Hoechst incubation) using prolong diamond antifade with DAPI (Life Technologies) on pre-cleaned glass slides (Fisher Scientific).

For deconvolution microscopy, image stacks (z-section distance: 0.2  $\mu\text{m}$ ) were acquired on a Deltavision PersonalDx microscope (Applied Precision) with a CCD camera using 20 $\times$ , 60 $\times$ , or 100 $\times$  lenses and deconvolved using Softworx. Super-resolution structured illumination microscopy (SR-SIM) images were acquired on a Zeiss ELYRA PS.1 system with a CCD camera and 60 $\times$ /100 $\times$  lenses, and processed via SIM/channel-alignment algorithms (Zen-2011; Zeiss). Line-intensity profiles were quantified using Imaris (Bitplane). z Sections on figures were exported using Imaris.

Images of FA patient marrow aspirates, marrow aspirates of patients diagnosed with immune-mediated aplastic anemia with negative chromosome breakage test results, marrow cytopins, and peripheral smears were obtained on a Zeiss Axiolab microscope with Axiocam-105 color camera.

## **Live Imaging**

Cells were plated at 10,000 cells per quadrant in a 35-mm Hi-Q4 (Ibidi) culture dish. The next day, time-lapse phase-contrast images (3 z sections, total = 6  $\mu\text{m}$ ) were acquired every 2 min for a period of 48 hours using a BioStation IM-Q time-lapse imaging system (Nikon) equipped with a 20 $\times$  0.8 NA Plan Fluor objective lens. NIS-Elements AR Analysis 4.10.02 or NIS-Elements Viewer 4.20 microscope imaging software (Nikon) was used for video analysis. Videos were exported via Imaris (Bitplane) and Adobe Photoshop. 112 *FANCA*<sup>+</sup> and 81 *FANCA*<sup>-/-</sup> JRAST fibroblasts were analyzed.

## **Quantification of intensities on CENPA spots**

Image stacks were transferred to Imaris software (version 7.7.1, *Bitplane*) for analysis. Each image was visualized in surpass view and the region of interest was segmented based on presence of DNA (blue channel). Next, xy diameter (0.3  $\mu\text{m}$ ) and ellipsoid size (0.6  $\mu\text{m}$ ) of each CENP-A stained kinetochore was manually estimated. Spots function was then used to detect CENP-A stained kinetochores based on fluorescence quality threshold (manually determined). The fluorescence quality threshold was set to exclude weak spots that represent background intensity. Background subtraction function in Imaris was enabled to exclude background signal. Statistical calculation was then performed on each CENP-A stained kinetochore and the mean intensity of the channel representing the protein of interest was exported and used in further analysis. A minimum of 300 kinetochores were used for the quantification.

## **Immunoblotting**

Whole cell extracts from HeLA cells or fibroblasts were prepared using M-PER Mammalian Protein Extraction Reagent (Thermo Scientific) containing protease inhibitor (Roche) and phosphatase inhibitor (Thermo Scientific) on ice for 10 minutes. Lysates were centrifuged at top-speed in a microcentrifuge for 10 minutes. Lysate protein concentrations were normalized using a bicinchoninic acid (BCA) assay kit (Pierce) followed by denaturation in NuPAGE sample-reducing agent and NuPAGE LDS sample buffer (Life Technologies) and boiled at 95°C for 5 minutes). Proteins were separated by 12.5% sodium dodecyl sulphate polyacrylamide gel electrophoresis (SDS-PAGE) and transferred to high-quality nitrocellulose membrane (Life Tech) in a solution of 20mM Tris, 150 mM glycine and 20% methanol at 250 mV for 2 hours at 4°C. After blocking in LiCor PBS blocking buffer (LI-COR Biosciences) for an hour, the membranes were incubated with primary antibodies at 1:1000 dilution in LiCor PBS blocking buffer overnight at 4°C. Following overnight exposure, the membranes were washed three times with 0.1% Tween 20 in PBS (PBS-T). Fluorescent-dye-conjugated secondary antibodies (LI-COR Biosciences) were used for infrared fluorescence-based detection (Odyssey CLX). Protein levels were quantified by measuring the relative fluorescence intensity of bands (normalized against loading controls (actin, GAPDH, tubulin, vinculin) using Image Studio 2.1 software.

For detection of FANCA protein expression, CD34+ cells were lysed in M-Per buffer (Thermo Scientific) containing phosphatase and protease inhibitors (Roche) and protein concentration was determined by BCA (Pierce). 15 µg of protein was loaded per well in a 4-12% gradient Bis-Tris gel (Life Tech). Membranes were blocked in 5% milk for 1 hour, and then incubated with anti-FANCA antibody (ab5063, Abcam) overnight diluted 1:2000 in 5% milk. Blots were washed with 0.1% Tween 20 in PBS (PBS-T) and incubated with anti-rabbit IgG horseradish peroxidase linked secondary antibody diluted in PBS-T and 0.5% milk. Signal was detected via the enhanced chemiluminescence system (Life Tech).

### **CD34+ CFU assay**

Transduced CD34+ cells were grown in triplicate (2500 cells/35 mm dish) in Methocult (H4434) methylcellulose-based medium containing recombinant cytokines (Stem Cell) and varying concentrations of MMC. Plates were incubated at 37°C, 5% O<sub>2</sub> for 11 days. Colonies were then counted, and defined as clusters of >50 cells.

### **Co-Immunoprecipitation (Co-IP)**

Whole HeLa cell extracts were collected and 1000µg protein lysate was incubated at 4°C overnight in columns prepared with rabbit anti-FANCA (Abcam) and mouse anti-BUB1 (Abcam) using the Pierce co-immunoprecipitation Kit

protocol (Thermo Scientific, Rockford, IL, USA). Each column was eluted per the protocol and subjected to immunoblotting analysis.

### **Flow cytometry**

To detect functional correction of isogenic-corrected patient fibroblasts, cells were treated with 33 nM MMC, and then harvested upon incubation with HyClone HyQTase (Fisher) detachment solution for 15 minutes. Cells were pelleted and resuspended dropwise in cold 70% ethanol, and stored at -20°C overnight. The following day, cells were spun down and resuspended in FxCycle PI/RNase Staining Solution (Life Tech) for cell cycle analysis. For quantification of mitotic cells, fibroblasts were treated with 1nM MMC or 1nM taxol for 9 days. Cells were then removed from tissue culture plates upon incubation with HyClone HyQTase (Fisher) detachment solution for 15 minutes at 37°C followed by 4% paraformaldehyde/PBS fixation for 10 minutes. Cells were pelleted, resuspended in 90% methanol and stored in -20°C overnight. The next day, cells were incubated in 0.5% BSA/PBS for 4 minutes, pelleted and stained with an Alexa Fluor 488-conjugated phospho-histone H3 antibody (Cell Signaling) diluted 1:50 in 0.5% BSA/PBS for 1 hour in the dark. The cells were next washed with PBS and analyzed on a FacsCalibur flow cytometer (Becton-Dickinson). Flow cytometry data analysis was performed using Flow Jo software.

### **Cytokinesis-block micronucleus assays**

Fibroblasts grown on coverslips were treated with cytochalasin-B (2  $\mu\text{g}/\text{mL}$ ) for 24 hours, followed by processing/imaging as described above; anti-CENPA immunofluorescence visualized endogenous kinetochores. For drug treatments, cells were exposed to 1 nmol/L taxol or MMC for 9 days before cytochalasin B for 24 hours. A micronucleus was defined based on the following criteria: (i) the diameter of the micronucleus must be less than half that of the main nucleus, and (ii) the nuclear boundary must be identified between the micronucleus and the nucleus. The presence of kinetochores was determined based on visualization of CENPA+ foci within the stack of z sections spanning the entire micronucleus.

For CD34+ experiments, primary human CD34+ cells transduced with green fluorescent protein (GFP)-tagged lentiviral shRNA constructs were cultured for 5 days, sorted on a SORP Aria FACS system, attached to coverslips via cytopsin (450 rpm, 7 min), and analyzed in immunofluorescence assays as described above.

### **Mitotic spindle assembly assay**

Culture plates with live fibroblasts on coverslips were removed from the 37°C incubator to replace growth medium with prechilled medium and kept at 4°C for 1 hour. Next, the cold medium was replaced with medium prewarmed to 37°C, and cells were returned to 37°C (15 sec) and immediately fixed (4% paraformaldehyde/PBS). For staining with anti-pericentrin and anti- $\alpha$ -tubulin, cells



were imaged via deconvolution microscopy. Imaris (Bitplane) was used to measure length of microtubules in z sections and count centrosome-associated microtubules within stacks.

### **S-phase quantification**

Cells grown on coverslips were treated for 9 days with 1nM MMC or 1nM taxol as described above, pulsed with EdU using the Click-iT® EdU Imaging Kit (Life Technologies) for 45 minutes, then fixed and stained per the manufacturer's protocol. Nuclei were counterstained with Hoechst 33342. Cells were imaged on the Deltavision deconvolution microscope and the fraction of EdU-positive nuclei was manually quantified.

### **Colony Forming Unit- Fibroblast (CFUF) assay and direct cell count assay**

500 corrected and uncorrected patient fibroblasts were plated on 10-cm cell culture dishes. After cellular adherence overnight in 37°C 5% CO<sub>2</sub> and 5% O<sub>2</sub> incubator, cells were treated with either PBS, MMC, Taxol, small molecule inhibitor or shRNA and returned to the incubator for total of 14 days followed by fixation and staining with 0.4% methylene blue/methanol (Fisher Scientific Company). Colonies were manually counted and plates were scanned using an Epson color scanner.

For direct cell counting, 6-well plates were seeded with  $1 \times 10^5$  cells/well and treated with indicated doses of MMC or taxol for 9 days. Cell counts were performed using a hemocytometer.

### **Small molecule inhibitors**

10 mg of MK 8776 (Cat No. S2375, Selleckchem) stock solution was diluted to 100 mM in dimethyl sulfoxide (DMSO) and further diluted in fibroblast growth medium to a final concentration of 30nM. 10 mg of Volasertib (Cat No. S2235, Selleckchem) stock solution was diluted to 100 mM in dimethyl sulfoxide (DMSO) and further diluted in fibroblast growth medium to a final concentration of 10nM. 5 mg of Roscovitine (R7772, Sigma) stock solution was diluted to 50 mM in dimethyl sulfoxide (DMSO) and further diluted in fibroblast growth medium to a final concentration of 10nM.

### **Bioinformatics analysis of cancer-associated FA mutations**

Somatic cancer-associated mutations of FANCA were identified within the COSMIC database (Forbes et al., 2015). Functional impact of mutations was examined with Mutation Assessor algorithm; mutations producing a Functional Impact Score (FIS)  $>1.938$  were considered potentially disruptive.

### ***in vitro* Kinase assay**

BUB1 antibody (Abcam) was used to immunoprecipitate BUB1 from FANCA patient fibroblasts (FANCA<sup>-</sup>), their corrected counterparts (FANCA<sup>+</sup>), or from HeLa cells using Pierce™ Crosslink IP Kit (Thermo Scientific). Protein kinase assays were performed in 30 µl reactions. Reaction mixture contained 1µg BUB1 immunoprecipitates, 2µg H2A (New England Biolabs), 30µM cold ATP, 100 nCi P<sup>32</sup> ATP (PerkinElmer) in kinase buffer (Cell Signaling). The reactions were incubated for 30 mins at room temperature. The reactions were then quenched with SDS buffer, resolved by SDS-PAGE, and analyzed by autoradiography to detect BUB1-dependent in-vitro phosphorylation of Histone 2A.

### **Antibodies**

The following primary antibodies were used for IF in this study: FANCA (ab201458 or ab5063, Abcam), BUB1 (ab54893, Abcam), CENPA (2186s, Cell Signaling Technologies; ab13939, Abcam), BUBR1 (ab54894, Abcam), BUBR1-Ac<sup>k250</sup> (gift from Dr. Hyunsook Lee), FANCD1 (Op45 or CA1033, millipore), AURKB (611082, BD Biosciences), FANCG (sc393382, Santa Cruz),  $\alpha$ -tubulin (11126, Life Technologies), PCAF (sc8999, Santa Cruz; 3378, Cell Signaling Technologies), anti-pericentrin (Abcam, 1:100), mouse anti-centrin 3 (Santa Cruz, 1:100), mouse anti- $\gamma$ -tubulin (Abcam, 1:100), rabbit anti-CEP170 (Abcam, 1:100). For immunofluorescence, Alexa 488-, Alexa 594-, and Alexa 647-conjugated antibodies (Life Technologies) were used for primary antibody detection.

For immunoblotting, the following primary antibodies were used: rabbit anti-FANCA (Abcam), rabbit anti-BRCA2/FANCD1 (millipore), mouse anti-BUB1 (Abcam), mouse anti-BUBR1 (Abcam), rabbit anti-acetylated BubR1 (gift from Dr. Hyunsook Lee), rabbit anti-cyclin B1 (Cell Signaling Technology), mouse anti-cdc27 (BD Biosciences), mouse anti-actin (Sigma-Aldrich), and rabbit anti-GAPDH (Cell Signaling Technology).

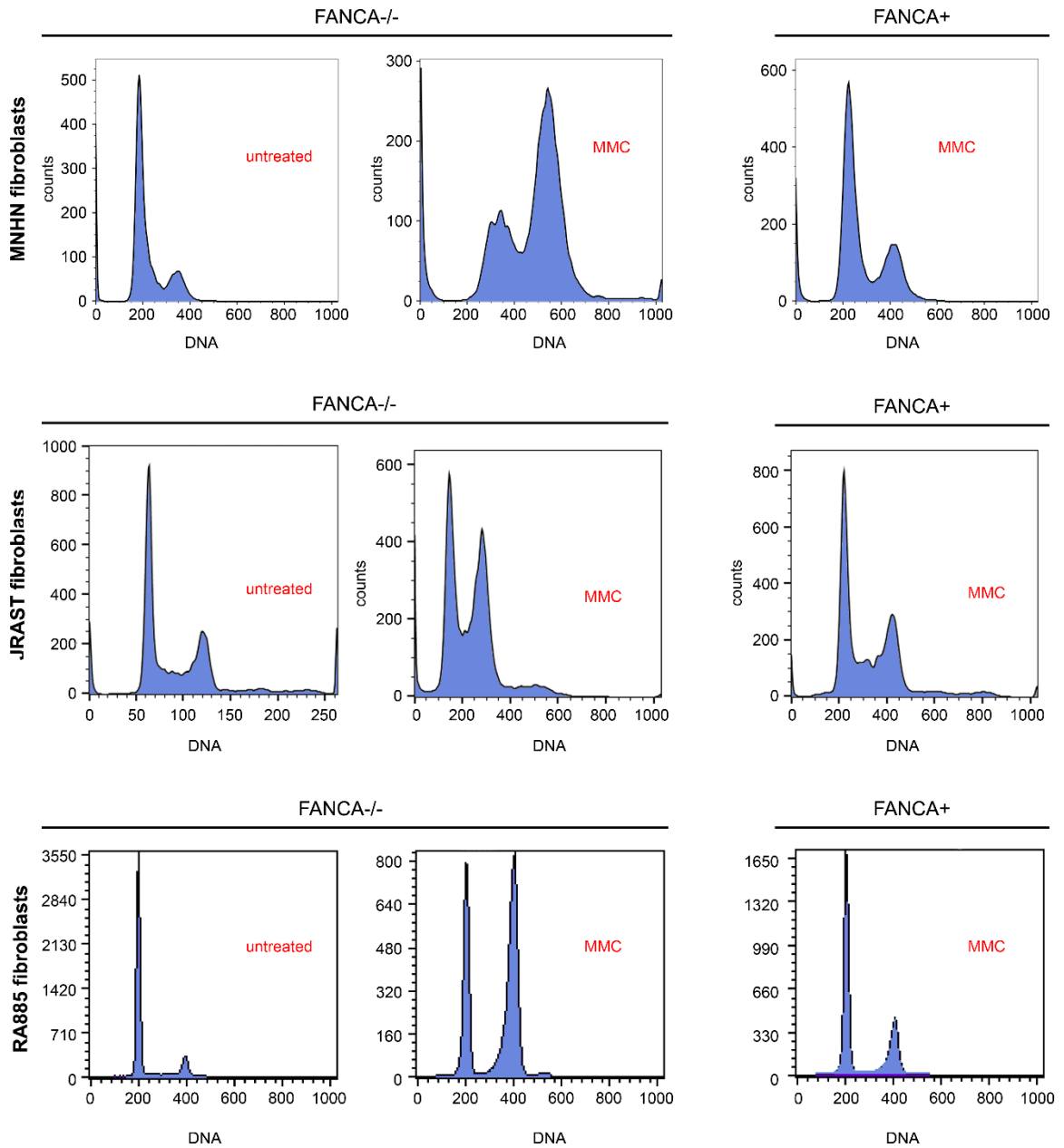


**Figure 3. Functional rescue of FANCA isogenic gene defect in primary patient fibroblasts.** Cell cycle flow profiles of *FANCA*-deficient patient line MNHN (top), JRAST (middle), and RA885 (bottom). Primary patient cells and their isogenic gene-corrected counterparts were either untreated or treated with MMC for 48 hours and analyzed for DNA content via flow cytometry to determine

functional FA correction. Note partial correction of MMC-induced G2/M arrest in *FANCA*<sup>-/-</sup> patient cells on correction with wild-type FANCA.

## CHAPTER THREE

### INTERPHASE AND MITOTIC ERRORS RESULT IN GENOMIC INSTABILITY IN FA

#### **Introduction**

Fanconi anemia (FA/BRCA) pathway is an intricate plexus of at least 21 proteins that maintain genomic stability, control growth and development, and prevent cancer. Bi-allelic germline disruption of any FA gene causes Fanconi anemia (FA), a genetic disorder characterized by developmental abnormalities, bone marrow failure (BMF), myelodysplasia and high risk of cancer, particularly acute myeloid leukemia (AML) (Alter, 2014; Alter et al., 2010; D'Andrea, 2010; Kottemann & Smogorzewska, 2013; P. S. Rosenberg et al., 2008). Heterozygous inborn mutations in the BRCA branch of FA network increase risk of breast and ovarian cancers as well as other tumors (D'Andrea, 2010; Howlett et al., 2002; Jones et al., 2009; Sawyer et al., 2015; Seal et al., 2006), and somatic mutations of FA/BRCA genes occur in malignancies in non-Fanconi patients (Narayan et al., 2004; Taniguchi et al., 2003; M. Tischkowitz et al., 2003; M. D. Tischkowitz et al., 2004). Thus, disruption of FA/BRCA signaling promotes malignancies in the inherited genetic syndromes and in the general population.

The FA/BRCA pathway prevents cancer by protecting genome integrity. In interphase, DNA damage response (DDR) initiates the assembly of the multi-protein FA complex at damage sites to arrest the cell cycle as the cascade of

effectors repairs the lesions (D'Andrea, 2010; Kottemann & Smogorzewska, 2013). These compartmentalized bursts of FA activity handle multiple genotoxic insults, from endogenous aldehydes (Garaycochea et al., 2012; Langevin et al., 2011) to replication errors and mutagen exposure. Thus, the FA/BRCA network provides a crucial line of defense against interphase mutagenesis (D'Andrea, 2010; Kottemann & Smogorzewska, 2013).

Less is known about the role of the FA/BRCA pathway during mitosis, but FA signaling has been recently implicated in the maintenance of normal centrosome count (Kim et al., 2013; Nalepa et al., 2013; Zou et al., 2013; Zou et al., 2014), spindle assembly checkpoint (SAC) (London & Biggins, 2014; Nalepa et al., 2013), repair of anaphase bridges (Chan et al., 2009; Naim & Rosselli, 2009a) and execution of cytokinesis (Daniels, Wang, Lee, & Venkitaraman, 2004; Mondal et al., 2012; Vinciguerra et al., 2010). Since chromosomal instability due to mitotic errors is a hallmark of cancer (Gordon, Resio, & Pellman, 2012; Hanahan & Weinberg, 2011) and a therapeutic target (Bakhoun & Compton, 2012), these findings may have translational relevance. However, it is unknown whether these *ex vivo* observations are applicable to *in vivo* hematopoiesis.

Here, we present quantitative evidence that loss of FA signaling disrupts mitosis during *in vivo* hematopoiesis in humans, and that both aberrant interphase and mitotic failure contribute to genomic instability due to FA deficiency. Super-resolution microscopy revealed that FANCA shuttles to the pericentriolar material



at mitotic entry to regulate centrosome-associated spindle nucleation. We found that primary *FANCA*<sup>-/-</sup> cells escape chemotherapy-induced SAC to replicate despite genomic instability. Our cell-survival assays showed that FA-deficient cells are hypersensitive to taxol (an antimitotic chemotherapeutic). Sublethal taxol doses exacerbated genomic instability in FA<sup>-/-</sup> cells through mitotic errors while low-dose MMC activated the G2/M checkpoint and DNA breakage. Therefore, distinct classes of chemotherapeutics inflict unique damage patterns in FA<sup>-/-</sup> cells, which may have implications for future strategies against FA-deficient cancers. Together, our findings provide insights into complex mechanisms of genomic instability in FA.

## Results

### *In vivo* error-prone mitosis during FA<sup>-/-</sup> hematopoiesis.

Mitotic failure was reported in FA cells *ex vivo*, and cytokinesis failure was documented in FA marrows (Nalepa et al., 2013; Vinciguerra et al., 2010). However, the *in vivo* evidence of abnormal early mitosis in hematopoietic cells of FA patients has been missing. To examine whether loss of *FANCA*, the gene most commonly disrupted in FA (D'Andrea, 2010), predisposes hematopoietic cells to erratic divisions *in vivo*, we quantified mitotic errors in marrow aspirates of two *FANCA*<sup>-/-</sup> patients with pancytopenia but no MDS/AML. Consistent with the role of *FANCA* in cell division, we observed increased frequency of abnormal mitotic figures in *FANCA*<sup>-/-</sup> marrows compared to marrow aspirates of patients diagnosed with immune-mediated aplastic anemia after excluding FA by negative chromosome breakage tests (**Figure 4A**,  $p=0.01$ ). Lack of chromosome congression leading to lagging chromosomes in anaphase and micronucleation at mitotic exit reflects weakened SAC or merotelic attachment due to centrosome malfunction (Nalepa et al., 2013). The DNA bridges in late mitosis may reflect impaired resolution of ultrafine anaphase bridges (Naim & Rosselli, 2009a). Interphase nuclear morphology in the erythroid lineage provided further evidence of *in vivo* mitotic abnormalities (**Figure 4B-C**). Erythroblast micronucleation (**Figure 4B**) suggests failure to segregate chromosomes into the daughter nuclei. Presence of bizarre erythroblasts with multilobed nuclei (**Figure 4B**) is consistent with impaired chromosome segregation due to erroneous SAC followed by

cytokinesis failure (Nalepa et al., 2013; Vinciguerra et al., 2010). Binucleated erythroblasts (**Figure 4B**) reflect lack of cytokinesis after normal chromosome division (Vinciguerra et al., 2010). These results provide quantitative *in vivo* evidence that abnormal mitoses occur with increased frequency in the hematopoietic cells of *FANCA*<sup>-/-</sup> patients before development of MDS/AML.

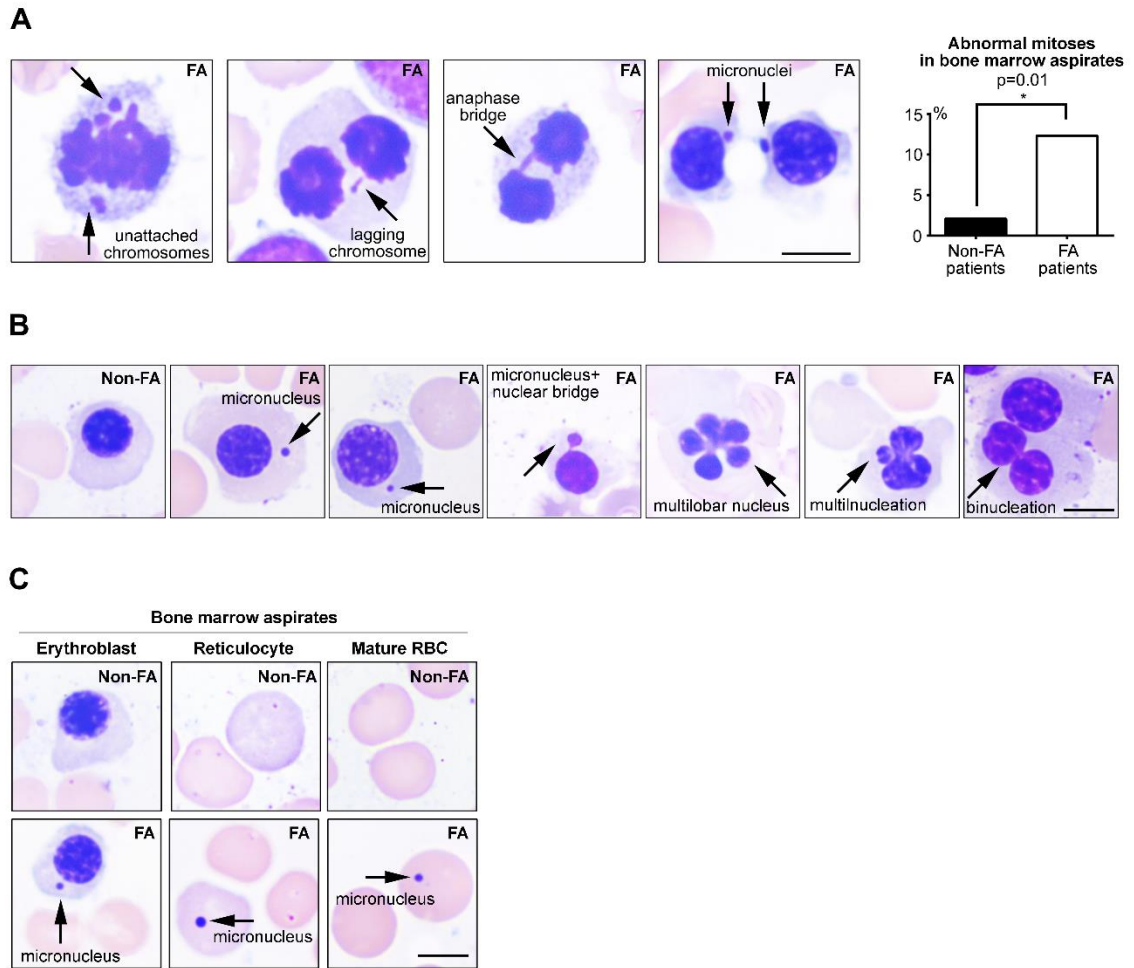


**Figure 4. Chromosomal instability and abnormal mitoses during hematopoiesis in human *FANCA*<sup>-/-</sup> patients. (A)** Representative abnormal mitoses in *FANCA*<sup>-/-</sup> patient bone marrow aspirates. Quantification (upper right) represents data from 2 different FA patients and 2 non-FA patients (96 mitoses in non-FA and 73 mitoses in FA; Fisher's exact test). Scale bars: 5  $\mu$ m. **(B)** Examples of abnormal interphase nuclear morphology in *FANCA*<sup>-/-</sup> patients' hematopoietic cells that have undergone aberrant mitoses compared to a normal non-FA interphase erythroblast. Scale bars: 5  $\mu$ m **(C)** Micronucleation of *FANCA*<sup>-/-</sup> bone marrow erythroblasts, reticulocytes and mature red blood cells top. Scale

bars: 5  $\mu\text{m}$  (top); 2 $\mu\text{m}$  (bottom). All specimens were imaged with Zeiss Axiolab system equipped with an Axiocam 105 color camera.

## **A combination of interphase and mitotic errors drives genomic instability in FA.**

Since BMF and hematopoietic malignancies are consistent clinical hallmarks of FA (D'Andrea, 2010; Kottemann & Smogorzewska, 2013), we quantified the contribution of interphase and mitotic abnormalities to genomic instability in FANCA-deficient hematopoietic cells. A modified micronucleus assay (**Figure 5A**) (Fenech, 2007) allowed to determine the origin of multinucleation in primary human CD34+ hematopoietic cells transduced with an shRNA (short hairpin RNA) against *FANCA* (Nalepa et al., 2013) compared to control CD34+ cells. We validated the *FANCA* shRNA in human CD34+ cells (**Figure 5B-C**). Upon *FANCA* knockdown, CD34+ cells were immunostained for endogenous CENPA (a kinetochore marker (Palmer, O'Day, Trong, Charbonneau, & Margolis, 1991)) and imaged by deconvolution microscopy to classify cells based on the presence of CENPA+ foci. As described (Fenech, 2007), additional kinetochore-positive nuclei arise through whole-chromosome missegregation in mitosis, and supernumerary kinetochore-negative nuclei result from DNA fragmentation (**Figure 5A**). *FANCA*-knockdown CD34+ cells developed higher multinucleation due to both chromosome breakage ( $p=0.0083$ ) and faulty chromosome segregation ( $p=0.0001$ ) compared to control CD34+ cells (**Figure 5D-E**). We concluded that silencing *FANCA* impairs both interphase and mitotic genome maintenance in human hematopoietic cells.

To validate this finding in primary FA-deficient patient cells and eliminate the possibility of non-specific shRNA-induced phenotype (Sigoillot et al., 2012), we pursued cytokinesis-block cytome assays (Fenech, 2007). Dividing cells are treated with cytochalasin B, a cytokinesis inhibitor, prior to CENPA immunofluorescence. Inhibition of cytokinesis generates binucleated cells upon error-free chromosome partition, and the presence of micronuclei indicates abnormal chromosome segregation during the last mitosis. Again, CENPA-positivity distinguishes mitotic-failure micronuclei from DNA-breakage micronuclei (**Figure 6**) (Schuler, Rupa, & Eastmond, 1997).

*FANCA*<sup>-/-</sup> fibroblasts had increased frequency of both chromosome missegregation ( $p=0.0391$ ) and chromosome breakage ( $p=0.0218$ ) compared to isogenic gene-corrected cells (**Figure 7A-B**). Thus, disruption of FA signaling impairs interphase and mitotic fidelity not only during hematopoiesis (**Figure 4**), but also in fibroblasts (**Figure 7**). These findings suggest that FANCA, a member of the FA/BRCA pathway, may play evolutionarily conserved roles in mitotic genome housekeeping.

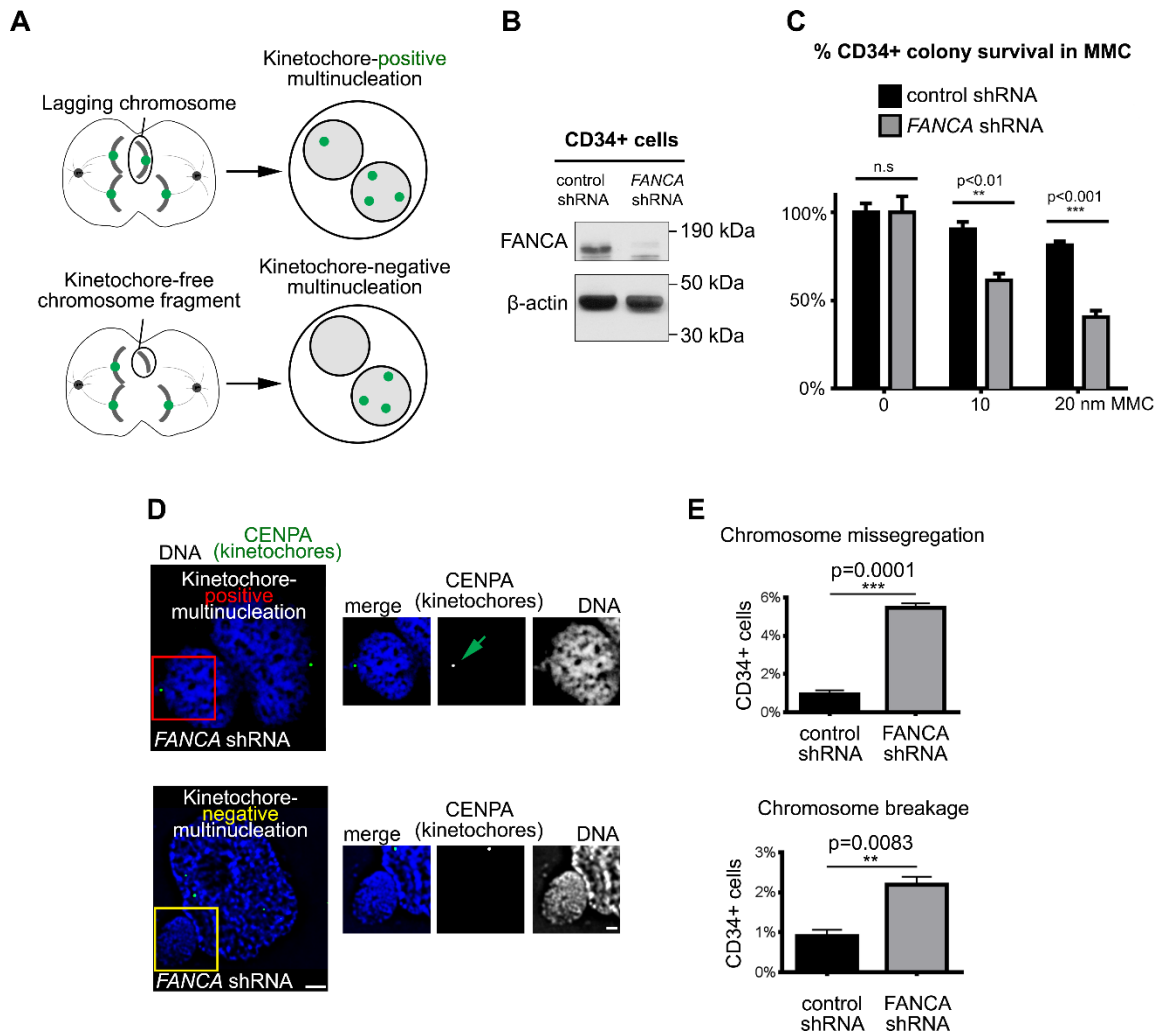


**Figure 5. FANCA maintains genomic integrity during interphase and mitosis in primary human CD34+ cells. (A)** Assay schematic.

Kinetochore/centrosome immunofluorescence staining distinguishes multinucleation generated through whole-chromosome missegregation from multinucleation resulting from DNA breakage. **(B)** *FANCA* shRNA efficiently knocks down FANCA protein in primary human CD34+ cells.  $\beta$ -actin serves as loading control. **(C)** Functional validation of *FANCA* shRNA in primary human CD34+ cells. *FANCA* shRNA renders CD34+ cells hypersensitive to mitomycin C compared to CD34+ cells compared with control shRNA. Error bars represent



mean  $\pm$  SEM and significance was determined using a two-way ANOVA with Sidak correction. **(D)** Representative images of multinucleation resulting from FANCA knockdown in human CD34<sup>+</sup> cells. Regions of interests are marked in red or yellow and enlarged on the right. Green arrow points to a CENPA-positive centromere/kinetochore within the supernumerary nucleus. Scale bars: 2 $\mu$ m (left) and 1 $\mu$ m (right) **(E)** Quantification of multinucleation resulting from weakened SAC or chromosome breakage in control and FANCA-knockdown CD34<sup>+</sup> cells. At least 500 cells per group were counted. Results were analyzed using a student's t-test and represented as mean  $\pm$  SEM.

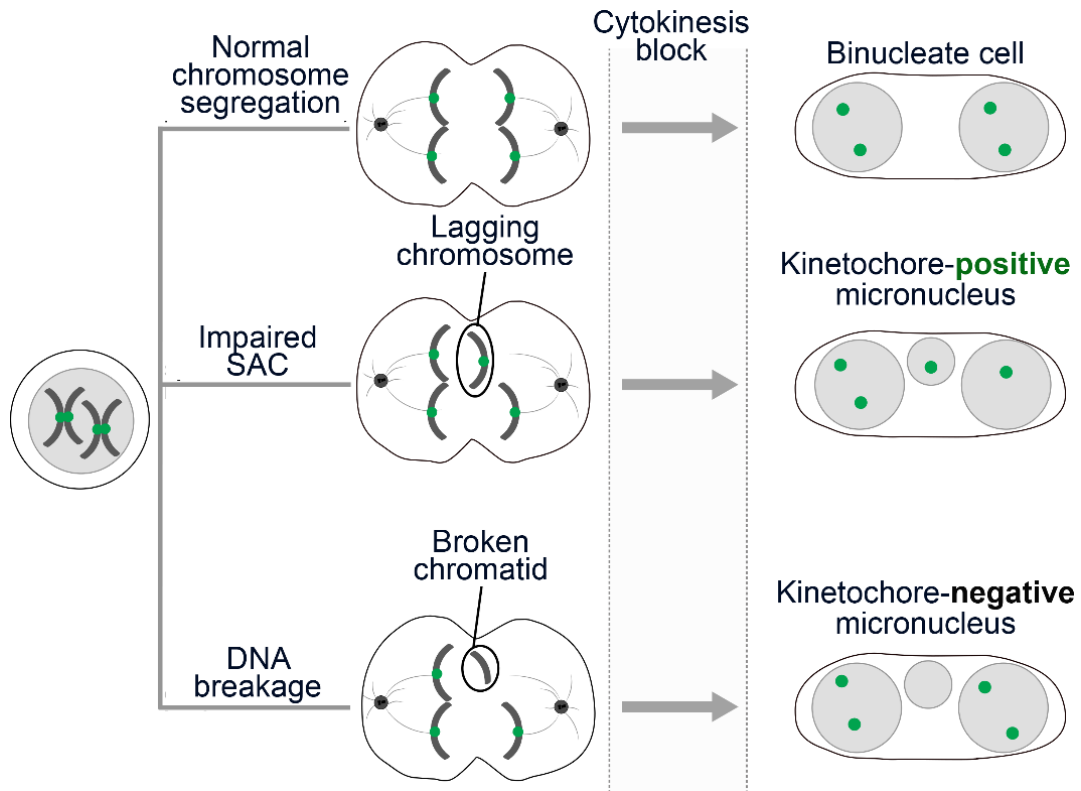


**Figure 6. Schematic representing micronucleus assay.** Schematic of the cytokinesis-block micronucleus test that delineated the origin of aneuploidy based on the presence or absence of kinetochores within micronuclei.

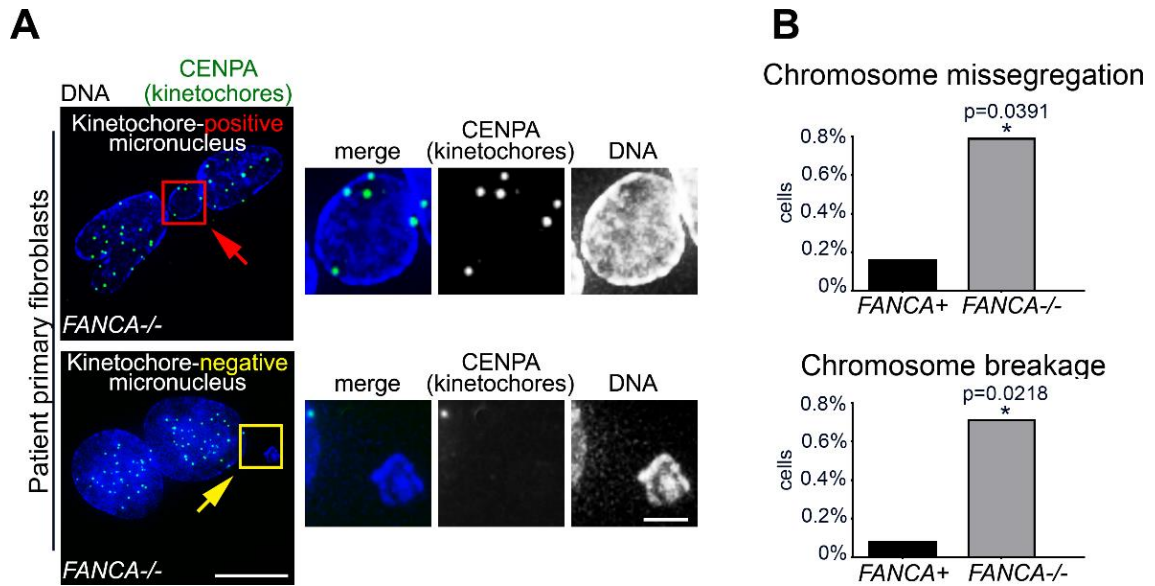


**Figure 7. Micronucleation upon loss of FA signaling results from a combination of interphase and mitotic errors. (A)** Representative images of micronuclei in *FANCA*<sup>-/-</sup> primary patient fibroblasts. Scale bars: 10µm (left) and 2µm (right) **(B)** Quantification of micronuclei resulting from whole-chromosome missegregation versus chromosome breakage in primary *FANCA*<sup>-/-</sup> and *FANCA*<sup>+</sup> fibroblasts. Error bars represent mean +/- SEM. At least 260 cells were counted per condition and significance was determined by student's t-test. Cells were imaged with deconvolution microscopy (Applied Precision personalDx) and deconvolved with Softworx imaging suite (10 iterations, ratio: conservative).

## **FANCA shuttles to the pericentriolar material during mitotic centrosome maturation.**

Multiple FA proteins, including FANCA (**Figure 8F-G**), localize to centrosomes and mitotic spindles (Kim et al., 2013; Nalepa et al., 2013; Zou et al., 2013). However, it is unknown whether FANCA association with centrosomes changes between interphase and mitosis, as expected of a *bona fide* regulator of mitotic centrosome/spindle function (Lee & Rhee, 2011; Sdelci et al., 2012).

Centrosome maturation prepares centrosomes for mitosis through reorganization of the pericentriolar material (PCM). A phosphosignaling circuit of cyclin-dependent kinases (CDKs), polo-like kinase 1 (PLK1) and Aurora A (Joukov, Walter, & De Nicolo, 2014) recruits pericentrin (Lee & Rhee, 2011) and  $\gamma$ -tubulin (Sdelci et al., 2012) to the PCM at mitotic entry to increase the spindle-nucleating centrosome activity (Zimmerman, Sillibourne, Rosa, & Doxsey, 2004). Since FANCA regulates spindle assembly (**Figure 8B-E**), we wondered whether FANCA is recruited to the PCM of maturing centrosomes similar to these other centrosome-spindle regulators. To examine FANCA sub-centrosomal localization, we employed deconvolution and super-resolution microscopy, which allows visualization of centrosomes beyond the diffraction limit imposed by conventional microscopes (Lawo, Hasegan, Gupta, & Pelletier, 2012; Mennella, Agard, Huang, & Pelletier, 2014). At mitotic entry, FANCA shuttled from centrioles towards the PCM and co-localized with pericentrin,  $\alpha$ -tubulin and the minus end of spindle microtubules until the mitotic exit (**Figure 8A-B, Figure 10-**

**11).** In interphase, FANCA returned to the mother centriole (**Figure 12**). These observations were confirmed with multiple primary antibodies and imaging of *FANCA*<sup>-/-</sup> patient cells stably expressing GFP-FANCA.

To thoroughly analyze FANCA distribution within the PCM, we analyzed individual 84-nm-thin super-resolution sections of mitotic centrosomes. At the mid-centrosome level, we observed well-organized FANCA fibers extending through and beyond the pericentrin-decorated PCM network from centrioles towards microtubule nucleation sites (**Figure 9B-C**). This dynamic relocalization of FANCA to the PCM during mitosis supports the newly discovered role of FANCA in spindle microtubule nucleation (**Figure 8**).

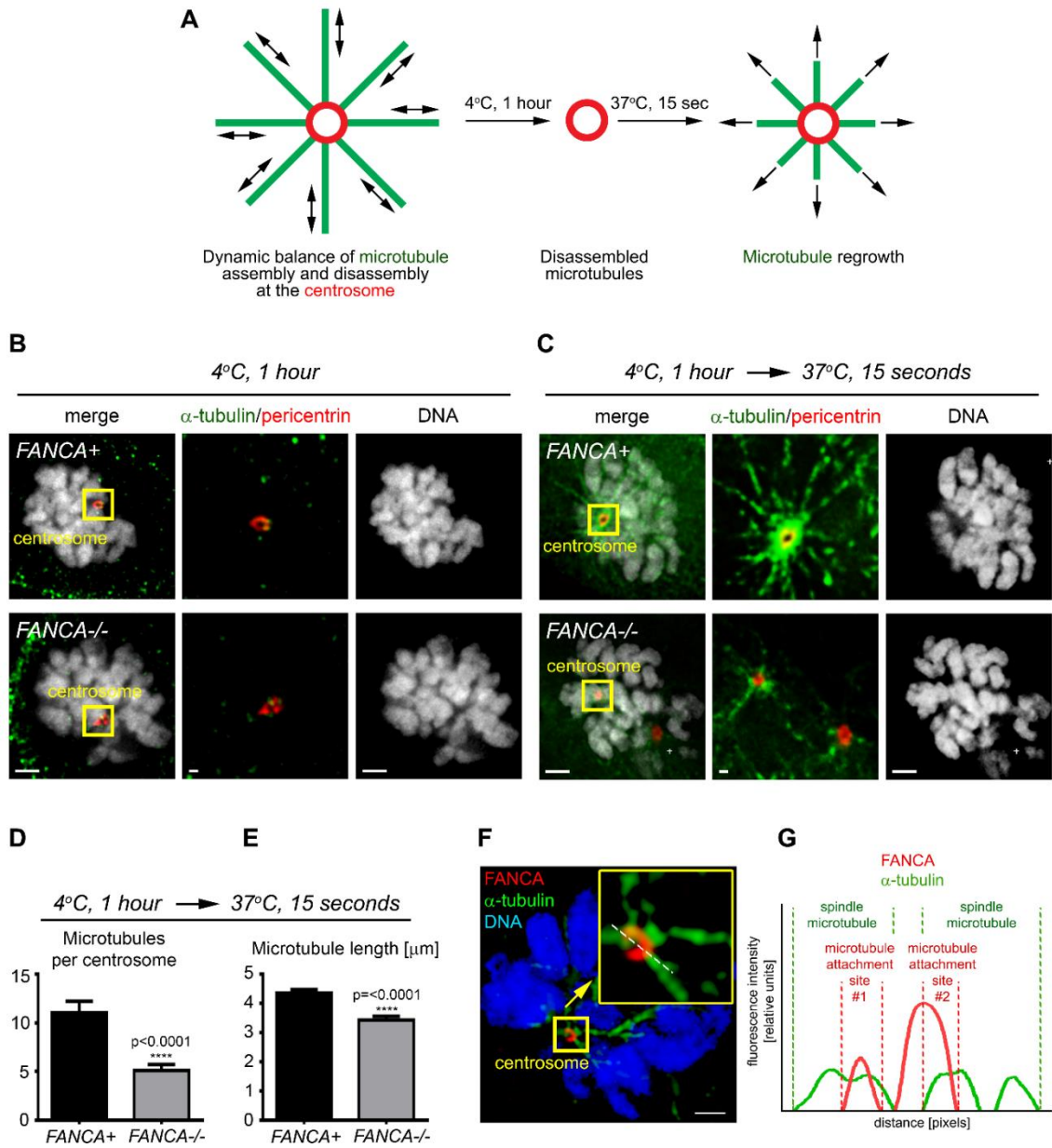


**Figure 8. Loss of FANCA disrupts spindle microtubule assembly at prometaphase centrosomes. (A)** Experiment design. Microtubules of living *FANCA*<sup>-/-</sup> and *FANCA*<sup>+</sup> cells were destabilized by cold treatment (4°C for 1 hour). Cells were then returned to 37°C to initiate microtubule reassembly and fixed with 4% paraformaldehyde 15 seconds later. **(B)** Cold treatment fully destabilizes microtubules in *FANCA*<sup>+</sup> and *FANCA*<sup>-/-</sup> prometaphase cells. **(C)**

Representative images of mitotic spindle assembly in *FANCA*<sup>+</sup> and *FANCA*<sup>-/-</sup> prometaphase cells stained with anti- $\alpha$ -tubulin (green) and anti-pericentrin (red) antibodies. Images were captured with 60x lens on the Deltavision deconvolution microscope. Scale bars: 2 $\mu$ m (left and right) and 500nm (region of interest showed in the center). **(D, E)** Quantification of spindle microtubules per centrosome **(D)** and the microtubule length ( $\mu$ M) **(E)** in gene-corrected and *FANCA*<sup>-/-</sup> cells treated as described in **(A)**. Data represents 2 independent experiments (n=130 microtubules/experiment), and error bars represent SEM. **(F)** Representative mitotic HeLa cell stained with anti-FANCA (red) and anti- $\alpha$ -tubulin (green) antibodies, imaged on an ELYRA PS.1 super-resolution microscope using SIM technology. Insert shows enlarged centrosome-containing region of interest. White line shows the line of fluorescence intensity profile. Scale bar: 2 $\mu$ m. Cells were imaged with deconvolution microscopy (Applied Precision personalDx) and deconvolved with Softworx imaging suite (10 iterations, ratio: conservative). **(G)** Fluorescence intensity profiles of FANCA (red) and  $\alpha$ -tubulin (green) signal.

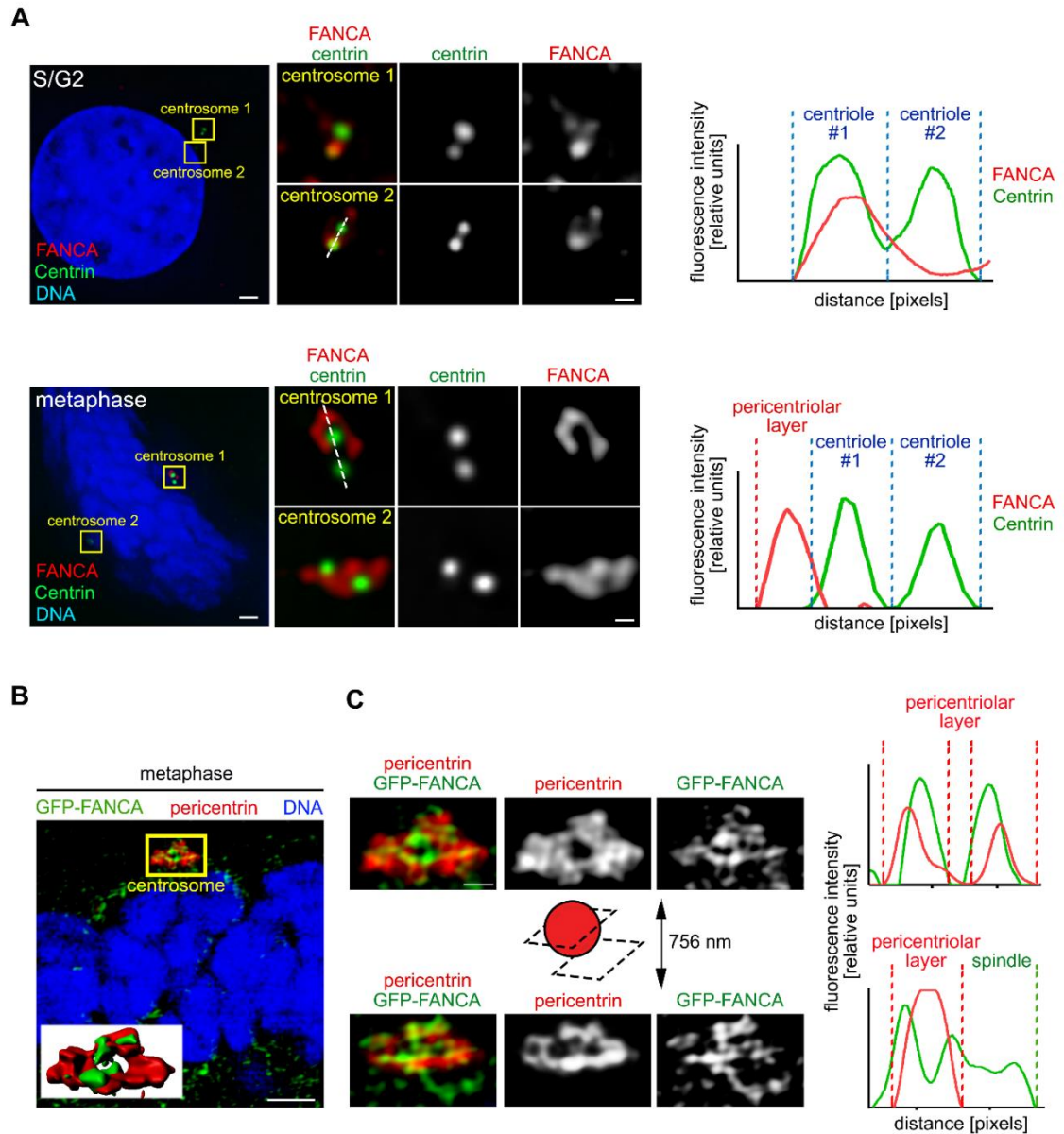


**Figure 9. FANCA shuttles to the pericentriolar material during mitosis. (A)**

HeLa cells were immunostained with antibodies against endogenous FANCA (red) and centrin (green), imaged with deconvolution microscopy (Applied Precision personalDx) and deconvolved with Softworx imaging suite (10 iterations, ratio: conservative). Fluorescence intensity profiles demonstrate that



FANCA colocalizes with centrin in interphase and migrates away from centrioles at metaphase. Scale bars: 1.5  $\mu\text{m}$  (left) and 300 nm (right) **(B)** Representative super-resolution image of human fibroblast stably expressing GFP-FANCA and stained with antibody against the pericentriolar material marker (pericentrin). Inserted 3D rendering of the centrosome shows colocalization of GFP-FANCA and pericentrin. Scale bars: 2  $\mu\text{m}$ . The yellow region of interest is magnified **(C)** to show FANCA fibers embedded within the PCM (centrosome cross-section) and extending towards the spindle (centrosome outer layer section). Fluorescence intensity profiles (right) of GFP-FANCA/pericentrin signal at PCM and spindle are shown on the right. Scale bar: 500 nm. SR-SIM images were acquired on Zeiss ELYRA PS.1 super-resolution microscopy system and exported using Imaris imaging suite.

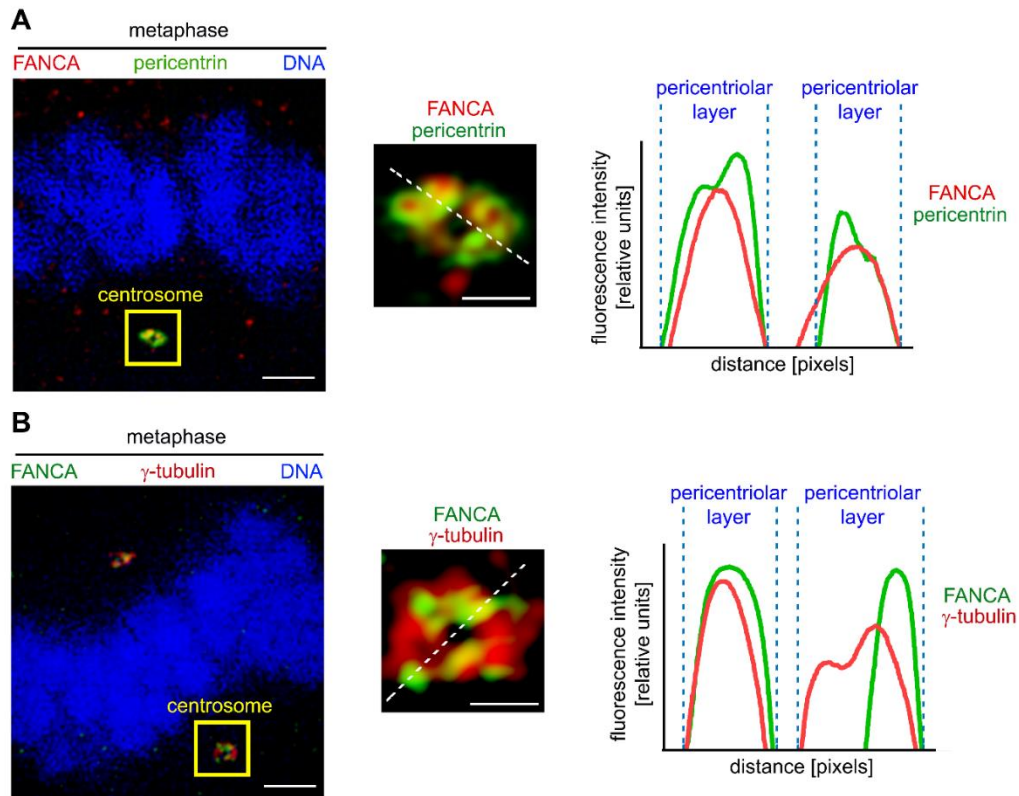


**Figure 10. Endogenous FANCA colocalizes with pericentrin and  $\gamma$ -tubulin during metaphase.** Representative super-resolution SIM images showing colocalization of endogenous FANCA with pericentrin (**A**) and  $\gamma$ -tubulin (**B**) in metaphase HeLa cells. White lines indicate location of fluorescence intensity profiles (right panels). Scale bars: 2  $\mu$ m (left) and 500 nm (right)

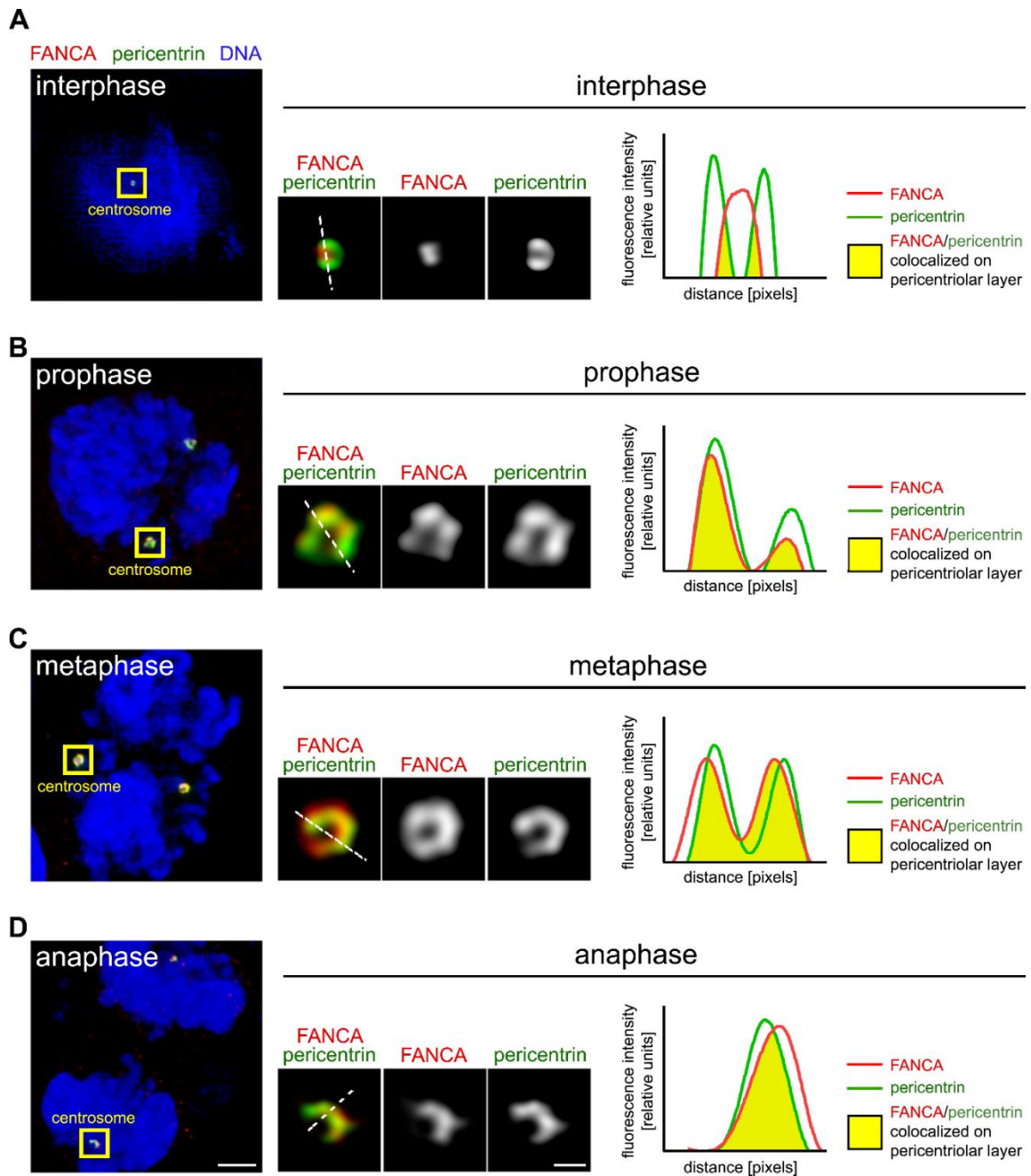


**Figure 11. Profile of FANCA and pericentrin localization profile throughout the cell cycle.** SIM images of HeLa cells stained with antibodies against endogenous FANCA (red) and pericentrin (green) during interphase (**A**), prophase (**B**), metaphase (**C**) and anaphase (**D**). Centrosomes were marked with yellow squares and enlarged in middle panels. FANCA and pericentrin

fluorescence line intensity profiles are depicted for each cell cycle stage. Note high overlap of FANCA and pericentrin peaks on mitotic centrosomes (**B-D**) compared to interphase centrosome (**A**). Scale bars: 3 $\mu$ m (**A-D**, left) and 500nm (**A-D**, right).

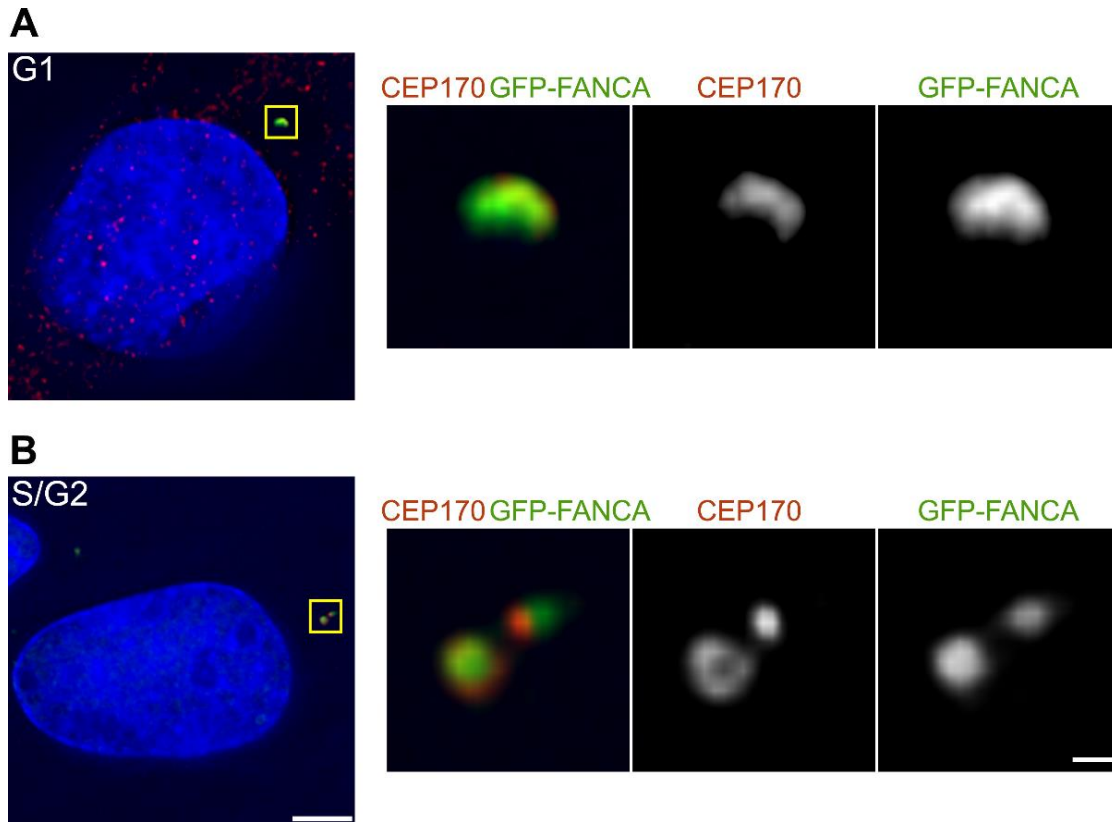


**Figure 12. FANCA localizes to the mother centriole during interphase.** SIM images of primary patient *FANCA*<sup>-/-</sup> fibroblasts stably expressing FANCA-GFP stained with the antibody against the mother centriole marker CEP170 (red) during **(A)** G1 and **(B)** S/G2 cell cycle phases. Hoechst 33342 was used to counterstain DNA. Areas of interest marked with yellow squares are magnified (right panels) to show colocalization of FANCA-GFP and CEP170. Scale bars: 5µm (left) and 500nm (right).

### **Loss of *FANCA* allows escape from SAC arrest and apoptosis.**

The FA/BRCA pathway repairs interphase DNA damage (Chandra et al., 2005; Heinrich et al., 1998) and participates in the spindle assembly checkpoint (SAC) (Nalepa et al., 2013). To examine the fate of *FANCA*-deficient cells upon SAC activation, we employed time-lapse imaging of primary *FANCA*<sup>-/-</sup> and gene-corrected cells treated with taxol, a microtubule-stabilizing chemotherapeutic (**Figure 13**). As described in other cells (Jordan et al., 1996; Woods, Zhu, McQueney, Bollag, & Lazarides, 1995), *FANCA*-corrected, taxol-exposed cells entered prolonged prometaphase arrest followed by cell death without exiting mitosis. *FANCA*<sup>-/-</sup> cells were more likely to escape taxol-induced SAC arrest and generate multinucleated interphase-like cells ( $p=0.0215$ ; **Figure 14A-D**). These findings validate the role of *FANCA* in the SAC and show that loss of *FANCA* facilitates the escape of chromosomally unstable cells from mitotic death caused by unsatisfied SAC (Woods et al., 1995).

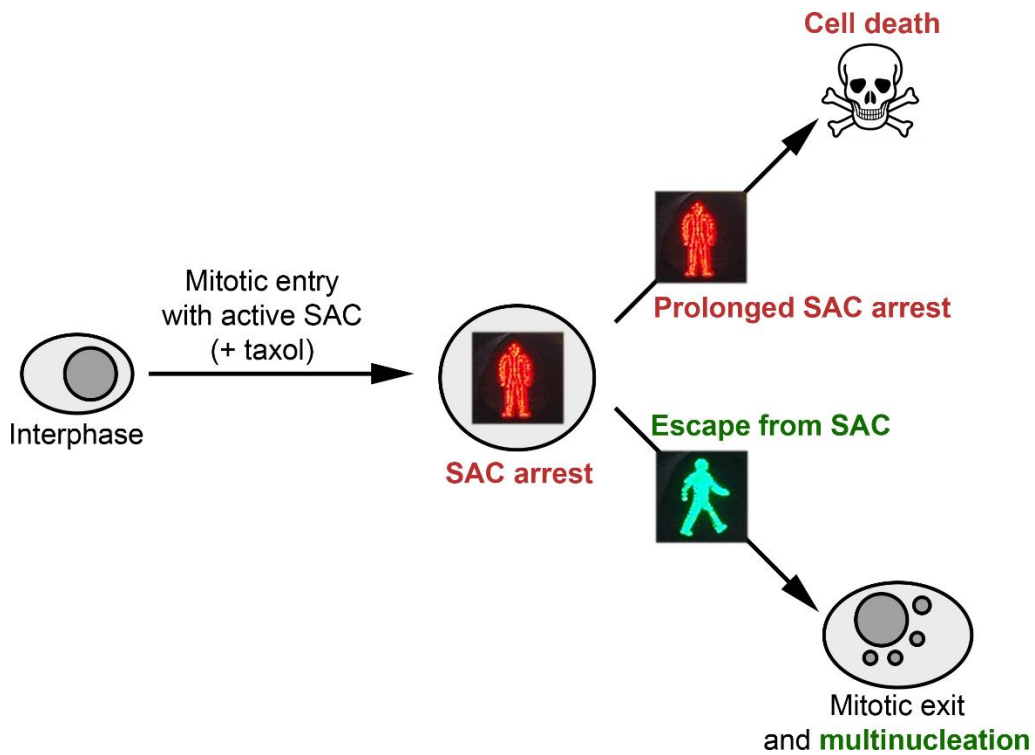


**Figure 13. SAC escape assay schematic.** Prolonged activation of SAC triggers cell death to prevent genomic instability by eliminating cells that cannot satisfy the checkpoint. Escape from SAC followed by erratic chromosome segregation and mitotic exit generates multinucleated cells.

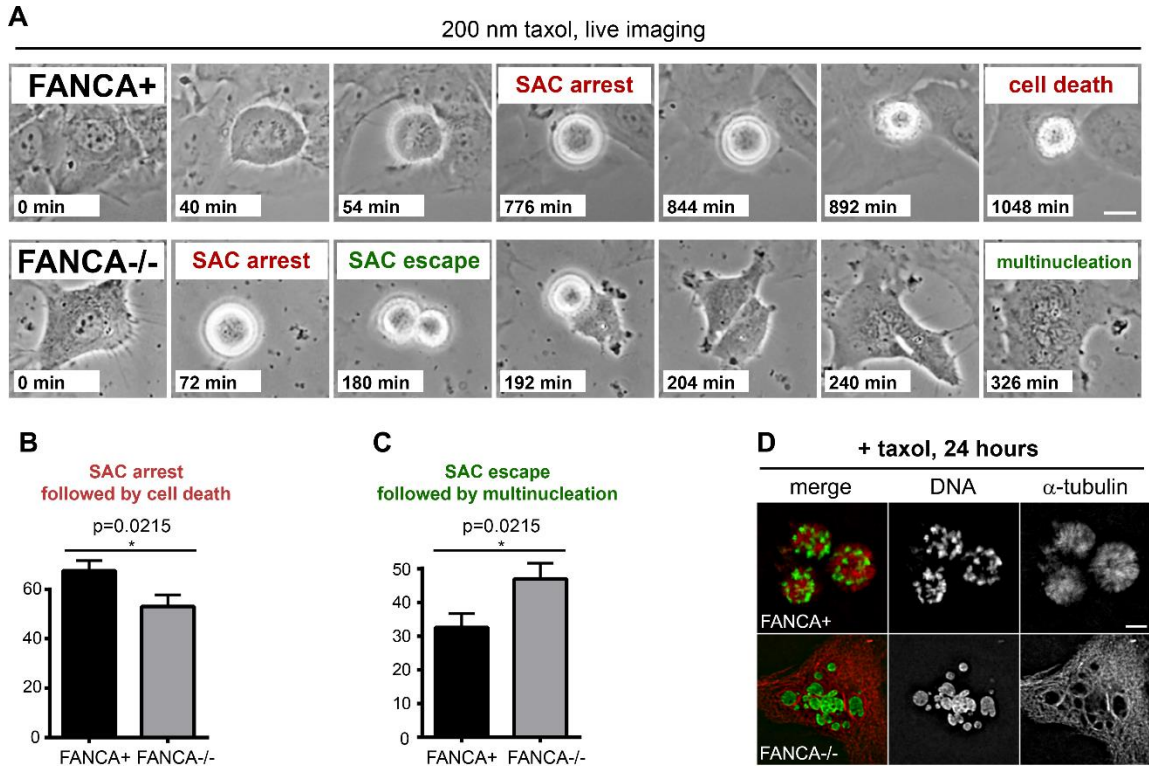


**Figure 14. *FANCA*<sup>-/-</sup> cells escape from taxol-induced SAC arrest. (A)**

Representative time-lapse imaging snapshots of *FANCA*<sup>+</sup> and *FANCA*<sup>-/-</sup> cells exposed to taxol. Note prolonged SAC arrest followed by cell death in gene-corrected cell and escape for SAC followed by cytokinesis failure and multinucleation in *FANCA*<sup>-/-</sup> cell. Scale bar: 15  $\mu$ m. Time from mitotic entry is shown for each frame. Time-lapse phase-contrast frames of cells grown in

DMSO supplemented with 10% FBS at 37°C, 5% CO<sub>2</sub> were acquired every 2 minutes for at least 24 hours on a Nikon Biostation live-imaging system (**B, C**)

Quantification of time-lapse imaging experiments. *FANCA*<sup>-/-</sup> cells are more likely to escape SAC and less likely to be eliminated through SAC-associated death compared to gene-corrected isogenic cells (p=0.0215). Data for 115 mitotic *FANCA*<sup>+</sup> cells and 129 mitotic *FANCA*<sup>-/-</sup> cells (three experimental replicates for



each cell line) were analyzed with two-tailed t-test. See Supplemental Movies 1-2. (D) Prolonged prometaphase arrest in *FANCA*<sup>+</sup> cells and multinucleation in *FANCA*<sup>-/-</sup> cells upon 24-hour exposure to taxol in an independent experiment. Images acquired on an Applied Precision personalDx deconvolution microscope.

### **FANCA<sup>-/-</sup> cells are hypersensitive to taxol.**

A significant fraction of multinucleated cells that escape taxol-induced arrest (Torres & Horwitz, 1998) or form upon failed mitosis (Cuomo et al., 2008; Mikule et al., 2007) is physiologically eliminated to prevent genomic instability (Crasta et al., 2012; Gordon et al., 2012). Complete SAC disruption causes chromosomal instability incompatible with cell survival (Dobles, Liberal, Scott, Benezra, & Sorger, 2000). Thus, we hypothesized that loss of *FANCA* may render cells hypersensitive to taxol.

Since previous studies evaluating response of *FA<sup>-/-</sup>* cells to anti-mitotic chemotherapeutics generated conflicting data (Kim et al., 2013; van der Heijden et al., 2005), we performed rigorous dose-response experiments to thoroughly examine this concept. We found that two separate *FANCA<sup>-/-</sup>* primary patient cell lines harboring different *FANCA* mutations are hypersensitive to taxol; stable *FANCA* expression rescued taxol hypersensitivity in both lines in two independent cell viability assays (**Figure 15A-C, Figures 16-17**). As expected (D'Andrea, 2010; Kottemann & Smogorzewska, 2013), *FANCA<sup>-/-</sup>* cells showed decreased survival upon exposure to the crosslinking agent mitomycin C (MMC) (**Figure 15B-C; Figure 18**). These findings, together with previously published work (Kim et al., 2013), indicate that loss of *FANCA* is synthetically lethal with exposure to anti-mitotic chemotherapeutics.

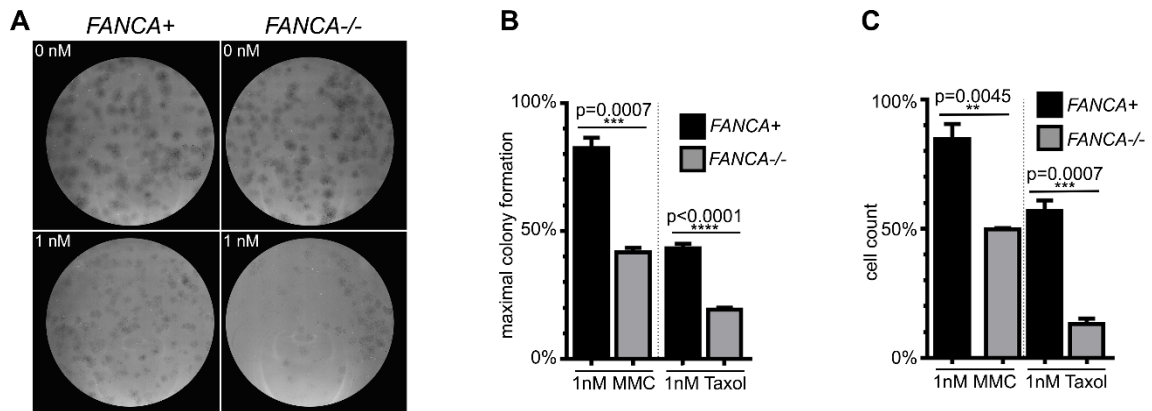


**Figure 15. *FANCA*<sup>-/-</sup> primary patient cells harboring different *FANCA* mutations are hypersensitive to taxol and MMC (A)** Representative colony-forming (CFU) assay plates. Primary *FANCA*<sup>-/-</sup> fibroblasts and *FANCA*<sup>+</sup> fibroblasts (500 cells per 10 cm<sup>2</sup> plate) were exposed to taxol for 11 days. Note decreased colony formation on *FANCA*<sup>-/-</sup> plates exposed to 1 nM of taxol. **(B)** Quantification of the CFU assay shown in **(C)**. *FANCA*<sup>-/-</sup> cells are more sensitive to 1 nM taxol than *FANCA*<sup>+</sup> cells in the CFU assay. 1 nM MMC was used as positive control. **(H)** Direct cell counts confirm that stable expression of *FANCA* rescues both taxol and MMC hypersensitivity of *FANCA*<sup>-/-</sup> patient cells. Two-way ANOVA with Sidak correction was used for data comparison. Data show pooled results of three separate experiments, expressed as the mean ± SEM in triplicates.

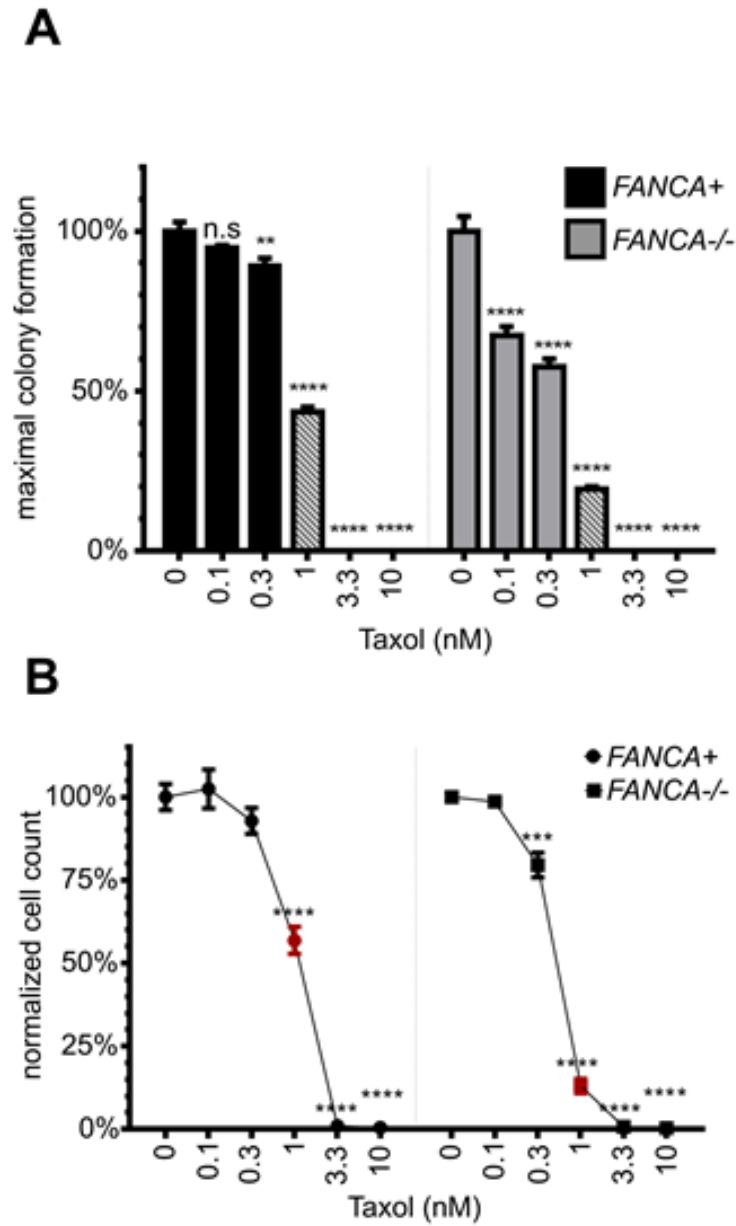


**Figure 16. Taxol dose-response curves of *FANCA*<sup>-/-</sup> and isogenic gene-corrected cells.** *FANCA*<sup>-/-</sup> cells are more sensitive to taxol than *FANCA*<sup>+</sup> cells in CFU assays (**A**) and in manual cell count assays (**B**). Two-way ANOVA with Sidak correction was used for data analysis. Figure shows pooled results of three

separate experiments, expressed as the mean  $\pm$  SEM in triplicates. \* $p \leq .05$ ; \*\* $p \leq .01$ ; \*\*\* $p \leq .001$ ; \*\*\*\* $p \leq .0001$ ; ns: not significant.

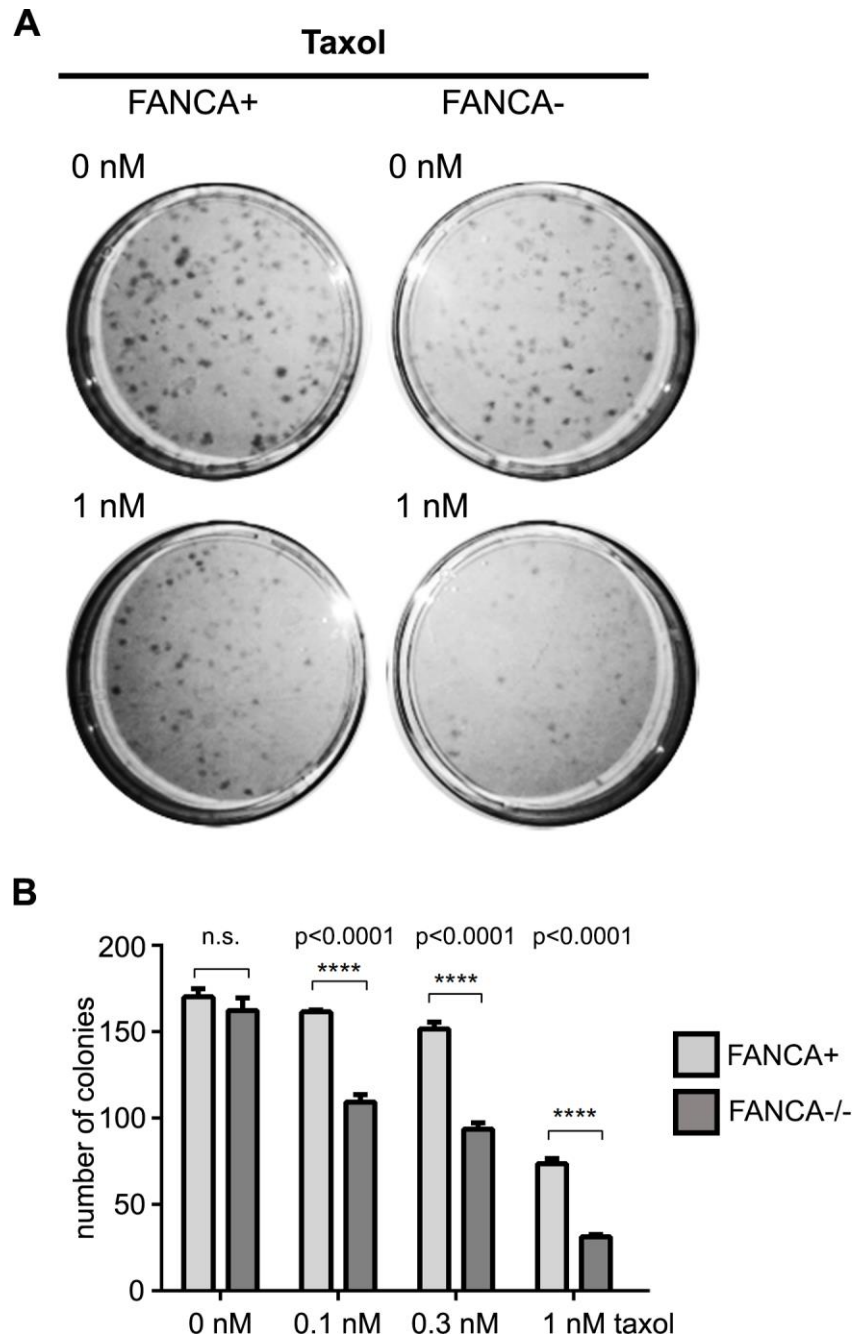


**Figure 17. Validation of taxol hypersensitivity in additional FANCA patient fibroblast cell lines.** Representative plates (**A**) and quantification (**B**) from colony-forming unit (CFU) assay in which *FANCA*<sup>+</sup> fibroblasts (patient line RA885) were exposed to low-dose taxol for 11 days. Error bars represent mean

+/- SEM, and a two-way ANOVA with Sidak correction was used to assess statistical significance.

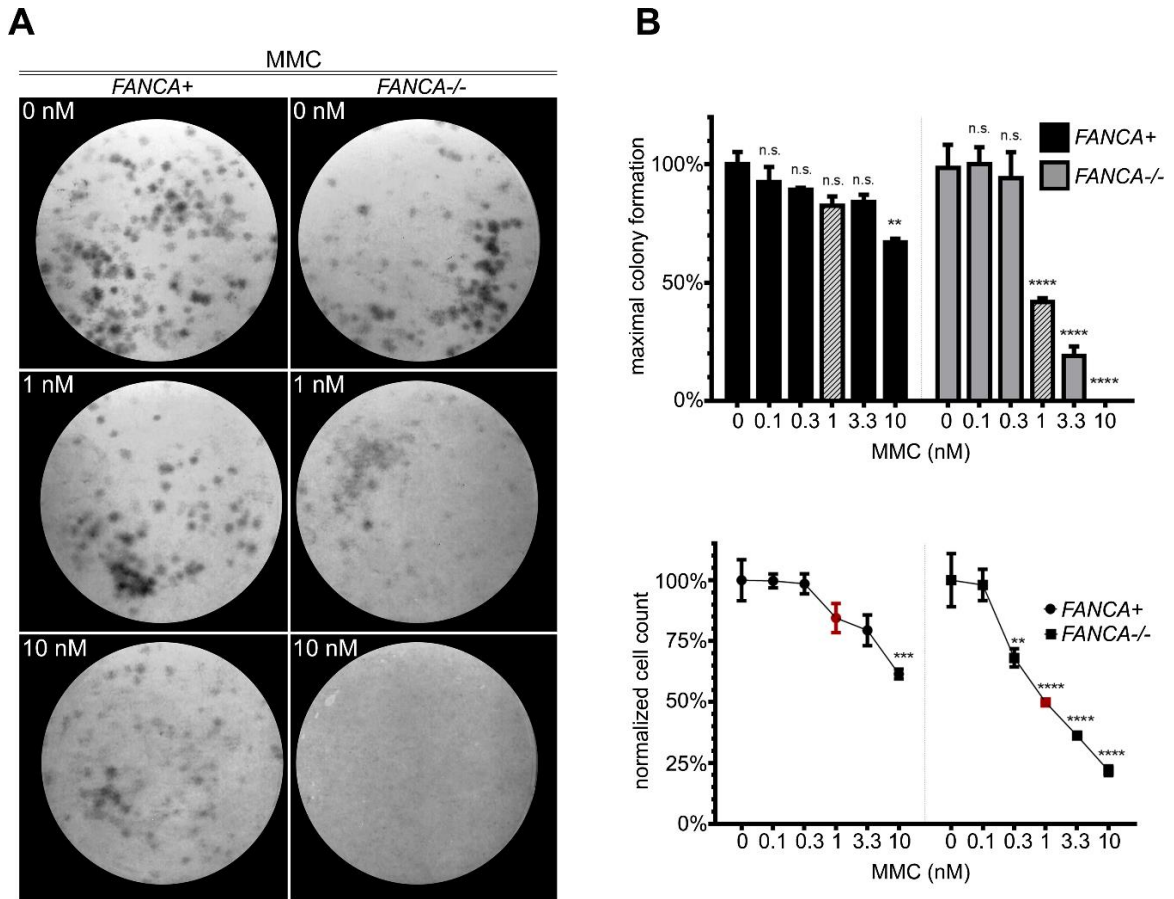


**Figure 18. Rescue of mitomycin C (MMC) hypersensitivity by *FANCA* gene correction in primary *FANCA*<sup>-/-</sup> patient cells. (A) Representative CFU assay plates of *FANCA*<sup>-/-</sup> or gene-corrected fibroblasts treated with indicated concentrations of MMC. (B) Normalized colony forming ability (top) of *FANCA*<sup>+</sup> or *FANCA*<sup>-/-</sup> fibroblasts treated with indicated concentrations of MMC for 11 days. (C) Cell count assay (bottom) of *FANCA*<sup>+</sup> and *FANCA*<sup>-/-</sup> fibroblasts. 6-well plates were seeded with  $1 \times 10^5$  cells/well and treated with indicated doses of MMC for 9 days. Cell counts were manually performed using a hemacytometer. Two-way ANOVA with Sidak correction was used for data comparison. Quantitation of data is representative of three separate experiments and results**



are shown as mean  $\pm$  SEM. \* $p \leq .05$ ; \*\* $p \leq .01$ ; \*\*\* $p \leq .001$ ; \*\*\*\* $p \leq .0001$ ; ns: not significant.

**Chemotherapy-exposed *FANCA*<sup>-/-</sup> cells develop distinct patterns of genomic instability due to separate interphase and mitotic checkpoint abnormalities.**

Having established the hypersensitivity of *FA*<sup>-/-</sup> cells to interphase DNA crosslinkers and anti-mitotic agents, we wanted to understand how loss of *FANCA* confers hypersensitivity to these separate classes of chemotherapeutics. Thus, we examined cell cycle and patterns of genomic instability in primary *FANCA*<sup>-/-</sup> and gene-corrected cells at baseline (**Figure 19**) and upon treatment with sublethal doses of MMC and taxol. We selected drug doses that decreased growth of *FANCA*<sup>-/-</sup> cells compared to isogenic *FANCA*<sup>+</sup> cells without fully arresting *FANCA*<sup>-/-</sup> cells or inducing cell death evidenced by increased sub-G1 fraction on flow cytometry (**Figure 20A** and not shown).

Prolonged treatment with 1 nM MMC reduced growth of *FANCA*<sup>-/-</sup> cells due to persistent activation of the G2/M checkpoint ( $p=0.0376$ ) reflected by decreased DNA replication ( $p<0.0001$ ) and decreased G1 fraction ( $p=0.0029$ ) (**Figure 20A-D**). This observation is consistent with the exaggerated MMC-induced G2/M arrest of *FA* cells due to the DDR failure (Chandra et al., 2005; Heinrich et al., 1998). In further support of this notion, exposure to low-dose MMC increased multinucleation due to DNA breakage ( $p=0.0223$ ) but not chromosome missegregation (**Figure 20F-H**). Sublethal taxol exposure affected *FANCA*<sup>-/-</sup> cells differently. Prolonged treatment with low-dose taxol (but not MMC) significantly decreased the mitotic fraction of *FANCA*<sup>-/-</sup> cells compared to gene-

corrected cells (**Figure 20I-J**,  $p < 0.0001$ ) consistent with impaired SAC (**Figure 15**). Furthermore, low-dose taxol increased multinucleation of *FANCA*<sup>-/-</sup> patient cells ( $p = 0.002$ ) secondary to mitotic chromosome missegregation ( $p < 0.0001$ ) as well as chromosome breakage ( $p = 0.0059$ ) (**Figure 20K-M**). Interestingly, multinucleated cells continued to enter S-phase (**Figure 21**) (Crasta et al., 2012; C. Z. Zhang et al., 2015).

In summary, these results (i) provide evidence that both impaired DDR and error-prone mitosis contribute to chromosomal instability in *FANCA*<sup>-/-</sup> cells *in vivo* and *ex vivo*, (ii) offer insights into the role of FA pathway in the response to DNA-crosslinking agents and anti-mitotic chemotherapeutics, and (iii) open potential new inroads towards synthetic lethal chemotherapy against FA-deficient cancers.

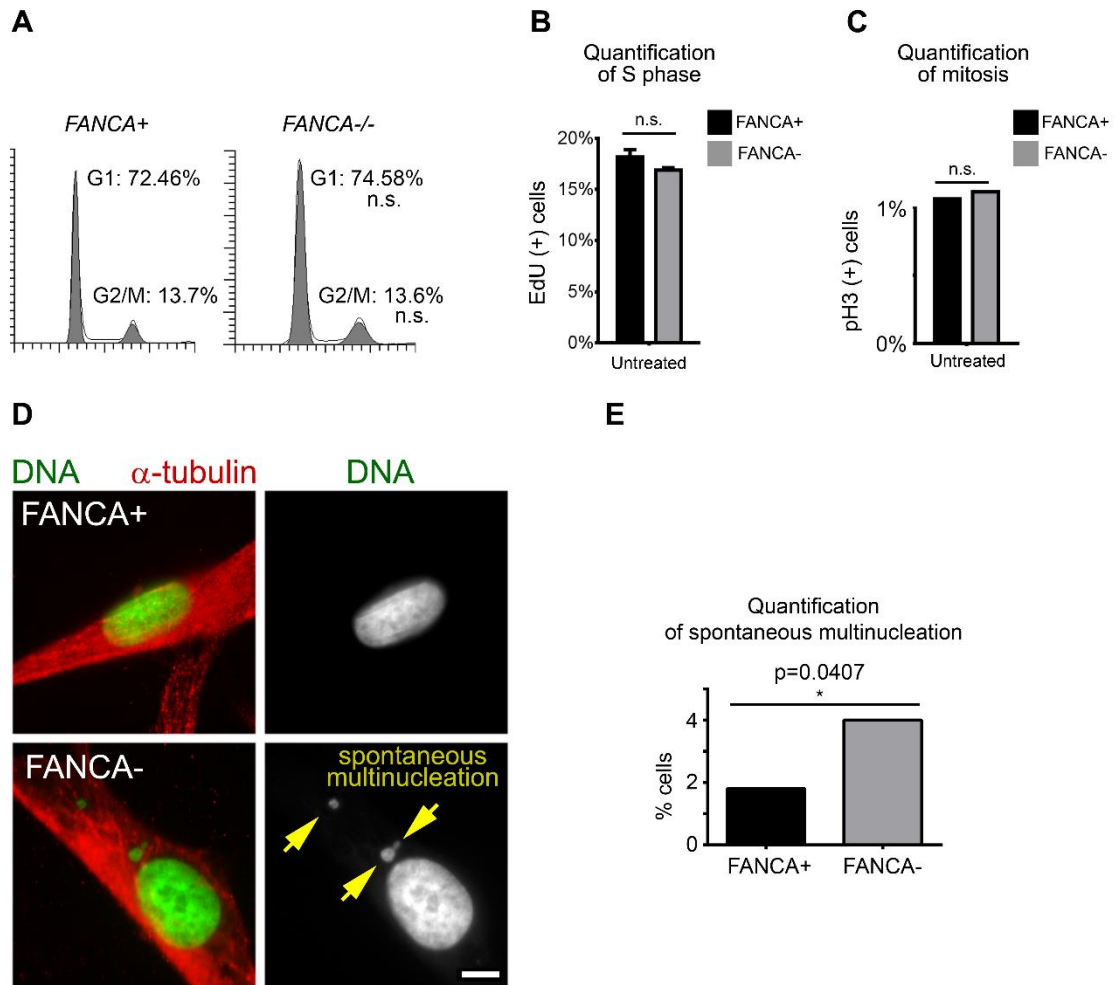
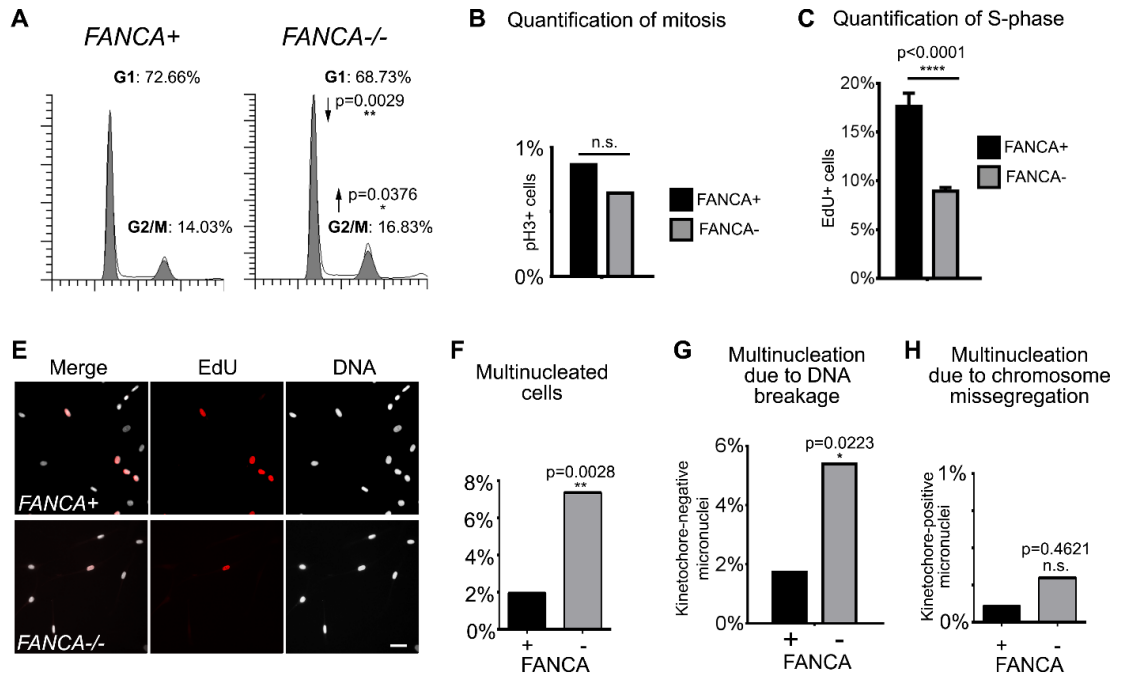


**Figure 19. Baseline cell cycle evaluation in *FANCA*<sup>-/-</sup> fibroblasts and *FANCA*-corrected isogenic cells.** *FANCA*<sup>-/-</sup> fibroblasts do not show significant differences in G1 or G2/M cell cycle fractions quantified by PI flow cytometry (**A**), S-phase fraction quantified by EdU incorporation via microscopy (**B**) and phospho-H3+ mitotic fraction quantified by flow cytometry (**C**) compared to isogenic gene-corrected cells. Increase in spontaneous micronucleation (**D-E**) is consistent with previous studies (Nalepa et al., 2013). Representative deconvolution microscopy images of cells of indicated genotypes are shown; scale bar=6  $\mu$ m. To quantify incidence of micronucleation, at least 500 cells/genotype were imaged via deconvolution microscopy as z-stacks spanning

whole cells and results were analyzed with Fisher's exact test. For flow cytometry analysis, data generated in 3 independent experiments were pooled and compared with two-tailed t-tests. EdU incorporation counts were compared via two-way ANOVA with Sidak's multiple comparisons test.

1 nM MMC for 9 days



1 nM taxol for 9 days

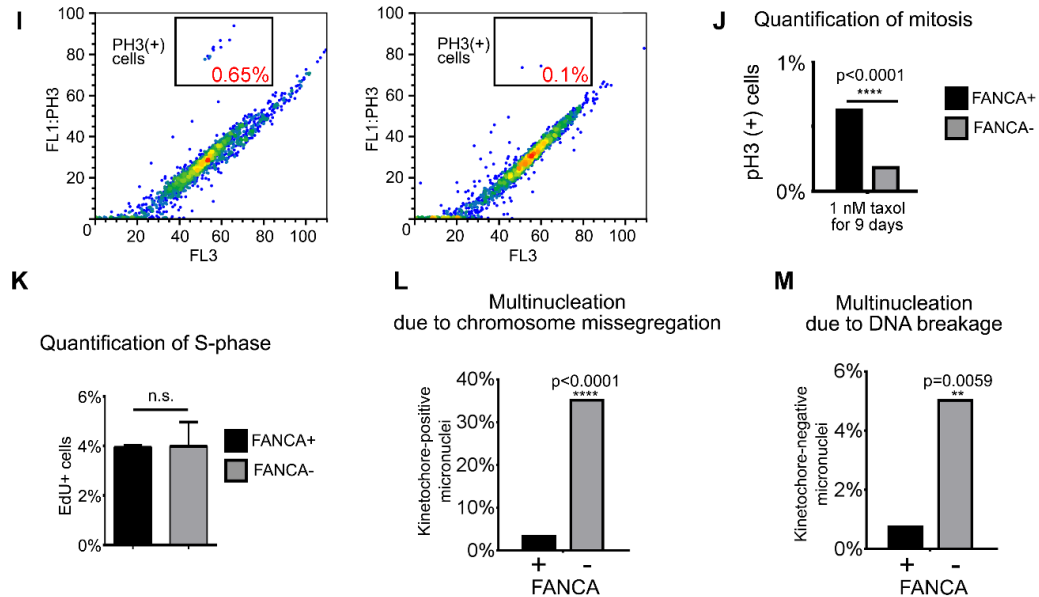


**Figure 20. *FANCA*<sup>-/-</sup> cells exposed to genotoxic stressors develop genomic instability through a combination of interphase and mitotic checkpoint abnormalities. (A)** Prolonged activation of the G2/M checkpoint in *FANCA*<sup>-/-</sup> cells grown in low-dose MMC for 9 days. **(B)** No difference in mitotic cell fraction

between MMC-treated *FANCA*<sup>-/-</sup> and *FANCA*<sup>+</sup> cells indicates that the increased *FANCA*<sup>-/-</sup> G2/M fraction shown in **(A)** reflects G2 arrest prior to mitotic entry. **(C, D)** DNA replication arrest in *FANCA*<sup>-/-</sup> cells exposed to 1 nM MMC is rescued by *FANCA* gene correction. S-phase cells were labeled red by EdU incorporation. **(E, F, G)** Increased multinucleation due to DNA breakage, but not chromosome missegregation, in *FANCA*<sup>-/-</sup> cells grown in low-dose MMC. **(H, I)** Flow cytometry shows decreased fraction of mitotic cells in *FANCA*<sup>-/-</sup> cells exposed to sublethal dose of taxol. **(J, K)** Treatment with taxol increases chromosome segregation errors and chromosome breakage in *FANCA*<sup>-/-</sup> cells. **(L)** Compound interphase and mitotic origins of genomic instability in FA-deficient cells (see text for discussion). Exponential accumulation of DNA damage may result in activation of cell cycle arrest/apoptosis (bone marrow failure) or malignant transformation (leukemia and solid tumors). All flow cytometry data represent pooled 3 replicates for each cell line and condition compared with two-tailed t-test. EdU incorporation counts were compared via two-way ANOVA with Sidak's multiple comparisons test.

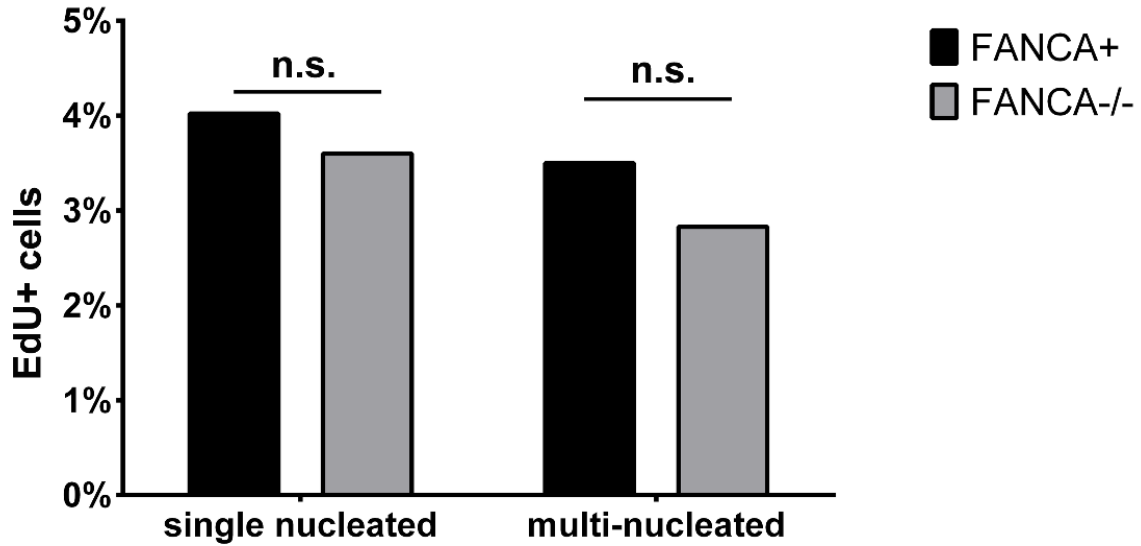


**Figure 21. Continued DNA replication in multi-nucleated *FANCA*<sup>-/-</sup> and gene-corrected cells.** *FANCA*<sup>-/-</sup> fibroblasts and isogenic *FANCA*-corrected cells were treated with 1 nM taxol for 9 days to induce multi-nucleation. Then, DNA replication in single-nucleated and multi-nucleated cells was quantified in EdU incorporation assays as shown on Figure 7. Multi-nucleated cells continue to replicate DNA upon abnormal mitotic exit, which may promote further accumulation of DNA damage in interphase-like multinucleated cells (Crasta et al., 2012; C. Z. Zhang et al., 2015). The frequency of S-phase entry in multinucleated cells is not *FANCA*-dependent ( $p=1$ ; Fisher's exact test;  $n=551$  *FANCA*<sup>-/-</sup> cells and 379 *FANCA*-corrected cells were analyzed).



## Discussion

Disrupted FA/BRCA signaling causes genomic instability and cancer. The FA/BRCA tumor suppressor network orchestrates interphase DDR and DNA replication (D'Andrea, 2010; Kottemann & Smogorzewska, 2013). Multiple lines of evidence implicated FA/BRCA signaling in centrosome maintenance and mitotic checkpoints (Kim et al., 2013; Naim & Rosselli, 2009a; Nalepa et al., 2013; Vinciguerra et al., 2010; Zou et al., 2013; Zou et al., 2014), but the *in vivo* importance of these findings is unknown. We found that both abnormal interphase and error-prone mitosis significantly contribute to the *in vivo* hematopoietic genomic instability in FA<sup>-/-</sup> humans, suggesting a role for the FA/BRCA network in genome surveillance throughout the cell cycle (**Figure 20**).

FANCA<sup>-/-</sup> patients' hematopoiesis is afflicted by mitotic errors. Lagging chromosomes due to an *in vivo* SAC impairment (Nalepa et al., 2013) and persistent anaphase/telophase bridges (Chan et al., 2009; Naim & Rosselli, 2009a) occur with increased frequency in FANCA<sup>-/-</sup> patients (**Figure 4**). In agreement with the work from the D'Andrea group (Vinciguerra et al., 2010), binucleated hematopoietic cells (**Figure 4**) are signs of faulty cytokinesis. The onset of FA-associated mitotic abnormalities precedes the MDS/AML (**Figure 4**), suggesting that impaired mitosis may contribute to carcinogenesis in FA. Indeed, FISH analysis detected chromosomally unstable clones in 15% of FA patients with morphologically normal marrows (Mehta et al., 2010), and gross chromosomal instability is a hallmark of MDS/AML in FA (Quentin et al., 2011).

More research is needed to quantify the impact of haphazard mitosis on FA-associated myelodysplasia and cancer.

The irregular mitosis during FA<sup>-/-</sup> hematopoiesis is a consistent but relatively rare event (**Figures 4-5**). Further, while multinucleated cells with centrosome clusters are easily seen in FA-deficient cancer cells (Nalepa et al., 2013), multinucleation in FA<sup>-/-</sup> primary cells is more subtle (**Figures 5-7**) (Nalepa et al., 2013), perhaps because cancers cannot eliminate mis-dividing cells through backup checkpoints. Indeed, centrosome abnormalities induce TP53-dependent cell cycle arrest (Mikule et al., 2007) and apoptosis (Cuomo et al., 2008), and activation of TP53 contributes to BMF in FA (Ceccaldi et al., 2012). TP53 inactivation boosts hematopoiesis but promotes MDS/AML in FA (Ceccaldi et al., 2011), and AML with bizarre karyotype instability occurred in an FA patient with somatic loss of heterozygosity of the TP53-harboring region of chromosome 17 (Woo et al., 2011). Thus, aneuploidy and centrosome disruption upon inactivation of the FA/BRCA signaling may trigger TP53-dependent checkpoints to limit the risk of leukemia at the cost of BMF.

The role of FANCA in mitosis is not clearly defined. Impaired FA signaling promotes accumulation of centrosomes due to DDR-induced centrosome over-replication (Zou et al., 2013; Zou et al., 2014) and deregulated mitosis (Nalepa et al., 2013; Vinciguerra et al., 2010). Supernumerary centrosomes promote chromosomal instability through multiple mechanisms (Ganem et al., 2009;

Gordon et al., 2012). We found that FANCA regulates centrosome-associated spindle assembly (**Figure 8**), and FANCA shuttles from centrioles to the PCM spindle attachment sites at mitotic entry (**Figures 8-9**). Dissecting FANCA-dependent mitotic centrosome-microtubule-kinetochore interactions in more detail will help understand how FANCA regulates the SAC (Nalepa et al., 2013). We hypothesize that functional and numerical centrosome abnormalities in FA-deficient cells may further promote chromosomal instability by promoting merotelic kinetochore attachment to spindle microtubules; this mechanism of genomic instability has been elucidated in non-FA cells acquiring supernumerary centrosomes (Ganem et al., 2009; Nam, Naylor, & van Deursen, 2015). Interestingly, as mentioned in the introduction of the thesis, FANCA is phosphorylated by the NIMA-related kinase 2 (NEK2) (Kim et al., 2013) and AKT kinase (Otsuki et al., 2002); FANCI and FANCD1 may regulate polo-like kinase 1 (PLK1) (Zou et al., 2013; Zou et al., 2014), which is essential for spindle function (Sumara et al., 2004); and FANCC binds the key mitotic cyclin-dependent kinase 1 (CDK1) (Kupfer et al., 1997), which co-immunoprecipitates with the FA core complex (Thomashevski et al., 2004). Moreover, loss of FANCA is synthetic lethal with PLK1 knockdown (Kennedy et al., 2007) and CDK inhibitors disrupt IR-induced formation of FANCD2 foci (Jacquemont, Simon, D'Andrea, & Taniguchi, 2012). Future work will examine these pathway connections to evaluate their translational relevance in cancer and FA.

We found that loss of FA signaling is synthetically lethal with taxol exposure, highlighting the role of FA-dependent SAC in cell survival. Kim *et al* observed hypersensitivity of *FANCA*-knockdown cells to nocodazole (Kim et al., 2013). Taxol and nocodazole are mechanistically different (Maresca & Salmon, 2010): nocodazole disrupts spindle-kinetochore attachment, while taxol renders the attached microtubules unable to stretch the kinetochores. Since the FA pathway is essential for taxol- and nocodazole-induced SAC (Nalepa et al., 2013), *FANCA* may regulate SAC by intra-kinetochore tension.

Of note, others have found that *FANCG/FANCC*-deficient pancreatic cancer cells exposed to taxol accumulate DNA at similar rate as gene-corrected cells in *in vitro* fluorescence assays (van der Heijden et al., 2005), and concluded that FA-/- cells are not hypersensitive to antimitotics. However, FA-/- cells multinucleate (**Figure 14**) (Kim et al., 2013; Nalepa et al., 2013) and replicate (**Figure 21**) upon exposure to antimitotics, suggesting why cell growth assays quantify taxol response with better specificity than total DNA measurements. Interestingly, low-dose taxol promotes chromosome missegregation and DNA breaks in *FANCA*-/- cells. Consistent with this notion, the Pellman group demonstrated that micronuclei produced by mitotic errors undergo excessive mutagenesis (Crasta et al., 2012) with secondary chromosome breakage (C. Z. Zhang et al., 2015) due to erratic replication. The micronucleus-associated chromosome breakage may be further exacerbated by failed DDR in *FANCA*-/- micronuclei.

Micronucleation has been noted in FA for decades (Barton et al., 1987; Willingale-Theune et al., 1989), but it was unclear whether it reflects interphase abnormalities or erratic mitoses. We addressed this question with quantitative high-resolution-imaging-based micronucleation assays validated in previous studies (Fenech, 2007). Given the key role of FA signaling in interphase (D'Andrea, 2010; Kottemann & Smogorzewska, 2013), we addressed whether kinetochore-containing micronuclei are not simply a product of impaired DDR. Importantly, DNA-crosslinking agent (MMC) produced “DNA breakage” micronuclei but not “chromosome missegregation” micronuclei (**Figure 20F-G**), confirming the assay specificity and sensitivity in distinguishing interphase from mitotic errors. Thus, we conclude that genomic instability results from DNA breakage and chromosome missegregation in multiple FA<sup>-/-</sup> hematopoietic and non-hematopoietic cell types (**Figures 4-5**). Based on these and other findings (Nalepa et al., 2013), we propose that FANCA deficiency causes genomic instability through a dual mechanism of impaired interphase DDR/replication and defective mitosis (Nalepa & Clapp, 2014) (**Figure 20L**). This model explains the FA-associated patterns of genetic instability and hypersensitivity to both DNA-crosslinkers and antimetabolites. Interphase errors exacerbate mitotic abnormalities and mitotic failure promotes interphase mutagenesis. Chromatid remnants generated through impaired DDR or replication are randomly segregated in mitosis. Defective midbody constriction (Mondal et al., 2012) and cytokinesis (Vinciguerra et al., 2010) may shatter lagging chromosomes resulting from impaired SAC(Choi et al., 2012; Nalepa et al., 2013) and break unresolved

anaphase bridges(Chan et al., 2009; Naim & Rosselli, 2009a). After mitotic exit, cells may attempt to repair splintered DNA through chromothripsis, the mutagenic process of randomly reconnecting chromosome fragments via non-homologous end joining (NHEJ) (Forment, Kaidi, & Jackson, 2012; Maher & Wilson, 2012; C. Z. Zhang, Leibowitz, & Pellman, 2013). Since FA<sup>-/-</sup> cells favor error-prone NHEJ over homologous recombination (Adamo et al., 2010), chromothripsis may have a particularly detrimental impact on genomic stability upon loss of the FA/BRCA network.

Our observations unveil the translational importance of mitotic defects caused by loss of FA/BRCA signaling. Somatic disruption of FA/BRCA genes occurs in malignancies in non-FA patients, including leukemia (Hess et al., 2008; M. Tischkowitz et al., 2003; M. D. Tischkowitz et al., 2004; Xie et al., 2000), cervical (Narayan et al., 2004), ovarian (Olopade & Wei, 2003; Taniguchi et al., 2003; Z. Wang, Li, Lu, Zhang, & Wang, 2006), breast (Wei et al., 2008), bladder (Neveling et al., 2007) and lung cancers (Marsit et al., 2004). Our analysis of the COSMIC (Forbes et al., 2015) database revealed multiple cancer-associated *FANCA*-inactivating mutations in non-FA patients (**Figure 22**). Since FA<sup>-/-</sup> cells are hypersensitive to antimetotics, future preclinical studies will determine whether targeting mitosis can be employed in FA-deficient cancers. This strategy may complement other evidence-driven precision medicine efforts against FA<sup>-/-</sup> cancers, such as targeting PARP-dependent DNA repair pathways (Bryant et al., 2005; Ceccaldi et al., 2015; Farmer et al., 2005), DNA damage kinases (C. C.

Chen, Kennedy, Sidi, Look, & D'Andrea, 2009) and selective use of crosslinkers (Jacquemont et al., 2012; Taniguchi et al., 2003).

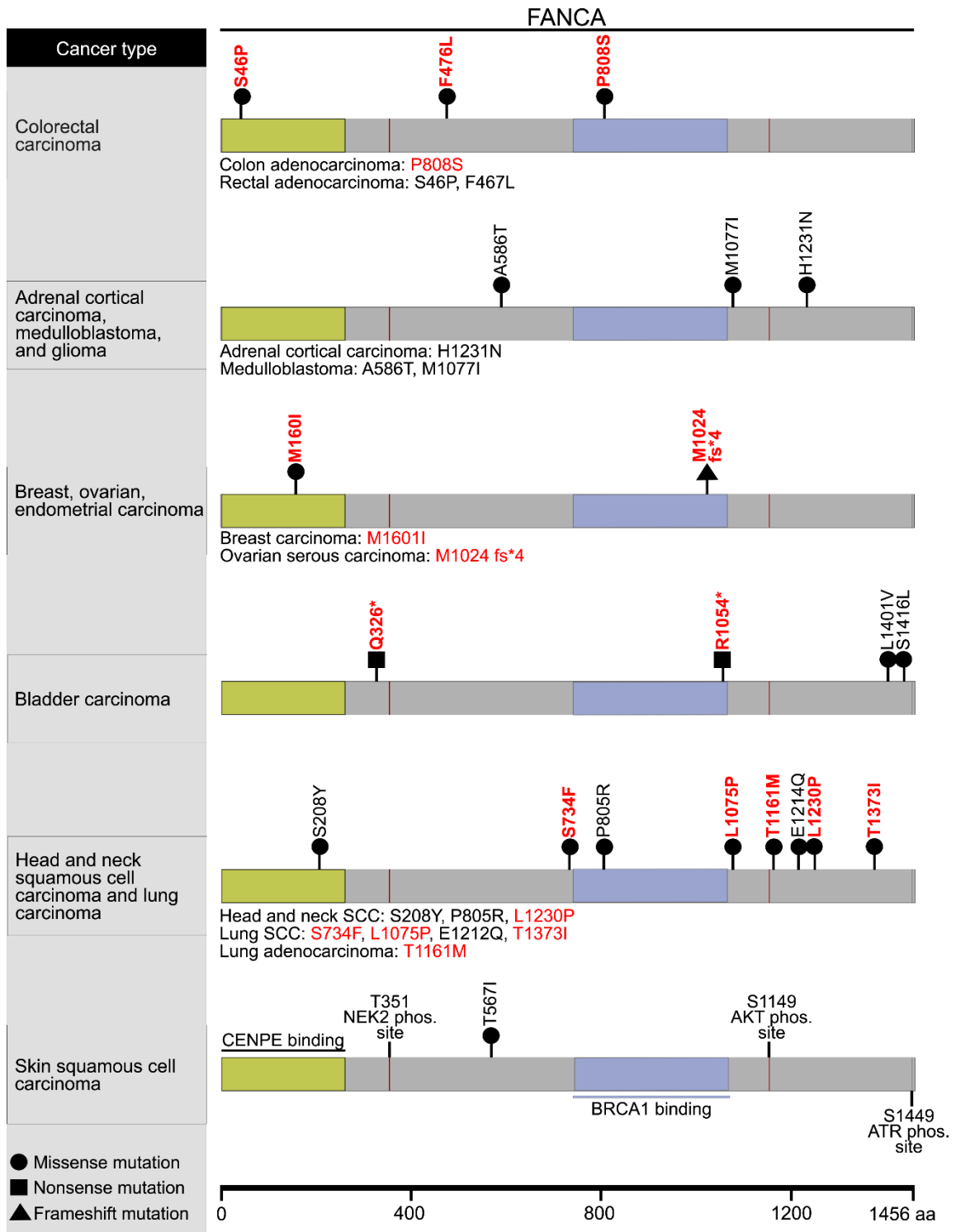


**Figure 22. Somatic mutations of *FANCA* in human malignancies.** Tumor samples harboring amino acid alterations resulting from confirmed missense (black circle), nonsense (black square), and frameshift gene mutations (black



triangle) in coding regions of *FANCA* are shown. Mutations that are predicted to adversely affect protein function are formatted in bold red, while mutations unlikely to affect protein function are shown in black. Cancers associated with indicated gene mutations are shown on the left. Protein binding and phosphorylation sites of *FANCA* are shown at the bottom. SCC: squamous cell carcinoma; \*= nonsense mutation; fs\*4=frame shift that causes a translation stop four amino acids after the insertion.

## CHAPTER FOUR

### FANCA MAINTAINS THE SAC THROUGH REGULATING BUBR1 ACETYLATION

#### **Introduction**

Fanconi Anemia (FA) is a genetic syndrome, characterized by progressive bone marrow failure and cancer predisposition, caused by bi-allelic mutations in one of 21 FA genes. Acquired somatic mutations in FA genes, such as *FANCA*, have been shown to result in AML and solid tumors in the general population (Nalepa G., *Nature Reviews*, 2017). FA pathway is well known for its role in orchestrating the DNA damage response (DDR) during interphase (D'Andrea, 2010; Kottmann & Smogorzewska, 2013). Recent work suggests perturbed mitotic processes, including spindle assembly checkpoint (SAC), to result in genomic instability upon loss of FA signaling (Nalepa et al., 2013; Vinciguerra et al., 2010). The SAC, a phosphosignaling network which includes tumor suppressor genes budding uninhibited by benzimidazoles 1 (BUB1) and budding uninhibited by benzimidazoles 1 Beta (BUBR1), ensures proper chromosomal segregation during mitosis. However, the mechanistic understanding for the cooperation between the SAC and FA signaling pathways remains unknown. Our data reveals that *FANCA*-deficient cells depend on SAC proteins, BUB1 and BUBR1, for their survival. More importantly, we showcase the BUBR1 signaling axis to serve as the common denominator between the SAC kinase network and the FA pathway. Our results not only suggest *FANCA* to play an important role in

regulating SAC proteins but also establish the dynamic role of FANCA during mitosis.

## Results

### Loss of FANCA is synthetic lethal with knockdown of mitotic SAC protein kinases

We have previously reported weakened SAC upon loss of FA signaling (**Figure 23 A-B, Figure 24, Figure 14**, (Nalepa et al., 2013)). The strength of SAC can also be assessed through live imaging (**Figure 25**). Here, we observed significantly decreased nuclear envelope breakdown to anaphase onset time in *FANCA* deficient primary patient fibroblasts (*FANCA*<sup>-/-</sup>) compared to *FANCA*-corrected primary patient fibroblasts (*FANCA*<sup>+</sup>) (**Figure 25B**). This faster mitotic exit is supported by decreased levels of mitotic markers, such as CCNB1 and Cdc20 in mitotically enriched *FANCA*<sup>-/-</sup> cells (**Figure 24A and B**). However, the molecular underpinnings between the FA pathway and SAC remain unknown. To interrogate the relationship between FA and SAC pathways in an unbiased fashion, we employed a kinome-wide synthetic lethality shRNA screen. *FANCA*<sup>-/-</sup> and *FANCA*<sup>+</sup> were transduced with a kinome viral library containing 5000 shRNAs targeting 512 protein kinases (**Figure 26**). Kinases targeted with at least one shRNA with a 5-fold copy number change between *FANCA*<sup>+</sup> and *FANCA*<sup>-/-</sup> cells were deemed significant (**Figure 26**). Bioinformatics program was used to categorize the significant kinases into relevant cellular pathways (**Figure 27**) that are depicted as a schematic showcasing the signaling networks that may be dysregulated in *FANCA*<sup>-/-</sup> cells (**Figure 28**). *FANCA*<sup>-/-</sup> cells were hypersensitive to silencing of DDR genes, such as *ATR*, *CHK1* and *CDK12*, which serves as

internal validation for our experimental approach. *FANCA*<sup>-/-</sup> cells were also hypersensitive to loss of kinases implicated in stress response, growth factor signaling, and cell cycle. Importantly, the screen identified genes implicated in mitotic processes, such as SAC, chromosome segregation and centrosome maintenance, to be essential for survival of *FANCA*<sup>-/-</sup> fibroblasts (**Figure 27**).

To confirm our findings and the validity of our screen, we tested whether clinically approved small molecule inhibitors, which target kinases that meet significance criteria from the screen, would selectively affect *FANCA*<sup>-/-</sup> cell survival compared to their gene-corrected counterparts. Indeed, colony forming unit-fibroblast (CFUF) assay (**Figure 29A**) revealed that *FANCA*<sup>-/-</sup> cells were hypersensitive to MK8776 (CHK1 inhibitor), Volasertib (PLK1 inhibitor) and Roscovitine (pan-CDK inhibitor) (**Figure 29B**). Next, we used screen-independent shRNAs targeting SAC kinases, BUB1 and BUBR1 (**Figure 30A-C**). Indeed, decreased CFUF formation was noted in *FANCA*<sup>-/-</sup> cells compared to *FANCA*<sup>+</sup> cells upon loss of BUB1 and BUBR1 (**Figure 30B-D**). We show that silencing cell cycle-specific kinases results in selective death of *FANCA*<sup>-/-</sup> cells.

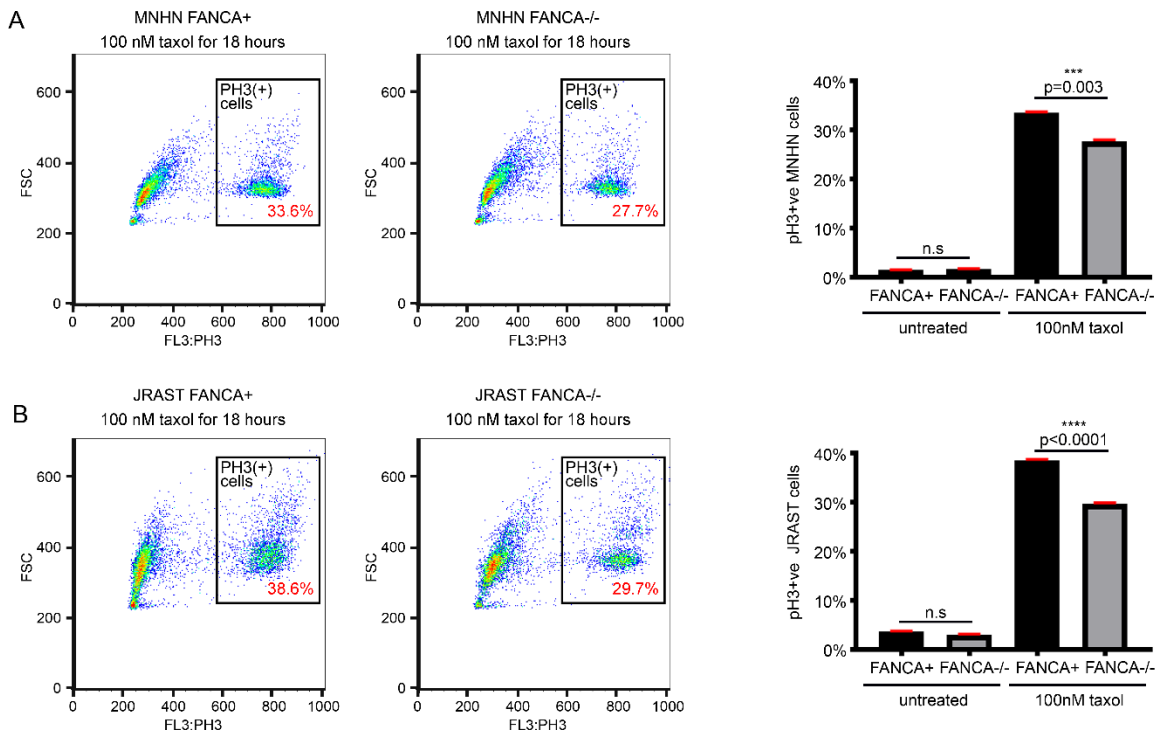


**Figure 23. Loss of *FANCA* results in escape from SAC.** Decreased fraction of mitotic cells are noted in *FANCA*<sup>-/-</sup> MNHN (A) and JRAST (B) fibroblasts exposed to 100 nM taxol compared to *FANCA*-corrected JRAST and MNHN fibroblasts via flow cytometry. No difference was observed in untreated fibroblasts. Flow cytometry data represents three replicates for each cell line and condition, which were analyzed with two-tailed student's t test.

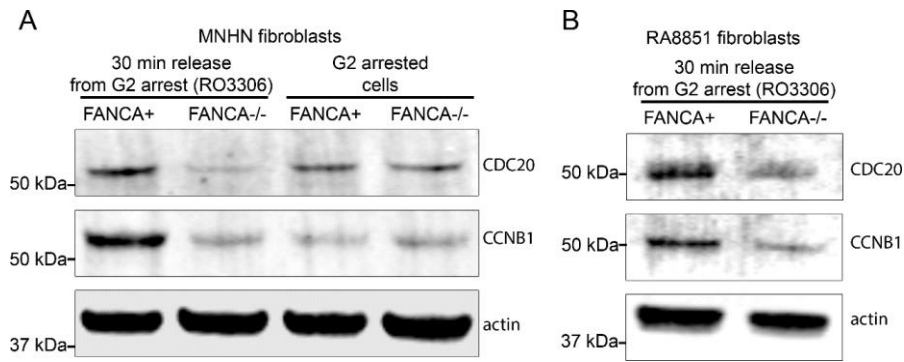


**Figure 24. Decreased CDC20 and CCNB1 levels upon loss of *FANCA*.** (A) Expression of CDC20 and CCNB1 proteins in *FANCA*<sup>-/-</sup> MNHN fibroblasts is decreased following 30-minute release from RO-3306 G2 arrest when compared to *FANCA*<sup>+</sup> counterparts. No significant difference is observed in CDC20 and CCNB1 levels in RO-3306 G2 arrested cells. (B) Western blot showing decreased CDC20 and CCNB1 protein levels in *FANCA*<sup>-/-</sup> RA8851 fibroblasts compared to *FANCA*<sup>+</sup> cells released from RO-3306-mediated G2 arrest.

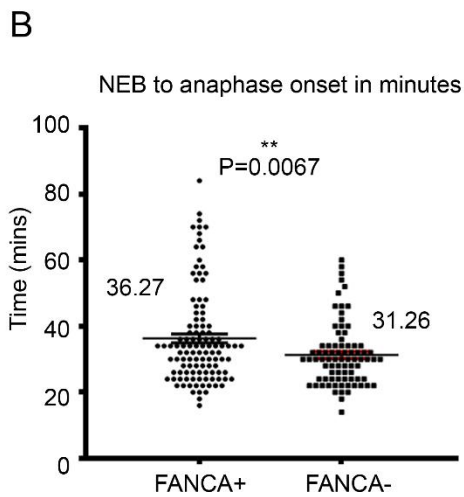
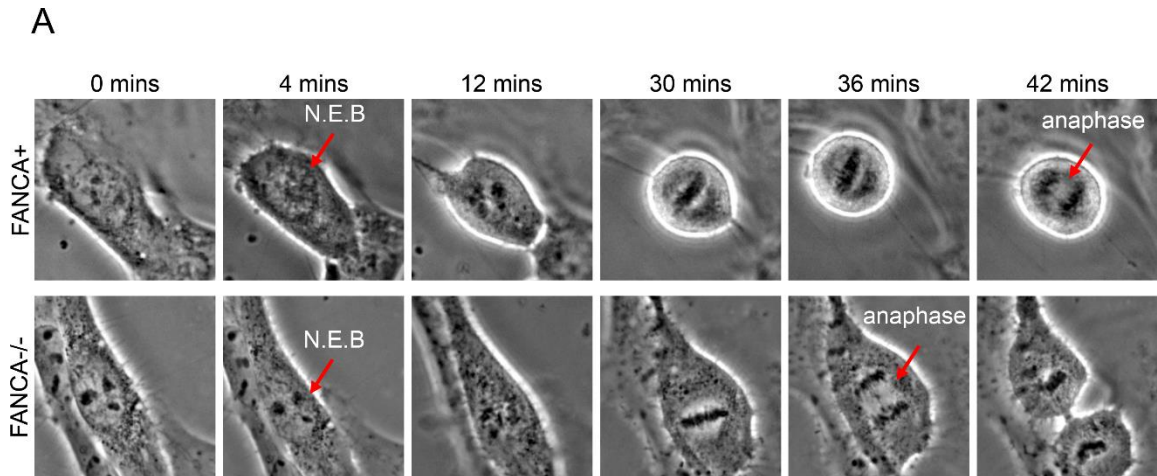


**Figure 25. *FANCA*<sup>-/-</sup> cells exit mitosis faster compared to *FANCA*<sup>+</sup> cells.** (A) Representative time-lapse imaging between nuclear envelope breakdown (NEB) and anaphase onset in *FANCA*<sup>+</sup> and *FANCA*<sup>-/-</sup> fibroblasts. (B) Decreased NEB to anaphase onset in *FANCA*<sup>-/-</sup> fibroblasts compared to *FANCA*<sup>+</sup> JRAST fibroblasts. \*\* $P < 0.005$ , two-tailed student's t-test was used to quantify 112 *FANCA*<sup>+</sup> and 81 *FANCA*<sup>-/-</sup> JRAST fibroblasts.



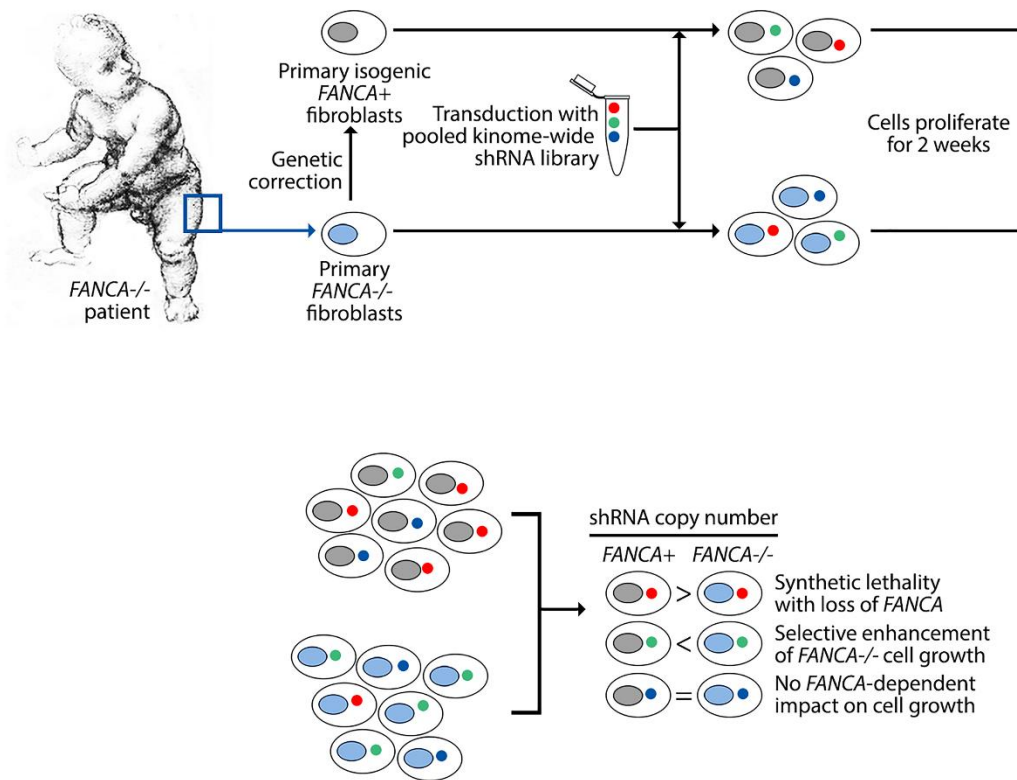


**Figure 26. Design of Kinome-wide screen using shRNAs.** *FANCA*<sup>-/-</sup> and *FANCA*<sup>+</sup> MNHN primary patient fibroblasts (2 replicates) were transduced in parallel with pooled lentiviral shRNA kinase library containing 5000 shRNAs targeting 512 human kinases. The cells were selected with puromycin, grown exponentially for 2 weeks, pelleted, flash-frozen and subjected to high-throughput sequencing to quantify individual clones within each biological replicate (sequencing depth: 1000x).

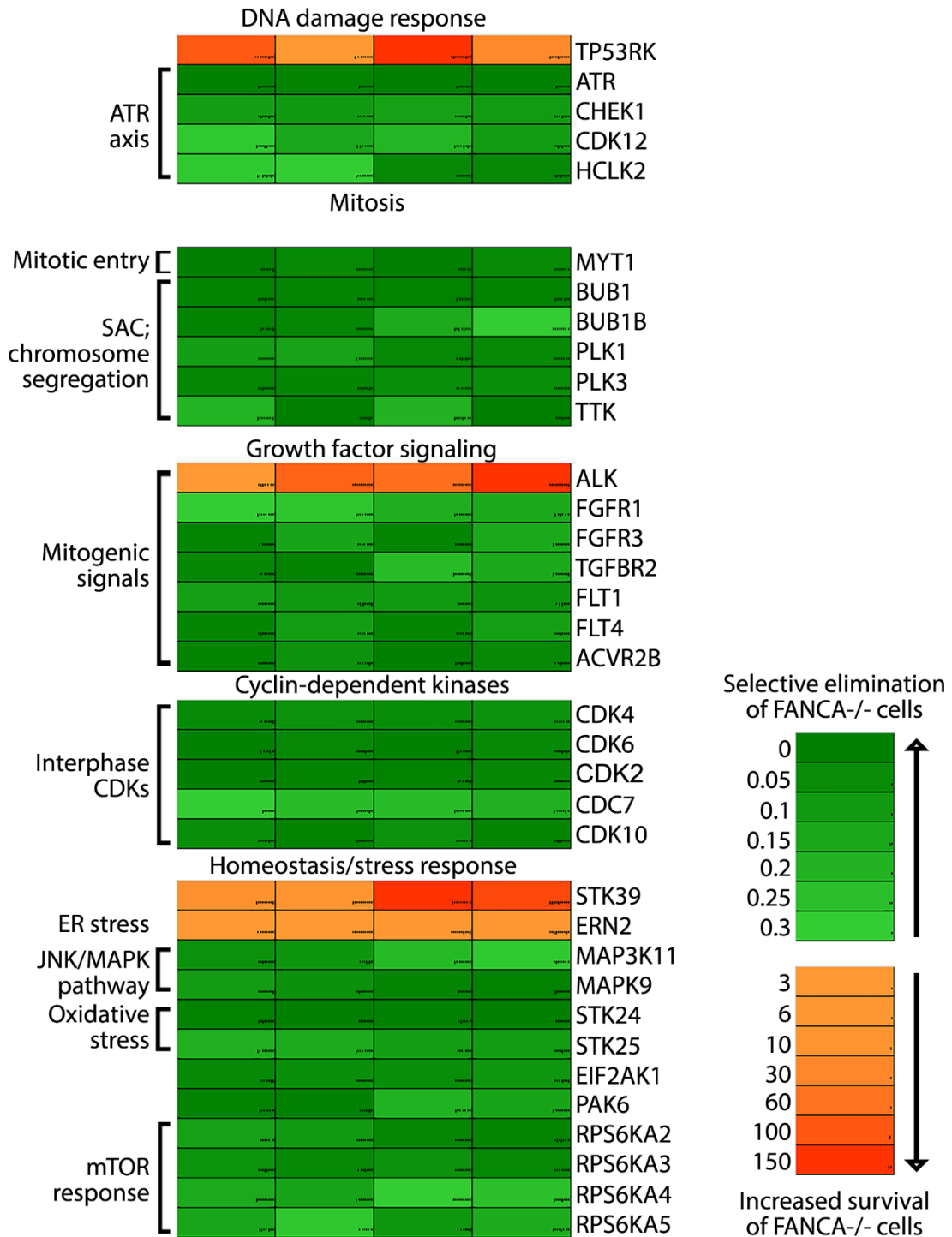


**Figure 27. Kinome-wide shRNA screen hits heat map.** A gene map was constructed into cellular pathways based on protein kinases with at least a 5-fold

copy number difference between *FANCA*<sup>-/-</sup> and *FANCA*<sup>+</sup> clones in all four ratios (described in methods).

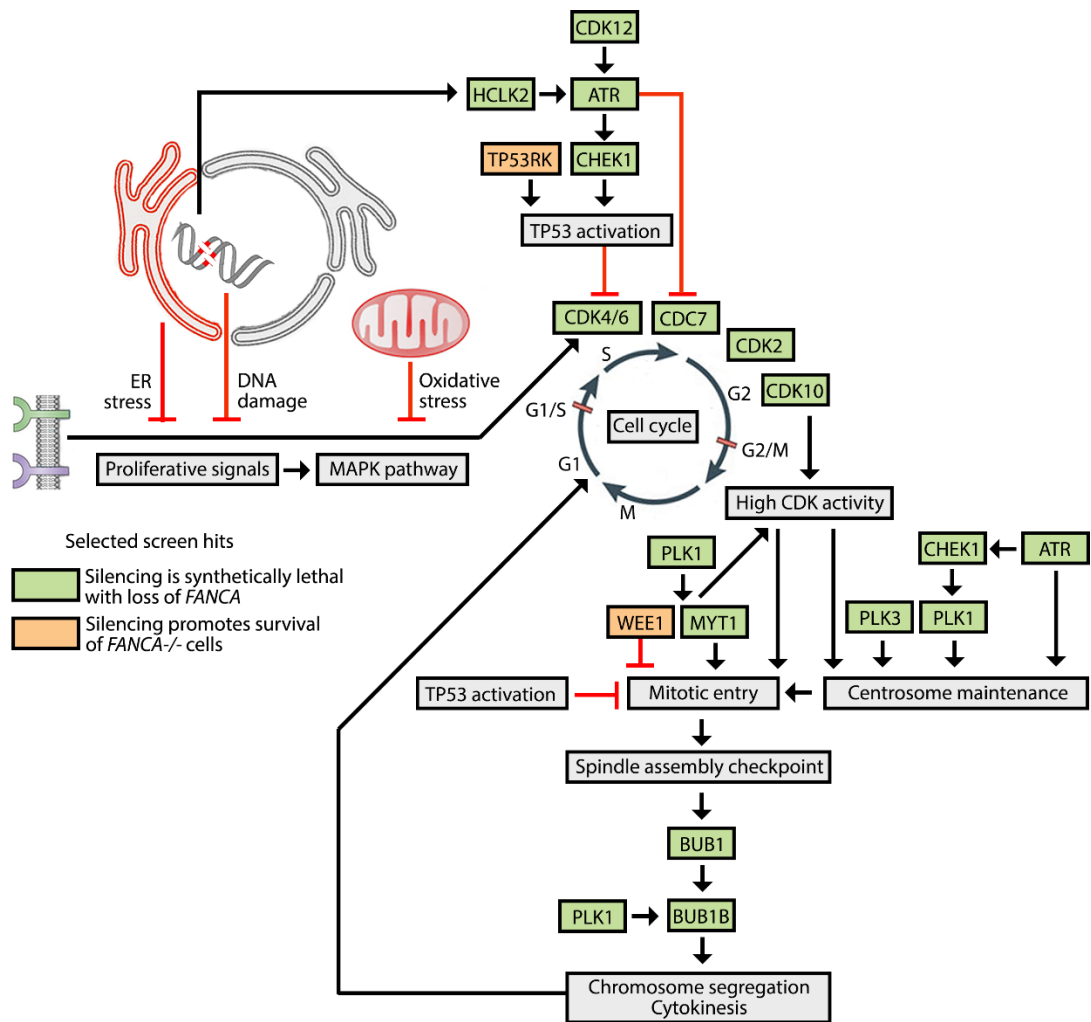
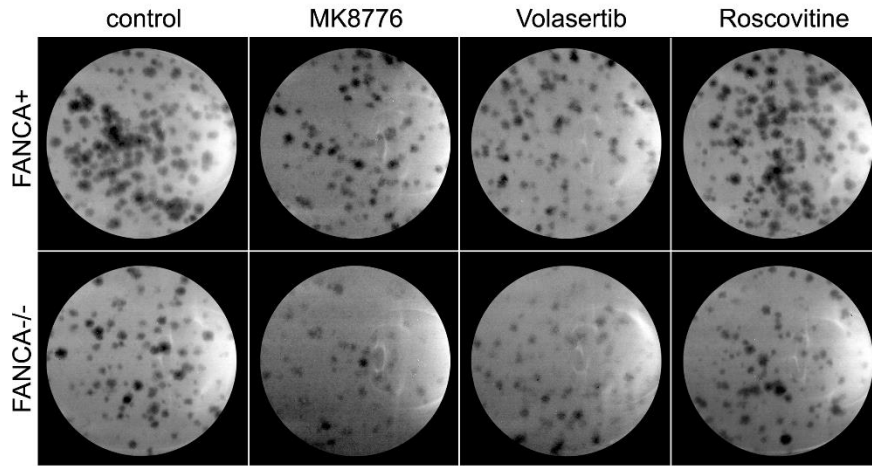


**Figure 28. Genes in mitotic pathways that are essential for survival of *FANCA*<sup>-/-</sup> primary patient fibroblasts.** Functional genomics provide a cellular blueprint of signaling pathways deemed necessary for survival of *FANCA*<sup>-/-</sup> cells. Loss of *FANCA* confers cellular lethality upon silencing of genes involved in DNA damage response, spindle assembly checkpoint (SAC) and chromosomal segregation.

A



B

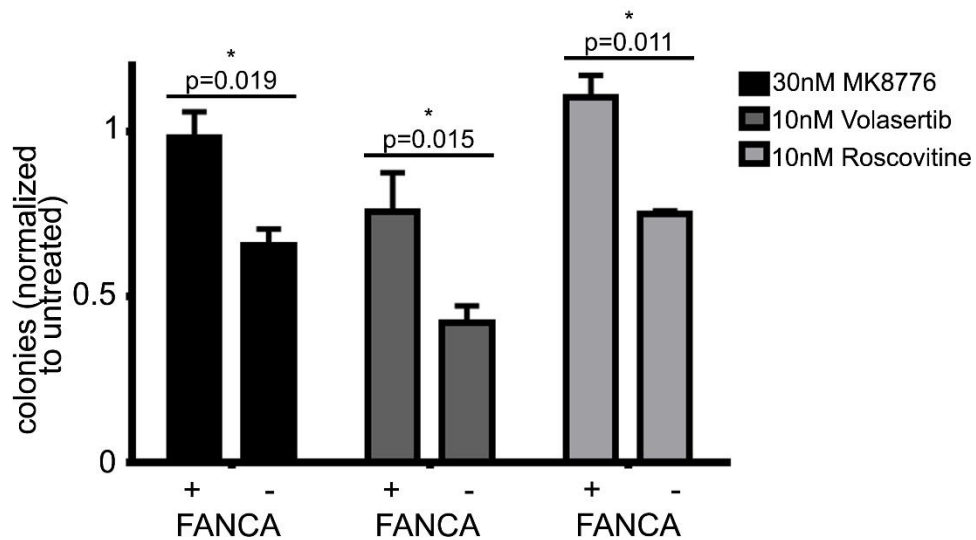


**Figure 29. *FANCA*<sup>-/-</sup> fibroblasts are hypersensitive to inhibition of kinases involved in DNA damage and cell cycle pathways using clinical grade small molecule inhibitors.** Left: Representative scans of colony-forming unit (CFU) assay plates of *FANCA* gene corrected and *FANCA*<sup>-/-</sup> patient MNHN fibroblasts grown in the presence of indicated inhibitors for 14 days. Right: Quantification of colony assays confirms that *FANCA*<sup>-/-</sup> cell survival depends on the activity of CHK1 (MK8776), PLK1 (volasertib) and CDKs (volasertib). \*P < 0.05, \*\*\*\*P <

0.0001, ns= non-significant, two-sided student's t-test. All experiments were performed in triplicates.

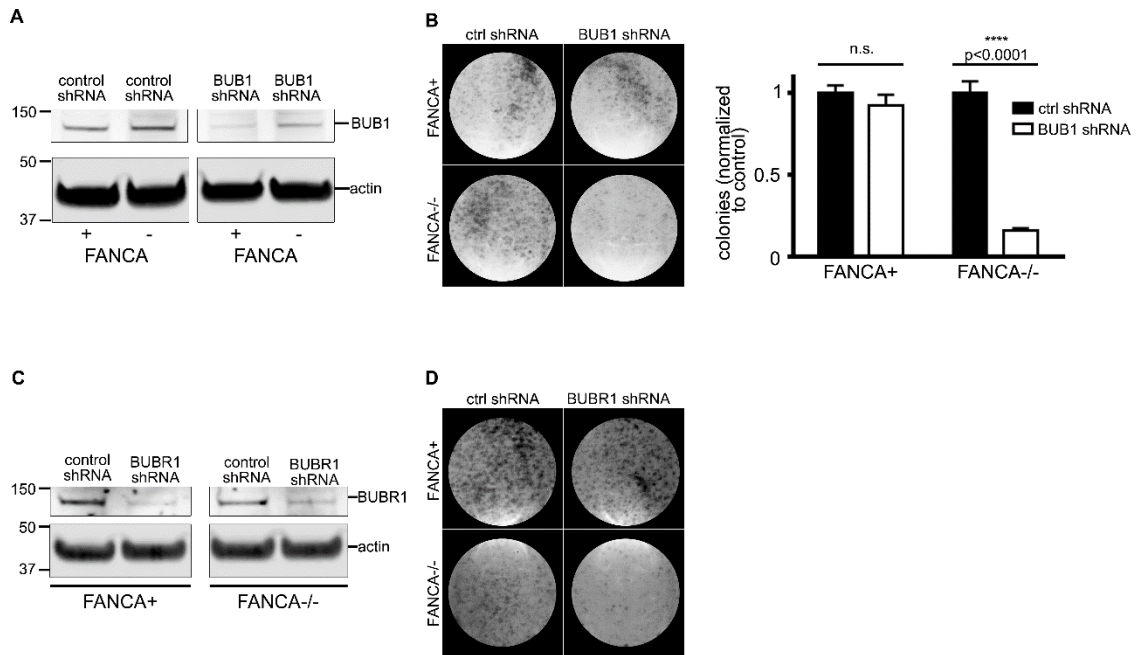


**Figure 30. shRNA-mediated silencing of SAC protein kinases, BUB1 and BUBR1, confers lethality of *FANCA*<sup>-/-</sup> MNHN fibroblasts. (A) BUB1**

knockdown is synthetically lethal with loss of *FANCA*. Western blot showing decreased BUB1 protein expression in *FANCA*<sup>+</sup> and *FANCA*<sup>-/-</sup> MNHN patient fibroblasts transduced with BUB1 shRNA when compared to control shRNA. (B) One representative of two independent BUB1 shRNAs, not included in the kinase library, demonstrated decreased colony formation in *FANCA*<sup>-/-</sup> fibroblasts in comparison to *FANCA*-corrected fibroblasts and confirmed by quantification of the colony assay. (C) BUBR1 knockdown confirmed by western blot, which shows decreased BUBR1 protein expression in *FANCA*<sup>+</sup> (left) and *FANCA*<sup>-/-</sup> (right) fibroblasts transduced with 2 screen independent BUBR1 shRNAs (#1 and #2) in comparison to control shRNA. (D) BUBR1 knockdown is synthetically lethal in *FANCA*<sup>-/-</sup> fibroblasts. Two independent BUBR1 shRNAs, not included in the screen, confirm the dependency of *FANCA*<sup>-/-</sup> cells on BUBR1 function using

CFUF assay. LacZ-targeting shRNA was used as negative control in all experiments. \*P < 0.05, \*\*\*\*P < 0.0001, ns= non-significant, two-tailed student's t-test. All experiments were performed in triplicates.



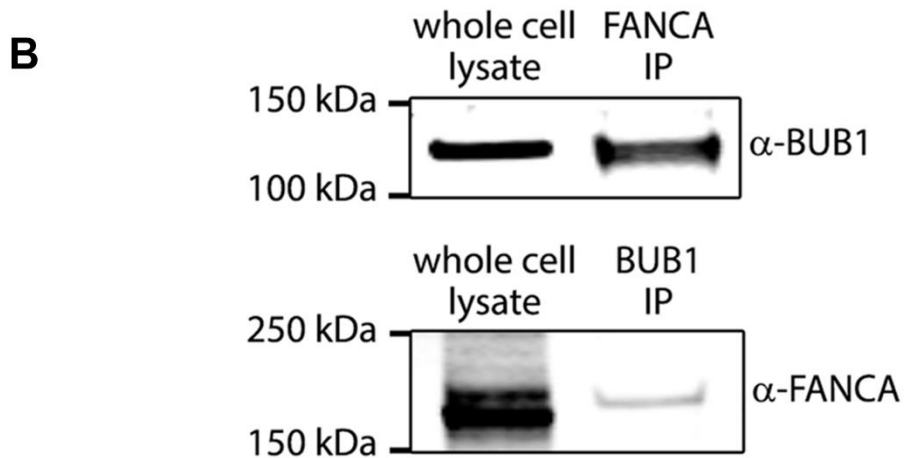
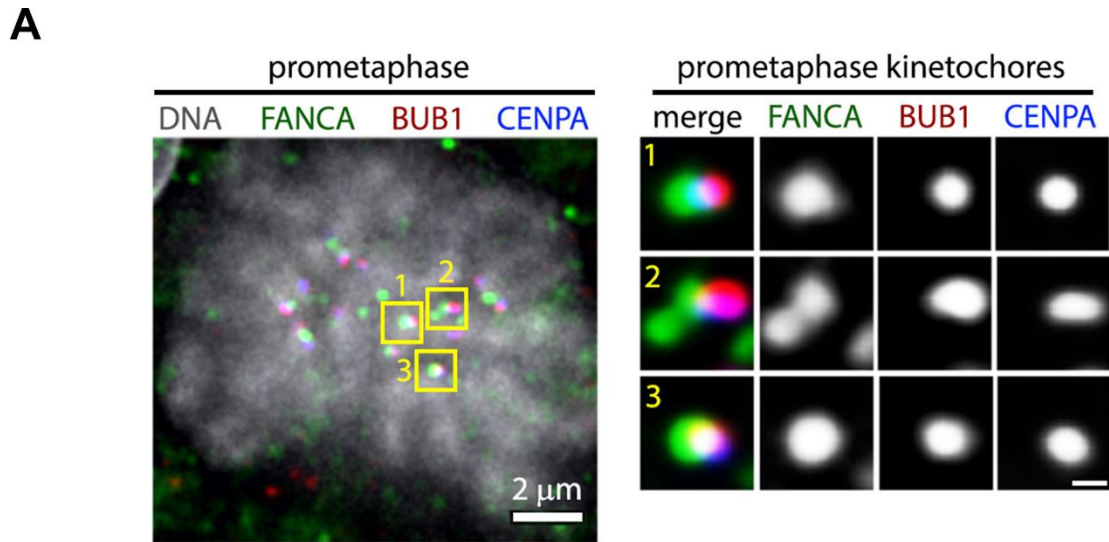
## **FANCA localizes to the mitotic kinetochore, when SAC is active**

FANCA, among other FA proteins, localizes to the mitotic spindle and is important for a robust SAC (Nalepa et al., 2013). Therefore, we focused our attention on synthetically lethal kinases regulating mitosis, specifically the SAC tumor suppressor genes BUB1 and BUBR1. BUB1 (budding uninhibited by benzimidazole 1) is a protein kinase essential for the SAC and chromosome alignment (Perera et al., 2007). BUB1 phosphorylates and inactivates CDC20, the anaphase promoting complex (APC/C) subunit that arrests anaphase until the SAC is satisfied (Tang, Shu, Oncel, Chen, & Yu, 2004). Further, BUB1 phosphorylates histone 2A (H2A) to maintain chromosomal stability by recruiting shugoshin (Kawashima, Yamagishi, Honda, Ishiguro, & Watanabe, 2010; Tang et al., 2004), Aurora B and other SAC components to kinetochores. BUB1 functions upstream in the SAC pathway and recruits other SAC proteins, including the BUBR1 (BUB1-related) kinase as well as MAD2 (Johnson, Scott, Holt, Hussein, & Taylor, 2004; Vigneron et al., 2004). We report that FANCA co-localizes with BUB1 at CENPA-associated kinetochores in HeLA cells during prometaphase (**Figure 31A, 32**), which is biochemically evident by the physical interaction between FANCA and BUB1 (**Figure 31B**). Next, we wondered if the biochemical interaction between FANCA and BUB1 is functionally relevant. BUB1 phosphorylates Cdc20 at S156 residue, preventing premature anaphase onset, and H2A, ensuring proper chromosome condensation (Kawashima et al., 2010; Tang et al., 2004). We show unchanged protein expression of phospho-Cdc20<sup>S156</sup> in *FANCA*<sup>-/-</sup> cells compared to their corrected counterparts (**Figure**

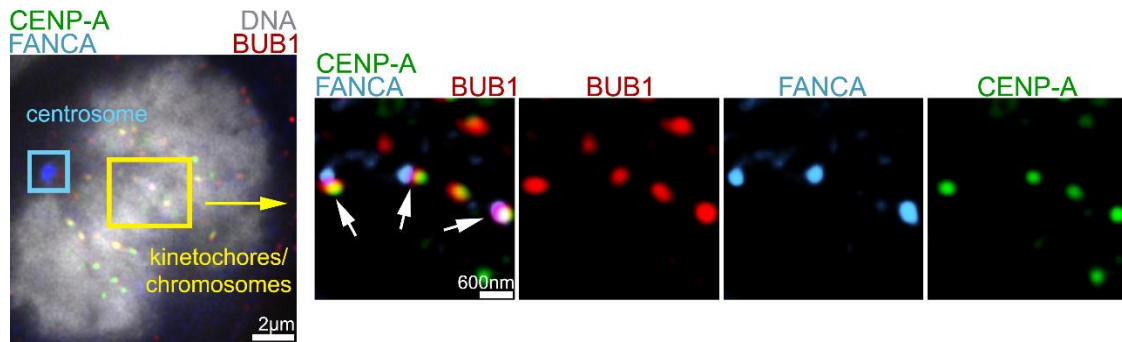
**33A**). In addition, BUB1 kinase activity towards substrates, H1 and H2A, was unchanged in cells transfected with FANCA siRNA when compared to control siRNA transfected HeLa cells (**Figure 33B and C**). Further, phosphorylation of H2A and its localization to kinetochores was unaffected in *FANCA*<sup>-/-</sup> fibroblasts (**Figure 33D and E**). Collectively, BUB1 activity was not affected upon loss of FANCA.

We next addressed whether FANCA is recruited to the kinetochore when the SAC is activated. Indeed, FANCA localization to kinetochores is the highest during prometaphase (**Figure 34**), with a gradual decrease in kinetochore localization as cells exit mitosis. This finding was corroborated by the expression of FANCA protein in cells released from G2 arrest (**Figure 35A and B**). SAC is activated either by lack of kinetochore-microtubule attachment or by lack of tension at the kinetochores (Li & Nicklas, 1995; Rieder, Cole, Khodjakov, & Sluder, 1995). To gain insight into how FANCA behaves in the context of an activated SAC, we used two microtubule-modulating drugs: nocodazole, which produces tensionless kinetochores in the absence of microtubules and taxol, which results in tensionless kinetochores in the presence of microtubules (**Figure 36**). We show that FANCA kinetochore localization pattern is distinct in taxol versus nocodazole treated cells. When microtubules are stabilized upon treatment of taxol, FANCA:BUB1 co-localization (**Figure 37, 38A and B**) and interaction (**Figure 40**) and co-localization is maximized. Interestingly, when treated with nocodazole, FANCA was found to co-localize with Aurora B kinase

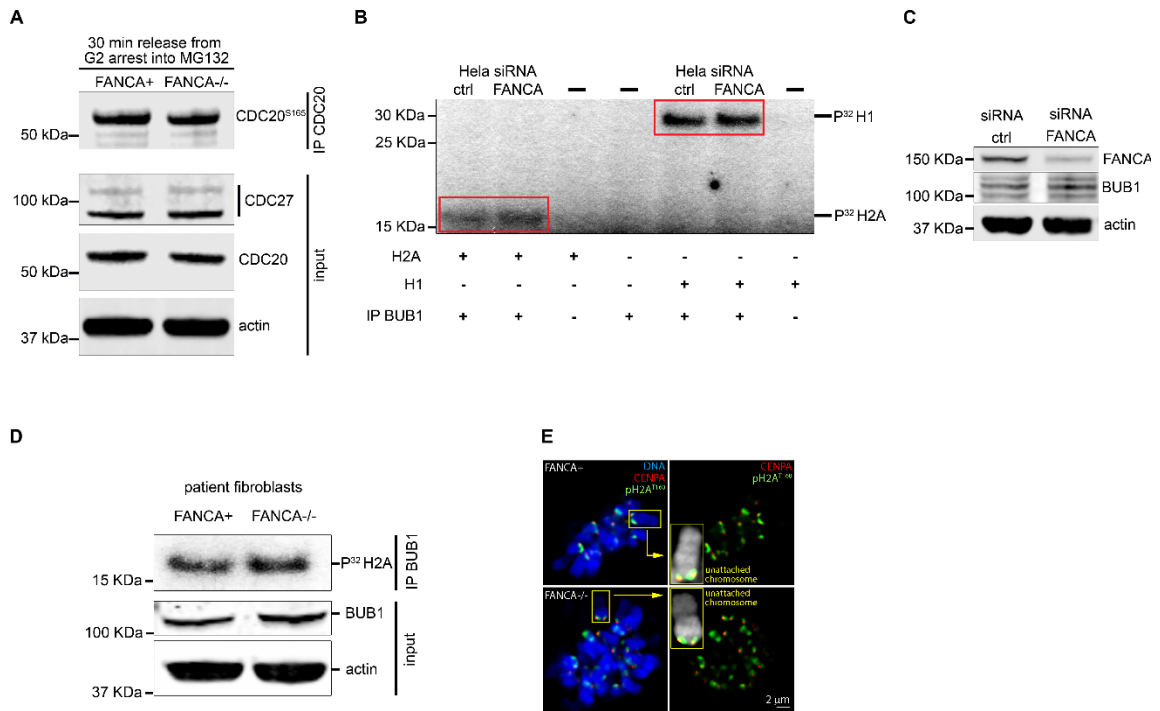
at the inter-centromeric region (**Figure 38-39**). These data suggest that FANCA localizes to kinetochores upon activation of SAC during prometaphase and interacts with SAC proteins, like BUB1, in a microtubule dependent manner.



**Figure 31. FANCA localizes to the kinetochore and interacts with SAC protein kinase, BUB1.** (A) Endogenous FANCA co-localizes with endogenous BUB1 on CENPA-associated kinetochores in HeLa cells during prometaphase. An enlarged region of interest (yellow square) shows a 200nm thin section through kinetochores. (B) A fraction of endogenous FANCA co-immunoprecipitates with endogenous BUB1 in co-IP experiments in Hela cells. Whole cell lysate lane serves as input.

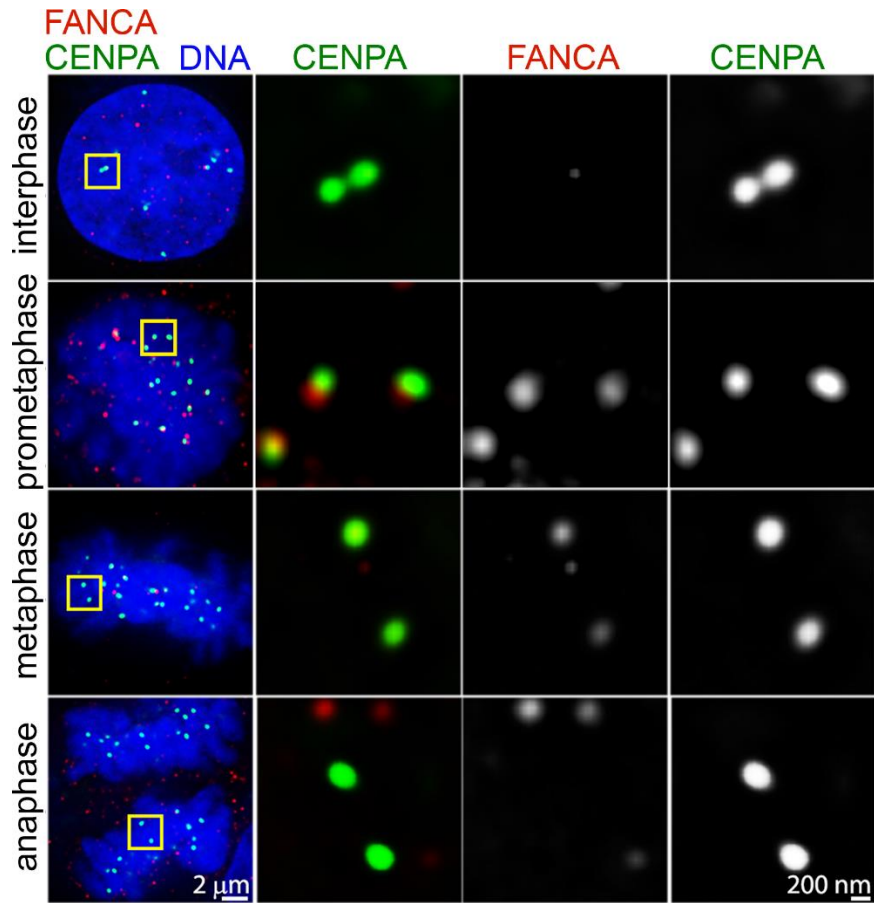


**Figure 32. Confirmation of FANCA:BUB1 co-localization by immunofluorescence microscopy.** Representative IF image using a different primary FANCA (blue) antibody (Ab5063) confirms FANCA co-localization with BUB1 (red) at kinetochores during prometaphase in HeLa cells. An enlarged region of interest (yellow squares) shows a 600nm thin section through kinetochores.



**Figure 33. Phosphorylation of BUB1 substrates upon loss of FANCA remains unchanged.** (A) Unchanged ratio of phospho-Cdc20<sup>S165</sup> to total Cdc20 was observed in *FANCA*-corrected compared to *FANCA*<sup>-/-</sup>. Cdc20 was immunoprecipitated from MNHN *FANCA*<sup>+</sup> and *FANCA*<sup>-/-</sup> fibroblasts and immunoblotted with phospho-Cdc20<sup>S165</sup>. Cdc20, actin and Cdc27 were equal in whole cell lysates. (B) FANCA knockdown does not affect BUB1 kinase activity in HeLa cells. BUB1 was immunoprecipitated from HeLa cells transfected with control or FANCA siRNA. H2A was used as a BUB1-specific substrate and H1 was used as a generic substrate to confirm that the assay was successful. No difference was observed in P<sup>32</sup> H2A and P<sup>32</sup> H1 in si-control versus si-FANCA transfected cells. (C) Western blot confirming successful knockdown of FANCA in HeLa cells. (D) BUB1 protein kinase activity is unchanged in *FANCA*<sup>+</sup> and *FANCA*<sup>-/-</sup> MNHN fibroblasts. BUB1 was immunoprecipitated from MNHN

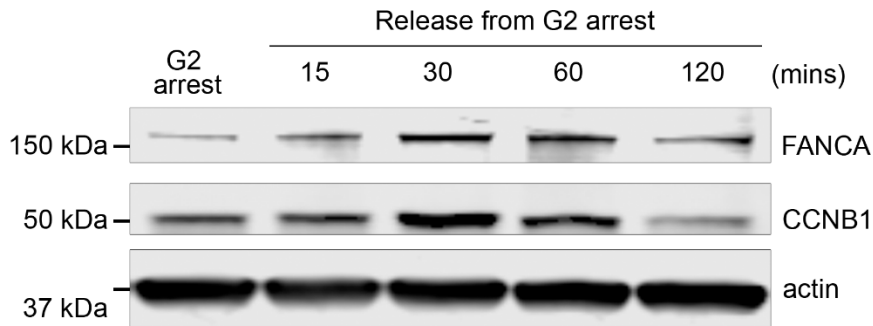
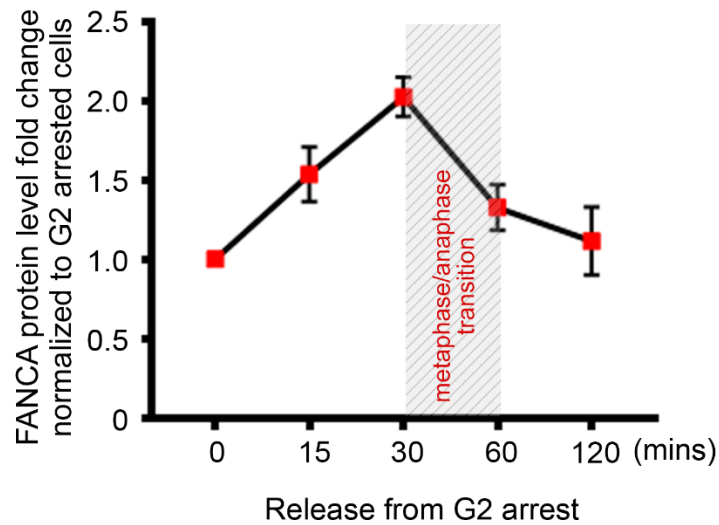
*FANCA*<sup>+</sup> and *FANCA*<sup>-/-</sup> fibroblasts and H2A was used as a substrate. P<sup>32</sup> H2A shows no difference between *FANCA*<sup>+</sup> and *FANCA*<sup>-/-</sup> MNHN fibroblasts with equal levels of BUB1 and Actin in whole cell lysates. (E) pH2A<sup>T160</sup>, BUB1 target, is equally recruited to the prometaphase kinetochores. Representative images showing prometaphase *FANCA*<sup>+</sup> (top panel) and *FANCA*<sup>-/-</sup> (bottom panel) MNHN fibroblasts stained with pH2A<sup>T160</sup> (green) CENPA (red) antibodies.



**Figure 34. Pattern of localization of FANCA during the cell cycle stages.**

FANCA localizes to HeLa CENPA-GFP marked kinetochores in prometaphase with decreasing kinetochore FANCA localization in late stages of mitosis.



**A****B**

**Figure 35. Expression of FANCA protein is increased in early mitotic stages.** (A) FANCA protein expression is increased as cells enter mitosis, when SAC is active, with a gradual decline as cells exit mitosis. CCNB1 serves as a mitotic marker. (B) Cell cycle dependent expression of FANCA is statistically significant.

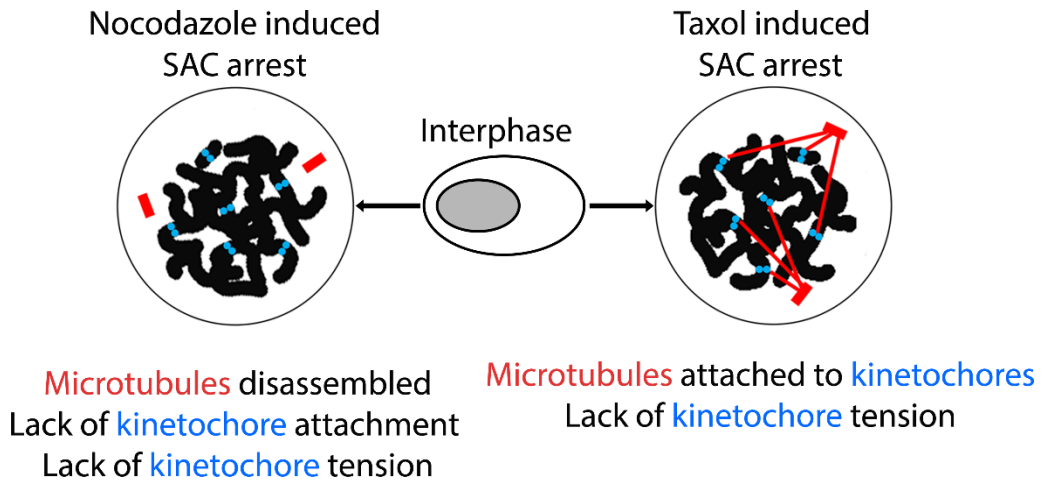


**Figure 36. Taxol and Nocodazole are drugs that modulate the microtubule.**

Schematic depicting microtubule status in cells treated with nocadazole or taxol.

Nocodazole causes microtubule disassembly in addition to lack of kinetochore attachment and tension while taxol results in microtubule stabilization and lack of kinetochore tension.

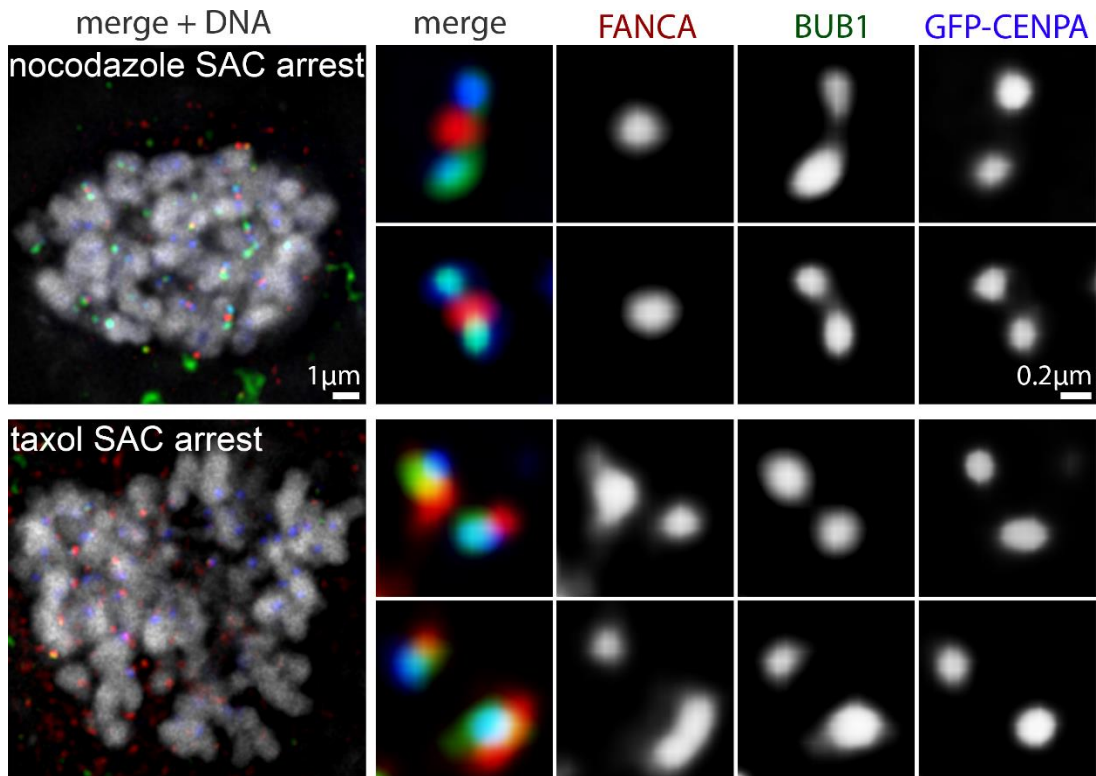


**Figure 37. Pattern of FANCA localization in nocodazole vs taxol treated cells.** Inter-centromeric localization of FANCA in nocodazole arrested HeLa cells compared to kinetochore co-localization of FANCA with BUB1 in taxol-arrested cells.

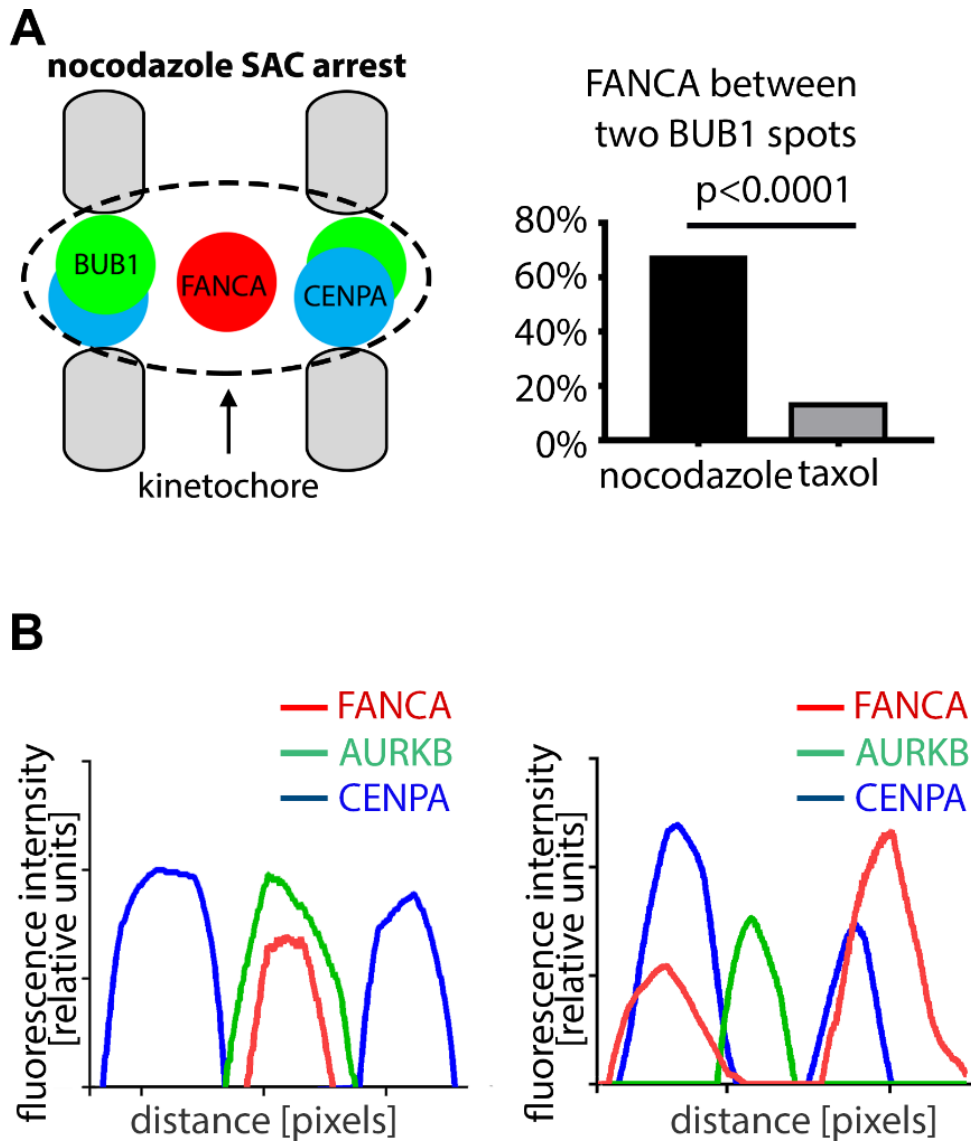


**Figure 38. FANCA interacts with SAC protein kinase, BUB1, in a cell cycle and microtubule-dependent manner.** (A) Representative schematic demonstrating inter-centromeric location of FANCA in the absence of microtubules in nocodazole-treated cells and a corresponding quantification of this localization. (B) Fluorescence intensity line profiles indicate that FANCA co-localizes with Aurora B in nocodazole and not in taxol-treated cells.

At least 300 kinetochores per cell line were counted. \*\*\*\* $P < 0.0001$  Fisher's exact test.

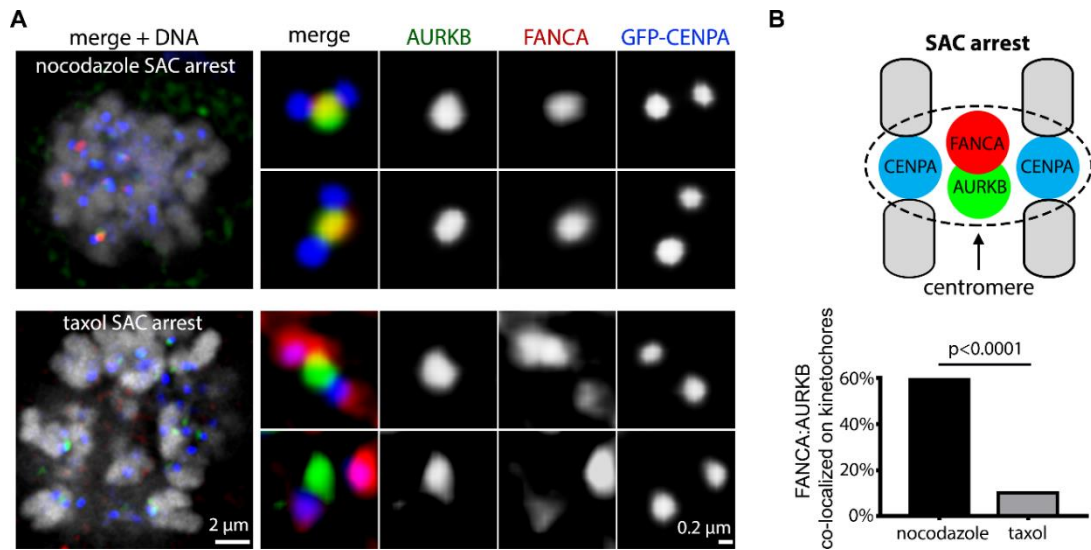


**Figure 39. Inter-centromeric localization of BUB1 with Aurora Kinase B (AURKB) following treatment with Nocodazole.** (A) Immunofluorescence images showing FANCA co-localizing with AURKB between two kinetochores (intercentromeric) in the presence of nocodazole, but not taxol. (B) Schematic (upper panel) depicting the FANCA:AURKB co-localization, which is significantly increased in nocodazole-treated cells when compared with taxol-treated cells upon quantification of this interaction on kinetochores. \*\*\*\* $P < 0.0001$  Fisher's exact test.

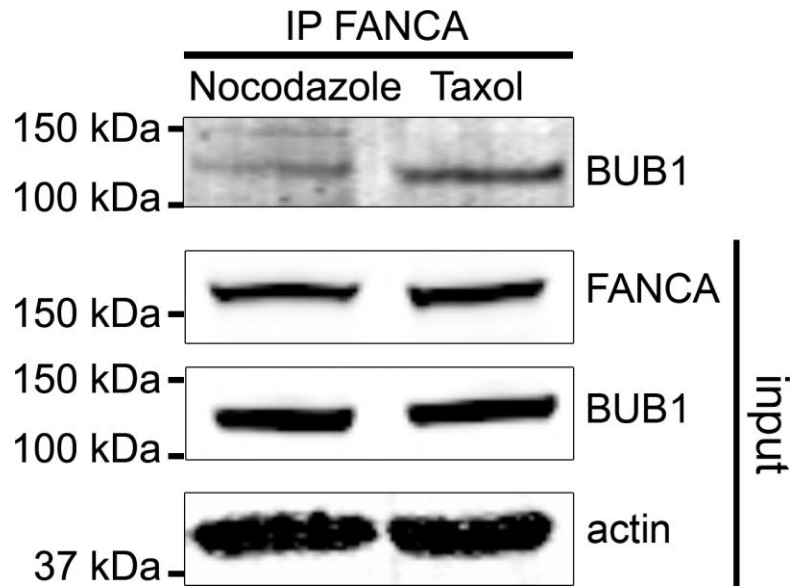


**Figure 40. FANCA interaction with BUB1 in the presence of microtubule-altering agents.** Increased FANCA:BUB1 interaction in the presence of taxol when compared to nocodazole treated Hela cells co-immunoprecipitated with FANCA and blotted for BUB1. No change is noted in FANCA and BUB1 protein expression in whole cell lysates.

## **FANCA regulates PCAF dependent BUBR1 acetylation promoting BUBR1 stability**

Next, we pursued the hypothesis that loss of FANCA affects BUBR1 mitotic functions. BUBR1 localizes to the kinetochore and interacts with CDC20, MAD2 and BUB3 to form the mitotic checkpoint complex (MCC), which sequesters CDC20 from anaphase promoting complex (APC/C) to prevent anaphase transition until SAC is satisfied (V. Sudakin et al., 2001). We asked whether faster anaphase onset and subsequent mitotic exit observed upon loss of FANCA (**Figure 25**, (Nalepa et al., 2013)) could be attributed to dysregulated BUBR1 signaling, especially since FANCA and BUBR1 were found to interact in the context of SAC activation (**Figure 41**). Indeed, BUBR1 protein levels are decreased in *FANCA*<sup>-/-</sup> cells in mitosis (**Figure 42A**) in a proteasome dependent manner (**Figure 42B**). This suggests faster BUBR1 degradation in *FANCA*<sup>-/-</sup> cells, which was confirmed by inhibition of de-novo protein synthesis upon cycloheximide treatment (**Figure 42C-43**). Given these findings, we addressed what the mechanism for accelerated BUBR1 degradation upon loss of *FANCA* might be.

Acetylation of BUBR1 at lysine residue K250 is important for its stability in prometaphase thus maintaining APC/Cdc20 inhibition until proper chromosome-spindle attachment is achieved (I. Park et al., 2013). We reasoned that dysregulated BUBR1 acetylation may explain decreased BUBR1 stability upon loss of FANCA. Indeed, experiments using published and validated antibody



recognizing acetylated lysine K250 residue on BUBR1 consistently showed diminished BUBR1<sup>Ac-K250</sup> kinetochore localization in *FANCA*-deficient patient fibroblasts (**Figure 44A**). Concomitantly, BUBR1<sup>Ac-K250</sup> protein expression was found to be decreased in two *FANCA*<sup>-/-</sup> patient fibroblast cell lines (**Figure 44B**, **Figure 45A**) and in HeLa cells transfected with *FANCA* siRNA (**Figure 45B**). Collectively, this shows that dysregulated BUBR1 acetylation contributes to decreased BUBR1 stability in *FANCA*<sup>-/-</sup> cells.

Choi et al also reported that BRCA2 (also known as FANCD1), a downstream effector of the FA pathway, is essential in recruiting PCAF acetyl transferase to kinetochores for BUBR1 acetylation (Choi et al., 2009). Our observation of decreased acetylated BUBR1 upon loss of *FANCA* prompted us to interrogate the PCAF- FANCD1 signaling chain during prometaphase. Indeed, immunofluorescence revealed that PCAF-positive kinetochores were diminished upon loss of *FANCA* in patient fibroblasts and in si-*FANCA* transfected Hela cells (**Figure 46-47**). We also demonstrate decreased BRCA2/FANCD1 recruitment to kinetochores in *FANCA*-deficient patient fibroblasts and in si-*FANCA* transfected Hela cells (**Figure 48-49**). Collectively, these results support a model in which *FANCA* is required for recruitment of FANCD1 and PCAF to kinetochores which acetylates and stabilizes BUBR1 allowing for error free chromosome segregation (**Figure 50**).

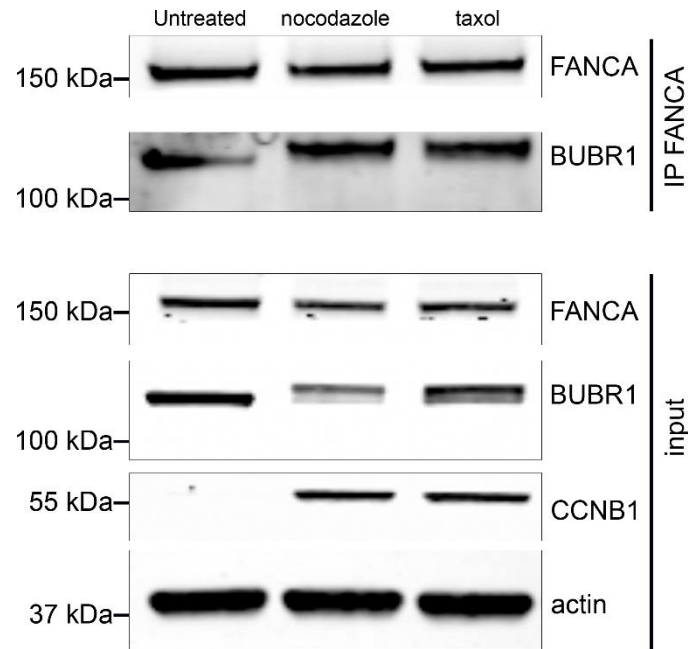


**Figure 41. FANCA interacts with BUBR1.** A fraction of endogenous FANCA co-immunoprecipitates with BUBR1 in co-IP experiments in HeLa cells treated with or without nocodazole or taxol. CCNB1 serves as a mitotic control and actin as a loading control.

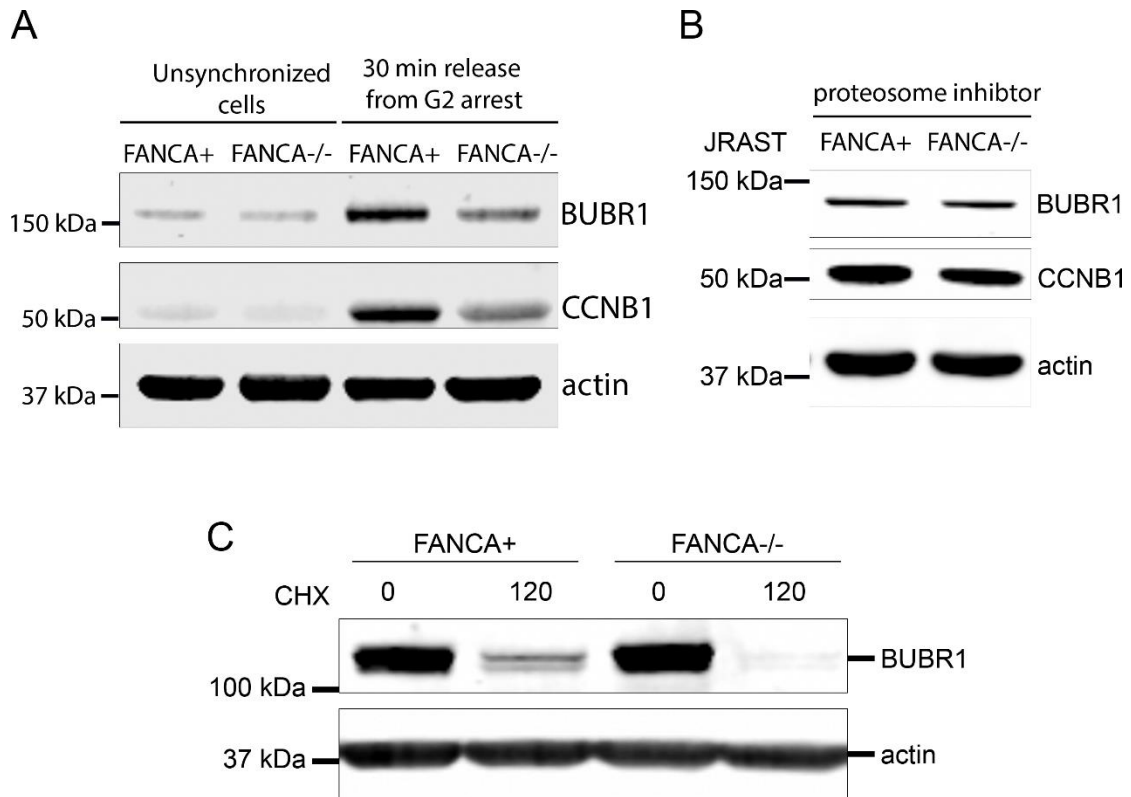


**Figure 42. Decreased BUBR1 stability upon loss of *FANCA*.** (A) Decreased BUBR1 and CCNB1 levels are observed in *FANCA*<sup>-/-</sup> JRAST fibroblasts compared to *FANCA*<sup>+</sup> cells following 30-minute release from RO-3306 induced G2 arrest. No significant difference in BUBR1 and CCNB1 is observed in unsynchronized *FANCA*<sup>+</sup> and *FANCA*<sup>-/-</sup> JRAST fibroblasts with equal protein loading indicated by Actin. (B) Western blot showing restored BUBR1 expression in *FANCA*<sup>-/-</sup> cells following 3-hour release from RO-3306 induced G2 arrest into MG132, a proteasome inhibitor. (C) Faster BUBR1 protein degradation is observed in *FANCA*<sup>-/-</sup> JRAST fibroblasts following 120-minute treatment with 20ug/ml cycloheximide (CHX) when compared to *FANCA*<sup>+</sup> counterparts following the same treatment. No difference in BUBR1 degradation is observed

at baseline (0 seconds). Actin serves as a loading control while CCNB1 serves as a mitotic marker.

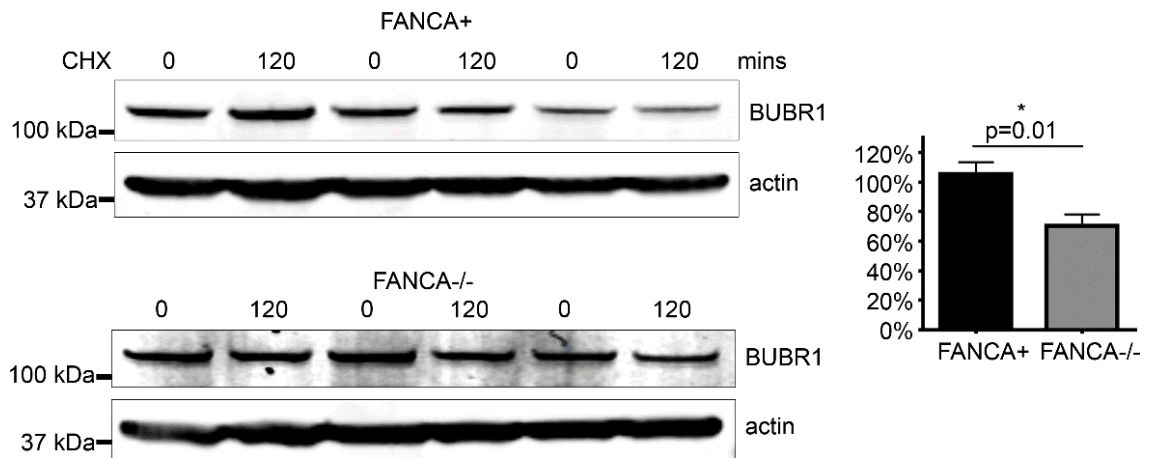


**Figure 43. *FANCA*<sup>-/-</sup> cells exhibit faster BUBR1 degradation.** (A) Western blot showing decreased BUBR1 protein levels in *FANCA*<sup>-/-</sup> JRAST cells (right) following 120-minute treatment with 20 µg/ml cyclohexamide (CHX) when compared to CHX treated *FANCA*<sup>+</sup> fibroblasts (left). Actin serves as a loading control. (B) BUBR1 levels in CHX treated cells were normalized to untreated cells. Quantification of normalized BUBR1 expression shows increased BUBR1 degradation in *FANCA*<sup>-/-</sup> cells. \*P < 0.05. two-sided student's t-test. Six different replicates were quantified (data not shown).

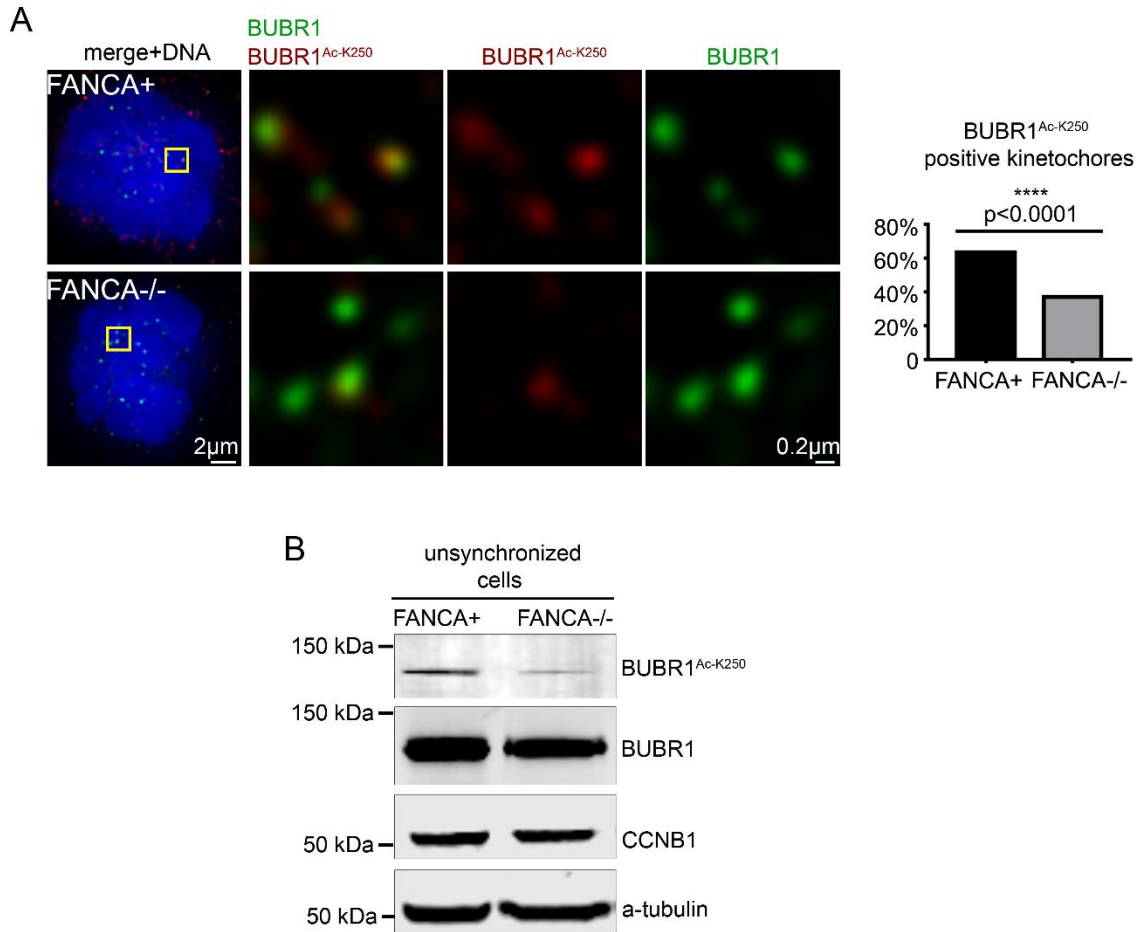


**Figure 44. FANCA is essential for BRCA2 mediated BUBR1 acetylation. (A)**

Immunofluorescence microscopy demonstrates decreased Ac-BUBR1 localization to kinetochores (left) in FANCA-deficient MNHN fibroblasts in comparison to FANCA corrected cells. Quantification shows significantly decreased BUBR1AcK250 positive kinetochores in *FANCA*<sup>-/-</sup> cells compared to *FANCA*<sup>+</sup>. (B) Unsynchronized *FANCA*<sup>-/-</sup> JRAST fibroblasts exhibit decreased acetylated BUBR1 expression when compared to *FANCA*<sup>+</sup> counterparts without a difference in CCNB1 or alpha-tubulin expression.

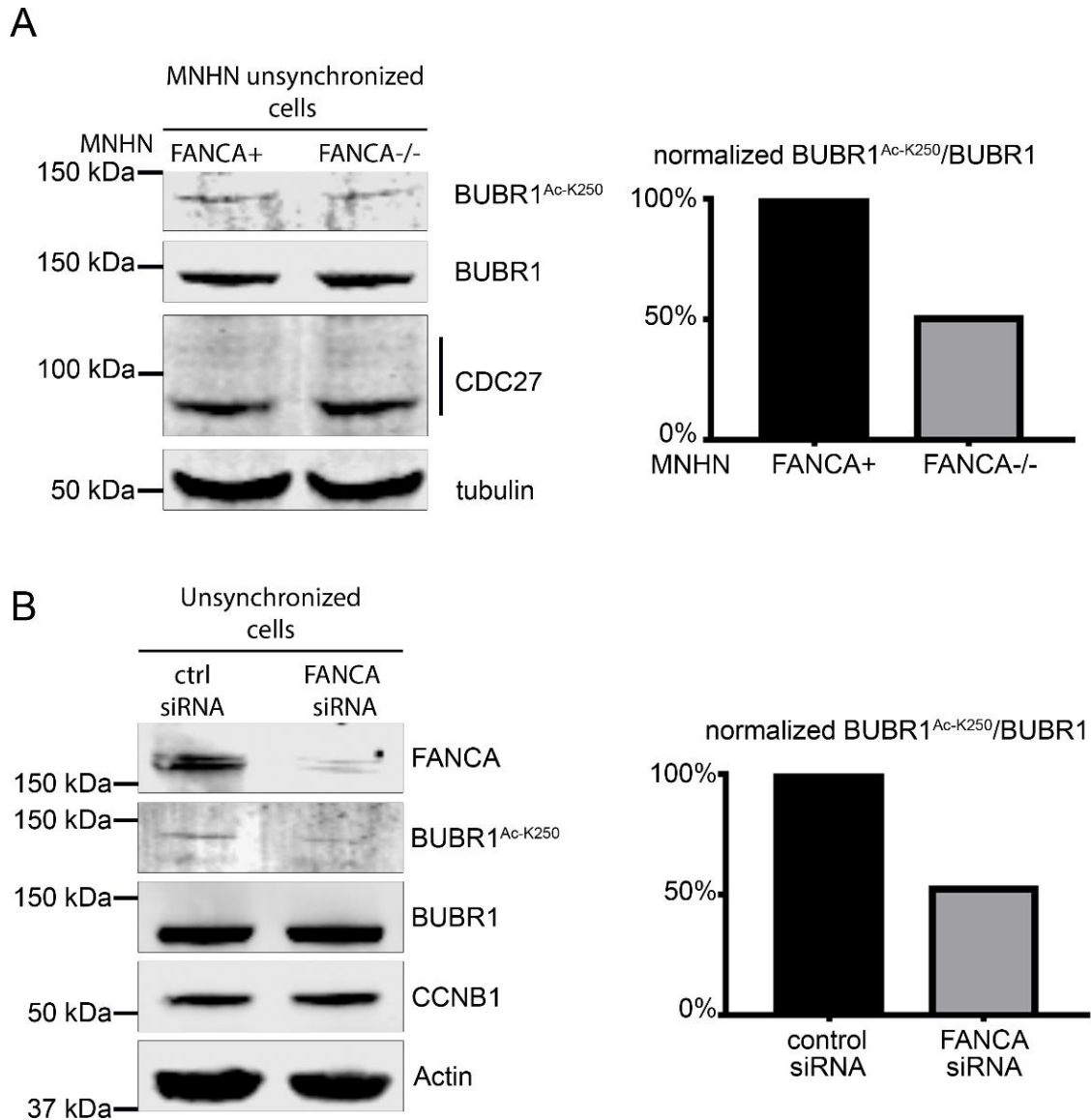


**Figure 45. Levels of acetylated BUBR1 protein is decreased upon loss of FANCA in unsynchronized cells.** (A) Decreased expression of acetylated-BUBR1 and quantification of BUBR1<sup>AcK250</sup>/BUBR1 ratio in unsynchronized FANCA<sup>-/-</sup> MNHN fibroblasts when compared to FANCA<sup>+</sup> counterparts. Quantification of BUBR1<sup>AcK250</sup>/BUBR1 ratio is shown on the right. No difference in CDC27 is noted among both cell lines suggesting equal mitotic cellular index. (B) FANCA siRNA transfected Hela cells exhibit decreased

BUBR1AcK250/BUBR1 expression compared to control siRNA with equal CCBN1 expression.



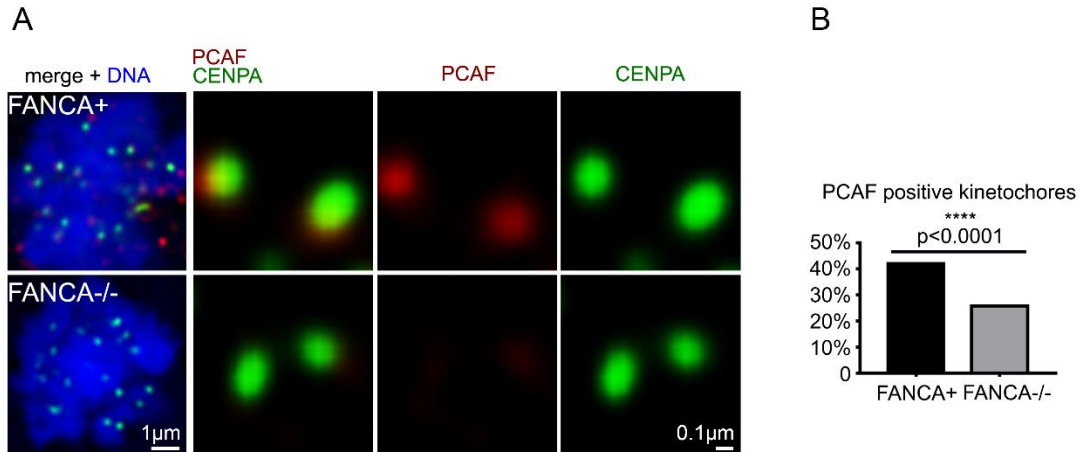


**Figure 46. Diminished localization of PCAF in *FANCA*<sup>-/-</sup> MNHN fibroblast**

**kinetochores.** (A) Representative microscopy images depicting decreased PCAF (red) positive CENPA (green) kinetochores in *FANCA*<sup>-/-</sup> MNHN (upper panel) fibroblasts compared to *FANCA*<sup>+</sup> MNHN fibroblasts (lower panel). (B) Quantification of at least 300 kinetochores demonstrates a statistically significant decrease in PCAF positive kinetochores in *FANCA*<sup>-/-</sup> fibroblasts compared to *FANCA*<sup>+</sup> counterparts. \*\*\*\*P < 0.0001 Fisher's exact test.

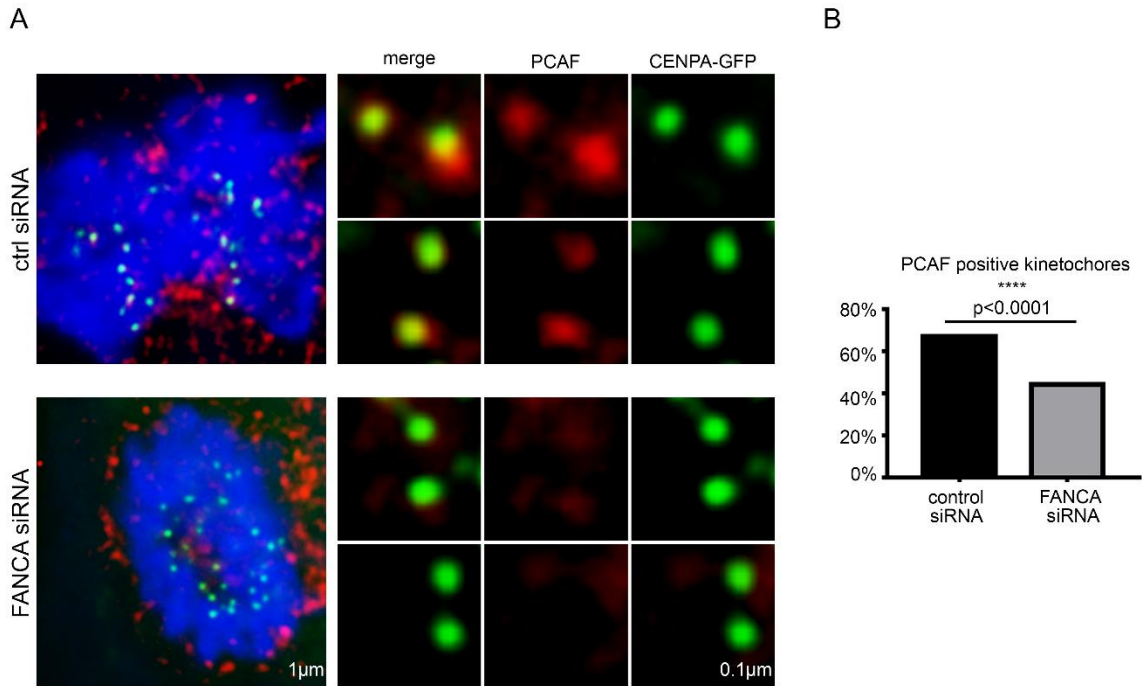


**Figure 47. PCAF recruitment is reduced upon loss of *FANCA*.** (A) Diminished PCAF (red) positive CENPA (green) kinetochores in *FANCA* siRNA transfected HeLa cells (upper panel) compared to control siRNA transfected HeLa cells (lower panel). (B) At least 300 kinetochores were used to quantify PCAF positive kinetochores, which shows a statistically significant decrease in PCAF recruitment in *FANCA* siRNA compared to control siRNA transfected HeLa cells. \*\*\*\* $P < 0.0001$  Fisher's exact test.

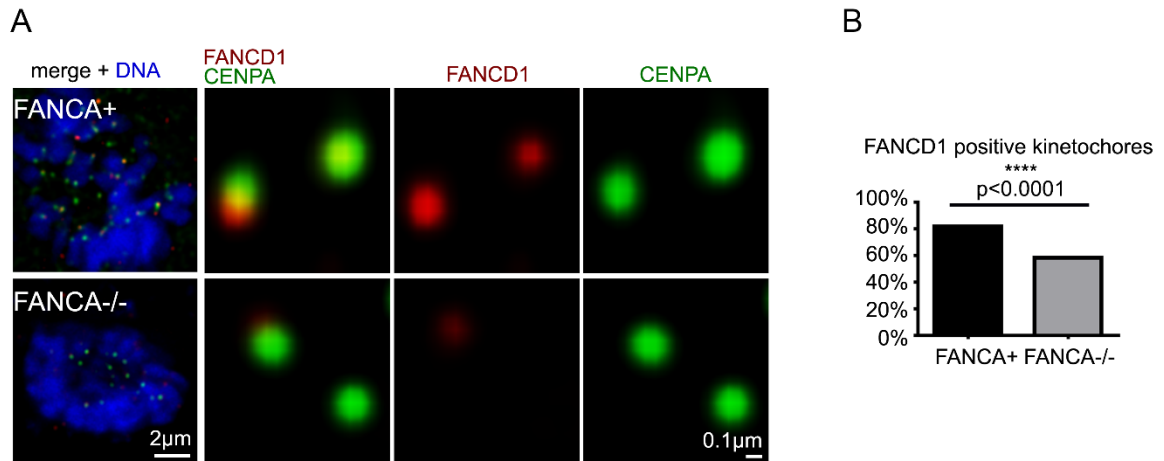


**Figure 48. Diminished localization of FANCD1 in *FANCA*<sup>-/-</sup> MNHN fibroblast kinetochores.** (A) Representative microscopy images depicting decreased FANCD1 (red) positive CENPA (green) kinetochores in *FANCA*<sup>-/-</sup> MNHN (upper panel) fibroblasts compared to *FANCA*<sup>+</sup> MNHN fibroblasts (lower panel). (B) Quantification of at least 300 kinetochores demonstrates a statistically significant decrease in FANCD1 positive kinetochores in *FANCA*<sup>-/-</sup> fibroblasts compared to *FANCA*<sup>+</sup> counterparts. \*\*\*\* $P < 0.0001$  Fisher's exact test.

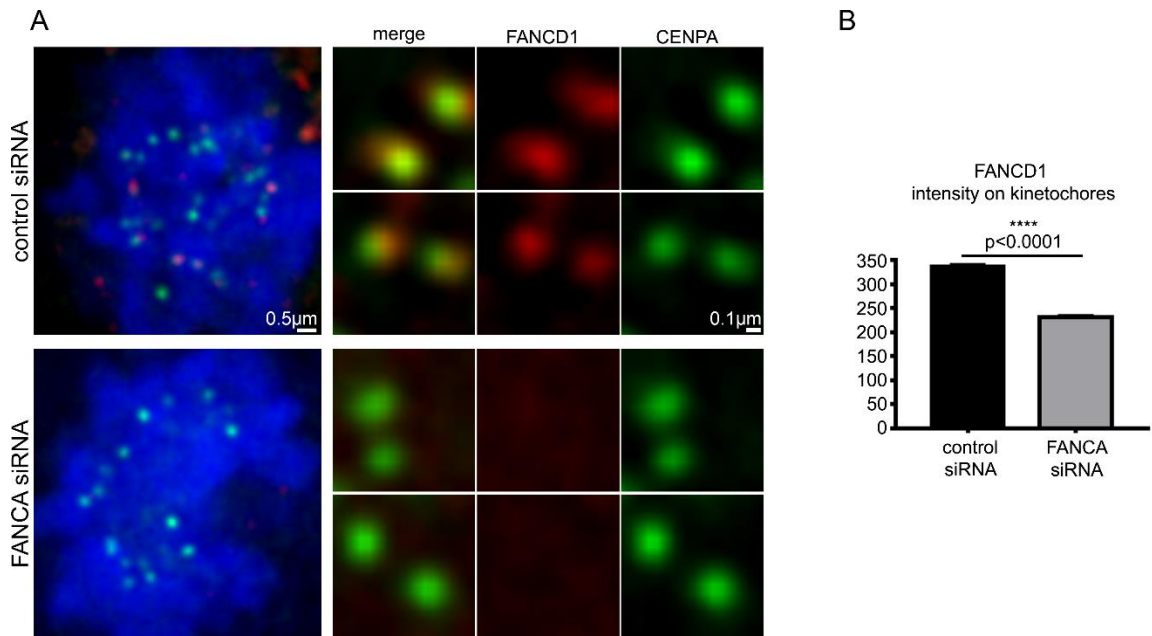


**Figure 49. Diminished FANCD1 localization is observed upon knockdown of FANCA.** (A) Diminished FANCD1 (red) positive CENPA (green) kinetochores in FANCA siRNA transfected HeLa cells (upper panel) compared to control siRNA transfected HeLa cells (lower panel). (B) At least 300 kinetochores were used to quantify FANCD1 positive kinetochores, which shows a statistically significant decrease in FANCD1 recruitment in FANCA siRNA compared to control siRNA transfected HeLa cells. \*\*\*\*P<0.0001 student T-test

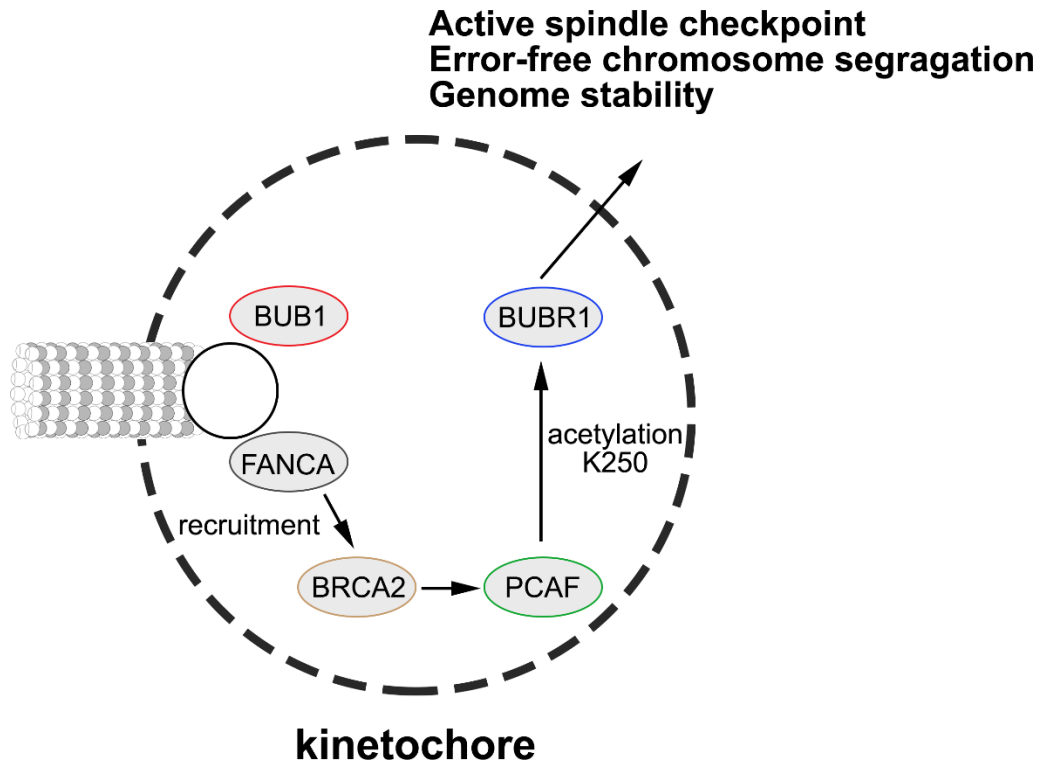


**Figure 50. FANCA maintains the SAC through a mechanism involving acetylation of BUBR1 protein.** Schematic showing the proposed mechanism for crosstalk between the SAC and FA pathway. FANCA is required for FANCD1 recruitment of PCAF to kinetochore and its acetylation of BUBR1, which ensures active SAC checkpoint error free chromosome segregation and genomic stability.

## Discussion

Our study uses an unbiased shRNA kinome screen that identified several kinases, including SAC kinases named BUB1 and BUBR1, to be synthetically lethal with loss of *FANCA*. We provide the first line of evidence that showcases *FANCA*'s role in ensuring a robust SAC by participating in the FANCD1:PCAF:BUBR1 acetylation cascade. Furthermore, revealing that *FANCA* regulates SAC through BUBR1 acetylation provides an explanation for BUB1 synthetic lethality in *FANCA*<sup>-/-</sup> cells. Indeed, losing *FANCA* and subsequently compromising BUBR1 inhibition of Cdc20 results in weakened SAC, but losing BUB1 as well may result in complete abrogation of the SAC and consequently cell death. Collectively, this study provides a mechanistic insight into the signaling pathways through which *FANCA* may exert its mitotic control. The synthetic lethality of BUB1 and BUBR1 provides therapeutic platform for targeting the SAC in *FANCA*<sup>-/-</sup> cells, which could prove to be an effective strategy for selective killing of *FANCA*-deficient cancers in Fanconi Anemia patients, in addition to, the general population.

## CHAPTER FIVE

### CONCLUSIONS AND FUTURE DIRECTIONS

Our understanding of the functions of the FA pathway in mitosis is only starting to take shape. In this study, we showed that genomic instability in FA arises from a combination of interphase DNA damage and mitotic aberrations. We also demonstrated that FANCA localizes to the prometaphase kinetochore to regulate the SAC through controlling BUBR1 acetylation. Our published and unpublished data suggest that FA proteins localize to the centrosome and are essential for centrosome maintenance (Kim et al., 2013; Nalepa et al., 2013; Zou et al., 2013; Zou et al., 2014). Still, many questions regarding the roles of FA proteins in mitosis remain unanswered. Future studies will focus the mechanism through which FANCA exerts its function in centrosome maintenance and spindle nucleation. It would be also interesting to understand how FANCA is targeted to the kinetochore and spindle.

Furthermore, our kinome-wide shRNA screen identified a number of candidate kinases whose silencing selectively impacts survival of *FANCA*<sup>-/-</sup> cells. Here we evaluated the mechanistic connection between FANCA and BUBR1 axis, but we are planning to systematically evaluate other candidates in our future studies as other kinases may also provide significant insights into FANCA-dependent mechanisms of cell division. In these studies, we will prioritize candidates that

can be effectively targeted with small-molecule chemotherapeutics as this would facilitate pre-clinical evaluation of the most promising candidates.



## REFERENCES

- Adamo, A., Collis, S. J., Adelman, C. A., Silva, N., Horejsi, Z., Ward, J. D., . . . La Volpe, A. (2010). Preventing nonhomologous end joining suppresses DNA repair defects of Fanconi anemia. *Mol Cell*, *39*(1), 25-35.  
doi:10.1016/j.molcel.2010.06.026
- Alter, B. P. (2014). Fanconi anemia and the development of leukemia. *Best Pract Res Clin Haematol*, *27*(3-4), 214-221. doi:10.1016/j.beha.2014.10.002
- Alter, B. P., & Clinician, S. (2014). Fanconi anemia and the development of leukemia. *Best Practice & Research Clinical Haematology*, *27*(3-4), 214-221.  
doi:10.1016/j.beha.2014.10.002
- Alter, B. P., Giri, N., Savage, S. A., Peters, J. A., Loud, J. T., Leathwood, L., . . . Rosenberg, P. S. (2010). Malignancies and survival patterns in the National Cancer Institute inherited bone marrow failure syndromes cohort study. *Br J Haematol*, *150*(2), 179-188. doi:10.1111/j.1365-2141.2010.08212.x
- Ameziane, N., May, P., Haitjema, A., van de Vrugt, H. J., van Rossum-Fikkert, S. E., Ristic, D., . . . Dorsman, J. C. (2015). A novel Fanconi anaemia subtype associated with a dominant-negative mutation in RAD51. *Nat Commun*, *6*, 8829.  
doi:10.1038/ncomms9829
- Auerbach, A. D. (2009). Fanconi anemia and its diagnosis. *Mutat Res*, *668*(1-2), 4-10. doi:10.1016/j.mrfmmm.2009.01.013
- Bakhoun, S. F., & Compton, D. A. (2012). Chromosomal instability and cancer: a complex relationship with therapeutic potential. *J Clin Invest*, *122*(4), 1138-1143.  
doi:10.1172/JCI59954

Barton, J. C., Parmley, R. T., Carroll, A. J., Huang, S. T., Goodnough, L. T., Findley, H. W., Jr., & Ragab, A. H. (1987). Preleukemia in Fanconi's anemia: hematopoietic cell multinuclearity, membrane duplication, and dysgranulogenesis. *J Submicrosc Cytol*, 19(2), 355-364.

Bryant, H. E., Schultz, N., Thomas, H. D., Parker, K. M., Flower, D., Lopez, E., . . . Helleday, T. (2005). Specific killing of BRCA2-deficient tumours with inhibitors of poly(ADP-ribose) polymerase. *Nature*, 434(7035), 913-917.

doi:10.1038/nature03443

Casado, J. A., Nunez, M. I., Segovia, J. C., Ruiz de Almodovar, J. M., & Bueren, J. A. (2005). Non-homologous end-joining defect in fanconi anemia hematopoietic cells exposed to ionizing radiation. *Radiation Research*, 164(5), 635-641.

Ceccaldi, R., Briot, D., Larghero, J., Vasquez, N., Dubois d'Enghien, C., Chamousset, D., . . . Soulier, J. (2011). Spontaneous abrogation of the G(2)DNA damage checkpoint has clinical benefits but promotes leukemogenesis in Fanconi anemia patients. *J Clin Invest*, 121(1), 184-194. doi:10.1172/JCI43836

Ceccaldi, R., Liu, J. C., Amunugama, R., Hajdu, I., Primack, B., Petalcorin, M. I., . . . D'Andrea, A. D. (2015). Homologous-recombination-deficient tumours are dependent on Poltheta-mediated repair. *Nature*, 518(7538), 258-262.

doi:10.1038/nature14184

Ceccaldi, R., Parmar, K., Mouly, E., Delord, M., Kim, J. M., Regairaz, M., . . . Soulier, J. (2012). Bone marrow failure in Fanconi anemia is triggered by an exacerbated p53/p21 DNA damage response that impairs hematopoietic stem

and progenitor cells. *Cell Stem Cell*, 11(1), 36-49.

doi:10.1016/j.stem.2012.05.013

Chan, K. L., Palmai-Pallag, T., Ying, S., & Hickson, I. D. (2009). Replication stress induces sister-chromatid bridging at fragile site loci in mitosis. *Nat Cell Biol*, 11(6), 753-760. doi:10.1038/ncb1882

Chandra, S., Levrán, O., Jurickova, I., Maas, C., Kapur, R., Schindler, D., . . . Williams, D. A. (2005). A rapid method for retrovirus-mediated identification of complementation groups in Fanconi anemia patients. *Mol Ther*, 12(5), 976-984. doi:10.1016/j.ymthe.2005.04.021

Cheeseman, I. M., & Desai, A. (2008). Molecular architecture of the kinetochore-microtubule interface. *Nat Rev Mol Cell Biol*, 9(1), 33-46. doi:10.1038/nrm2310

Chen, C. C., Kennedy, R. D., Sidi, S., Look, A. T., & D'Andrea, A. (2009). CHK1 inhibition as a strategy for targeting Fanconi Anemia (FA) DNA repair pathway deficient tumors. *Mol Cancer*, 8, 24. doi:10.1186/1476-4598-8-24

Chen, M., Tomkins, D. J., Auerbach, W., McKerlie, C., Youssoufian, H., Liu, L., . . . Buchwald, M. (1996). Inactivation of Fac in mice produces inducible chromosomal instability and reduced fertility reminiscent of Fanconi anaemia. *Nat Genet*, 12(4), 448-451. doi:10.1038/ng0496-448

Chen, R.-H., Waters, J. C., Salmon, E. D., & Murray, A. W. (1996). Association of spindle assembly checkpoint component X MAD2 with unattached kinetochores. *Science*, 274(5285), 242.

Choi, E., Choe, H., Min, J., Choi, J. Y., Kim, J., & Lee, H. (2009). BubR1 acetylation at prometaphase is required for modulating APC/C activity and timing of mitosis. *Embo Journal*, 28(14), 2077-2089. doi:10.1038/emboj.2009.123

Choi, E., Park, P. G., Lee, H. O., Lee, Y. K., Kang, G. H., Lee, J. W., . . . Lee, H. (2012). BRCA2 fine-tunes the spindle assembly checkpoint through reinforcement of BubR1 acetylation. *Dev Cell*, 22(2), 295-308. doi:10.1016/j.devcel.2012.01.009

Crasta, K., Ganem, N. J., Dagher, R., Lantermann, A. B., Ivanova, E. V., Pan, Y., . . . Pellman, D. (2012). DNA breaks and chromosome pulverization from errors in mitosis. *Nature*, 482(7383), 53-58. doi:10.1038/nature10802

Cuomo, M. E., Knebel, A., Morrice, N., Paterson, H., Cohen, P., & Mitnacht, S. (2008). p53-Driven apoptosis limits centrosome amplification and genomic instability downstream of NPM1 phosphorylation. *Nat Cell Biol*, 10(6), 723-730. doi:10.1038/ncb1735

D'Andrea, A. D. (2010). Susceptibility pathways in Fanconi's anemia and breast cancer. *N Engl J Med*, 362(20), 1909-1919. doi:10.1056/NEJMra0809889

D'Andrea, A. D., & Grompe, M. (2003). The Fanconi anaemia/BRCA pathway. *Nat Rev Cancer*, 3(1), 23-34. doi:10.1038/nrc970

Daniels, M. J., Wang, Y., Lee, M., & Venkitaraman, A. R. (2004). Abnormal cytokinesis in cells deficient in the breast cancer susceptibility protein BRCA2. *Science*, 306(5697), 876-879. doi:10.1126/science.1102574

Desai, A., Rybina, S., Muller-Reichert, T., Shevchenko, A., Shevchenko, A., Hyman, A., & Oegema, K. (2003). KNL-1 directs assembly of the microtubule-

binding interface of the kinetochore in *C. elegans*. *Genes Dev*, 17(19), 2421-2435. doi:10.1101/gad.1126303

Dobles, M., Liberal, V., Scott, M. L., Benezra, R., & Sorger, P. K. (2000). Chromosome missegregation and apoptosis in mice lacking the mitotic checkpoint protein Mad2. *Cell*, 101(6), 635-645.

Dong, H., Nebert, D. W., Bruford, E. A., Thompson, D. C., Joenje, H., & Vasiliou, V. (2015). Update of the human and mouse Fanconi anemia genes. *Hum Genomics*, 9, 32. doi:10.1186/s40246-015-0054-y

Du, J., Chen, L. J., & Shen, J. L. (2009). Identification of FANCA as a protein interacting with centromere-associated protein E. *Acta Biochim Biophys Sin (Shanghai)*, 41(10), 816-821. doi:10.1093/abbs/gmp074

Dunn, J., Potter, M., Rees, A., & Runger, T. M. (2006). Activation of the Fanconi anemia/BRCA pathway and recombination repair in the cellular response to solar ultraviolet light. *Cancer Research*, 66(23), 11140-11147. doi:10.1158/0008-5472.CAN-06-0563

Farmer, H., McCabe, N., Lord, C. J., Tutt, A. N., Johnson, D. A., Richardson, T. B., . . . Ashworth, A. (2005). Targeting the DNA repair defect in BRCA mutant cells as a therapeutic strategy. *Nature*, 434(7035), 917-921. doi:10.1038/nature03445

Fenech, M. (2007). Cytokinesis-block micronucleus cytome assay. *Nat Protoc*, 2(5), 1084-1104. doi:10.1038/nprot.2007.77

Ferrer, M., Rodriguez, J. A., Spierings, E. A., de Winter, J. P., Giaccone, G., & Kruyt, F. A. E. (2005). Identification of multiple nuclear export sequences in

Fanconi anemia group A protein that contribute to CRM1-dependent nuclear export. *Hum Mol Genet*, 14(10), 1271-1281. doi:10.1093/hmg/ddi138

Forbes, S. A., Beare, D., Gunasekaran, P., Leung, K., Bindal, N., Boutselakis, H., . . . Campbell, P. J. (2015). COSMIC: exploring the world's knowledge of somatic mutations in human cancer. *Nucleic Acids Res*, 43(Database issue), D805-811. doi:10.1093/nar/gku1075

Forment, J. V., Kaidi, A., & Jackson, S. P. (2012). Chromothripsis and cancer: causes and consequences of chromosome shattering. *Nat Rev Cancer*, 12(10), 663-670. doi:10.1038/nrc3352

Ganem, N. J., Godinho, S. A., & Pellman, D. (2009). A mechanism linking extra centrosomes to chromosomal instability. *Nature*, 460(7252), 278-282. doi:10.1038/nature08136

Garaycochea, J. I., Crossan, G. P., Langevin, F., Daly, M., Arends, M. J., & Patel, K. J. (2012). Genotoxic consequences of endogenous aldehydes on mouse haematopoietic stem cell function. *Nature*, 489(7417), 571-575. doi:10.1038/nature11368

Giampietro, P. F., Davis, J. G., Adler-Brecher, B., Verlander, P. C., Auerbach, A. D., & Pavlakis, S. G. (1993). The need for more accurate and timely diagnosis in Fanconi anemia: a report from the International Fanconi Anemia Registry. *Pediatrics*, 91(6), 1116-1120.

Gluckman, E., Auerbach, A. D., Horowitz, M. M., Sobocinski, K. A., Ash, R. C., Bortin, M. M., . . . Gale, R. P. (1995). Bone marrow transplantation for Fanconi anemia. *Blood*, 86(7), 2856-2862.

Gluckman, E., Broxmeyer, H. A., Auerbach, A. D., Friedman, H. S., Douglas, G. W., Devergie, A., . . . et al. (1989). Hematopoietic reconstitution in a patient with Fanconi's anemia by means of umbilical-cord blood from an HLA-identical sibling. *N Engl J Med*, 321(17), 1174-1178. doi:10.1056/NEJM198910263211707

Goldberg, J. I., & Borgen, P. I. (2006). Breast cancer susceptibility testing: past, present and future. *Expert Rev Anticancer Ther*, 6(8), 1205-1214. doi:10.1586/14737140.6.8.1205

Gollin, S. M. (2005). Mechanisms leading to chromosomal instability. *Semin Cancer Biol*, 15(1), 33-42. doi:10.1016/j.semcancer.2004.09.004

Gordon, D. J., Resio, B., & Pellman, D. (2012). Causes and consequences of aneuploidy in cancer. *Nat Rev Genet*, 13(3), 189-203. doi:10.1038/nrg3123

Green, A. M., & Kupfer, G. M. (2009). Fanconi anemia. *Hematol Oncol Clin North Am*, 23(2), 193-214. doi:10.1016/j.hoc.2009.01.008

Gregan, J., Polakova, S., Zhang, L., Tolic-Norrelykke, I. M., & Cimini, D. (2011). Merotelic kinetochore attachment: causes and effects. *Trends Cell Biol*, 21(6), 374-381. doi:10.1016/j.tcb.2011.01.003

Guo, Y., Kim, C., Ahmad, S., Zhang, J., & Mao, Y. (2012). CENP-E--dependent BubR1 autophosphorylation enhances chromosome alignment and the mitotic checkpoint. *J Cell Biol*, 198(2), 205-217. doi:10.1083/jcb.201202152

Hagting, A., Den Elzen, N., Vodermaier, H. C., Waizenegger, I. C., Peters, J.-M., & Pines, J. (2002). Human securin proteolysis is controlled by the spindle checkpoint and reveals when the APC/C switches from activation by Cdc20 to Cdh1. *J Cell Biol*, 157(7), 1125-1137.

Hahn, S. A., Greenhalf, B., Ellis, I., Sina-Frey, M., Rieder, H., Korte, B., . . .  
Bartsch, D. K. (2003). BRCA2 germline mutations in familial pancreatic carcinoma. *J Natl Cancer Inst*, *95*(3), 214-221.

Hanahan, D., & Weinberg, R. A. (2011). Hallmarks of cancer: the next generation. *Cell*, *144*(5), 646-674. doi:10.1016/j.cell.2011.02.013

Heinrich, M. C., Hoatlin, M. E., Zigler, A. J., Silvey, K. V., Bakke, A. C., Keeble, W. W., . . . Bagby, G. C. (1998). DNA cross-linker-induced G2/M arrest in group C Fanconi anemia lymphoblasts reflects normal checkpoint function. *Blood*, *91*(1), 275-287.

Hess, C. J., Ameziane, N., Schuurhuis, G. J., Errami, A., Denkers, F., Kaspers, G. J., . . . Waisfisz, Q. (2008). Hypermethylation of the FANCC and FANCL promoter regions in sporadic acute leukaemia. *Cell Oncol*, *30*(4), 299-306.

Howlett, N. G., Taniguchi, T., Durkin, S. G., D'Andrea, A. D., & Glover, T. W. (2005). The Fanconi anemia pathway is required for the DNA replication stress response and for the regulation of common fragile site stability. *Hum Mol Genet*, *14*(5), 693-701. doi:10.1093/hmg/ddi065

Howlett, N. G., Taniguchi, T., Olson, S., Cox, B., Waisfisz, Q., De Die-Smulders, C., . . . D'Andrea, A. D. (2002). Biallelic inactivation of BRCA2 in Fanconi anemia. *Science*, *297*(5581), 606-609. doi:10.1126/science.1073834

Hwang, W. W., Venkatasubrahmanyam, S., Ianculescu, A. G., Tong, A., Boone, C., & Madhani, H. D. (2003). A conserved RING finger protein required for histone H2B monoubiquitination and cell size control. *Mol Cell*, *11*(1), 261-266.



Imoto, Y., Yoshida, Y., Yagisawa, F., Kuroiwa, H., & Kuroiwa, T. (2011). The cell cycle, including the mitotic cycle and organelle division cycles, as revealed by cytological observations. *Journal of electron microscopy*, 60(suppl 1), S117-S136.

Jablonski, S., Chan, G., Cooke, C., Earnshaw, W., & Yen, T. (1998). The hBUB1 and hBUBR1 kinases sequentially assemble onto kinetochores during prophase with hBUBR1 concentrating at the kinetochore plates in mitosis. *Chromosoma*, 107(6), 386-396.

Jacquemont, C., Simon, J. A., D'Andrea, A. D., & Taniguchi, T. (2012). Non-specific chemical inhibition of the Fanconi anemia pathway sensitizes cancer cells to cisplatin. *Mol Cancer*, 11, 26. doi:10.1186/1476-4598-11-26

Joenje, H., & Patel, K. J. (2001). The emerging genetic and molecular basis of Fanconi anaemia. *Nat Rev Genet*, 2(6), 446-457. doi:10.1038/35076590

Johnson, V. L., Scott, M. I., Holt, S. V., Hussein, D., & Taylor, S. S. (2004). Bub1 is required for kinetochore localization of BubR1, Cenp-E, Cenp-F and Mad2, and chromosome congression. *J Cell Sci*, 117(Pt 8), 1577-1589. doi:10.1242/jcs.01006

Jones, S., Hruban, R. H., Kamiyama, M., Borges, M., Zhang, X., Parsons, D. W., . . . Klein, A. P. (2009). Exomic sequencing identifies PALB2 as a pancreatic cancer susceptibility gene. *Science*, 324(5924), 217. doi:10.1126/science.1171202

Jordan, M. A., Wendell, K., Gardiner, S., Derry, W. B., Copp, H., & Wilson, L. (1996). Mitotic block induced in HeLa cells by low concentrations of paclitaxel

(Taxol) results in abnormal mitotic exit and apoptotic cell death. *Cancer Res*, 56(4), 816-825.

Joukov, V., Walter, J. C., & De Nicolo, A. (2014). The Cep192-organized aurora A-Plk1 cascade is essential for centrosome cycle and bipolar spindle assembly. *Mol Cell*, 55(4), 578-591. doi:10.1016/j.molcel.2014.06.016

Kawashima, S. A., Yamagishi, Y., Honda, T., Ishiguro, K., & Watanabe, Y. (2010). Phosphorylation of H2A by Bub1 Prevents Chromosomal Instability Through Localizing Shugoshin. *Science*, 327(5962), 172-177. doi:10.1126/science.1180189

Kennedy, R. D., Chen, C. C., Stuckert, P., Archila, E. M., De la Vega, M. A., Moreau, L. A., . . . D'Andrea, A. D. (2007). Fanconi anemia pathway-deficient tumor cells are hypersensitive to inhibition of ataxia telangiectasia mutated. *J Clin Invest*, 117(5), 1440-1449. doi:10.1172/JCI31245

Kim, S., Hwang, S. K., Lee, M., Kwak, H., Son, K., Yang, J., . . . Lee, C. H. (2013). Fanconi anemia complementation group A (FANCA) localizes to centrosomes and functions in the maintenance of centrosome integrity. *Int J Biochem Cell Biol*, 45(9), 1953-1961. doi:10.1016/j.biocel.2013.06.012

Knudson, A. G., Jr. (1971). Mutation and cancer: statistical study of retinoblastoma. *Proc Natl Acad Sci U S A*, 68(4), 820-823.

Kops, G. J., Foltz, D. R., & Cleveland, D. W. (2004). Lethality to human cancer cells through massive chromosome loss by inhibition of the mitotic checkpoint. *Proc Natl Acad Sci U S A*, 101(23), 8699-8704.

Kottemann, M. C., & Smogorzewska, A. (2013). Fanconi anaemia and the repair of Watson and Crick DNA crosslinks. *Nature*, *493*(7432), 356-363.

doi:10.1038/nature11863

Kumari, U., Ya Jun, W., Huat Bay, B., & Lyakhovich, A. (2014). Evidence of mitochondrial dysfunction and impaired ROS detoxifying machinery in Fanconi anemia cells. *Oncogene*, *33*(2), 165-172. doi:10.1038/onc.2012.583

Kupfer, G. M., Yamashita, T., Naf, D., Suliman, A., Asano, S., & D'Andrea, A. D. (1997). The Fanconi anemia polypeptide, FAC, binds to the cyclin-dependent kinase, cdc2. *Blood*, *90*(3), 1047-1054.

Langevin, F., Crossan, G. P., Rosado, I. V., Arends, M. J., & Patel, K. J. (2011). Fancd2 counteracts the toxic effects of naturally produced aldehydes in mice. *Nature*, *475*(7354), 53-58. doi:10.1038/nature10192

Lawo, S., Hasegan, M., Gupta, G. D., & Pelletier, L. (2012). Subdiffraction imaging of centrosomes reveals higher-order organizational features of pericentriolar material. *Nat Cell Biol*, *14*(11), 1148-1158. doi:10.1038/ncb2591

Lee, K., & Rhee, K. (2011). PLK1 phosphorylation of pericentrin initiates centrosome maturation at the onset of mitosis. *J Cell Biol*, *195*(7), 1093-1101.

doi:10.1083/jcb.201106093

Levrn, O., Erlich, T., Magdalena, N., Gregory, J. J., Batish, S. D., Verlander, P. C., & Auerbach, A. D. (1997). Sequence variation in the Fanconi anemia gene FAA. *Proc Natl Acad Sci U S A*, *94*(24), 13051-13056.

Li, X., & Nicklas, R. B. (1995). Mitotic forces control a cell-cycle checkpoint.

*Nature*, *373*(6515), 630-632. doi:10.1038/373630a0

Liu, J. M., Otsuki, T., Young, D. B., & Mercurio, F. (2000). Fanconi anemia protein complex is a novel target of the IKK signalsome. *Blood*, *96*(11), 229a-229a.

London, N., & Biggins, S. (2014). Signalling dynamics in the spindle checkpoint response. *Nat Rev Mol Cell Biol*, *15*(11), 736-747. doi:10.1038/nrm3888

MacMillan, M. L., DeFor, T. E., Young, J. A. H., Dusenbery, K. E., Blazar, B. R., Slungaard, A., . . . Wagner, J. E. (2015). Alternative donor hematopoietic cell transplantation for Fanconi anemia. *Blood*, *125*(24), 3798-3804. doi:10.1182/blood-2015-02-626002

MacMillan, M. L., & Wagner, J. E. (2010). Haematopoietic cell transplantation for Fanconi anaemia - when and how? *Br J Haematol*, *149*(1), 14-21. doi:10.1111/j.1365-2141.2010.08078.x

Maher, C. A., & Wilson, R. K. (2012). Chromothripsis and human disease: piecing together the shattering process. *Cell*, *148*(1-2), 29-32. doi:10.1016/j.cell.2012.01.006

Mamrak, N. E., Shimamura, A., & Howlett, N. G. (2016). Recent discoveries in the molecular pathogenesis of the inherited bone marrow failure syndrome Fanconi anemia. *Blood Rev*. doi:10.1016/j.blre.2016.10.002

Maresca, T. J., & Salmon, E. D. (2010). Welcome to a new kind of tension: translating kinetochore mechanics into a wait-anaphase signal. *J Cell Sci*, *123*(Pt 6), 825-835. doi:10.1242/jcs.064790

Marsit, C. J., Liu, M., Nelson, H. H., Posner, M., Suzuki, M., & Kelsey, K. T. (2004). Inactivation of the Fanconi anemia/BRCA pathway in lung and oral

cancers: implications for treatment and survival. *Oncogene*, 23(4), 1000-1004.

doi:10.1038/sj.onc.1207256

Meetei, A. R., Levitus, M., Xue, Y., Medhurst, A. L., Zwaan, M., Ling, C., . . .

Joenje, H. (2004). X-linked inheritance of Fanconi anemia complementation group B. *Nat Genet*, 36(11), 1219-1224. doi:10.1038/ng1458

Mehta, P. A., Harris, R. E., Davies, S. M., Kim, M. O., Mueller, R., Lampkin, B., . . .

. Smolarek, T. A. (2010). Numerical chromosomal changes and risk of development of myelodysplastic syndrome--acute myeloid leukemia in patients with Fanconi anemia. *Cancer Genet Cytogenet*, 203(2), 180-186.

doi:10.1016/j.cancergencyto.2010.07.127

Mennella, V., Agard, D. A., Huang, B., & Pelletier, L. (2014). Amorphous no

more: subdiffraction view of the pericentriolar material architecture. *Trends Cell Biol*, 24(3), 188-197. doi:10.1016/j.tcb.2013.10.001

Mikule, K., Delaval, B., Kaldis, P., Jurczyk, A., Hergert, P., & Doxsey, S. (2007).

Loss of centrosome integrity induces p38-p53-p21-dependent G1-S arrest. *Nat Cell Biol*, 9(2), 160-170.

Mondal, G., Rowley, M., Guidugli, L., Wu, J., Pankratz, V. S., & Couch, F. J.

(2012). BRCA2 localization to the midbody by filamin A regulates cep55 signaling and completion of cytokinesis. *Dev Cell*, 23(1), 137-152.

doi:10.1016/j.devcel.2012.05.008

Morgan, N. V., Tipping, A. J., Joenje, H., & Mathew, C. G. (1999). High frequency

of large intragenic deletions in the Fanconi anemia group A gene. *Am J Hum Genet*, 65(5), 1330-1341. doi:10.1086/302627

Musacchio, A., & Salmon, E. D. (2007). The spindle-assembly checkpoint in space and time. *Nat Rev Mol Cell Biol*, 8(5), 379-393. doi:10.1038/nrm2163

Naf, D., Kupfer, G. M., Suliman, A., Lambert, K., & D'Andrea, A. D. (1998). Functional activity of the fanconi anemia protein FAA requires FAC binding and nuclear localization. *Mol Cell Biol*, 18(10), 5952-5960.

Naim, V., & Rosselli, F. (2009a). The FANC pathway and BLM collaborate during mitosis to prevent micro-nucleation and chromosome abnormalities. *Nat Cell Biol*, 11(6), 761-768. doi:10.1038/ncb1883

Naim, V., & Rosselli, F. (2009b). The FANC pathway and mitosis: a replication legacy. *Cell Cycle*, 8(18), 2907-2911.

Nalepa, G., & Clapp, D. W. (2014). Fanconi anemia and the cell cycle: new perspectives on aneuploidy. *F1000Prime Rep*, 6, 23. doi:10.12703/P6-23

Nalepa, G., Enzor, R., Sun, Z., Marchal, C., Park, S. J., Yang, Y., . . . Clapp, D. W. (2013). Fanconi anemia signaling network regulates the spindle assembly checkpoint. *J Clin Invest*, 123(9), 3839-3847. doi:10.1172/JCI67364

Nam, H. J., Naylor, R. M., & van Deursen, J. M. (2015). Centrosome dynamics as a source of chromosomal instability. *Trends Cell Biol*, 25(2), 65-73. doi:10.1016/j.tcb.2014.10.002

Narayan, G., Arias-Pulido, H., Nandula, S. V., Basso, K., Sugirtharaj, D. D., Vargas, H., . . . Murty, V. V. (2004). Promoter hypermethylation of FANCF: disruption of Fanconi Anemia-BRCA pathway in cervical cancer. *Cancer Research*, 64(9), 2994-2997.

Neveling, K., Kalb, R., Florl, A. R., Herterich, S., Friedl, R., Hoehn, H., . . .  
Schindler, D. (2007). Disruption of the FA/BRCA pathway in bladder cancer. *Cytogenet Genome Res*, 118(2-4), 166-176. doi:10.1159/000108297

O'Brien, P. J., Siraki, A. G., & Shangari, N. (2005). Aldehyde sources, metabolism, molecular toxicity mechanisms, and possible effects on human health. *Crit Rev Toxicol*, 35(7), 609-662.

Olopade, O. I., & Wei, M. (2003). FANCF methylation contributes to chemoselectivity in ovarian cancer. *Cancer Cell*, 3(5), 417-420.

Otsuki, T., Furukawa, Y., Ikeda, K., Endo, H., Yamashita, T., Shinohara, A., . . .  
Liu, J. M. (2001). Fanconi anemia protein, FANCA, associates with BRG1, a component of the human SWI/SNF complex. *Hum Mol Genet*, 10(23), 2651-2660.

Otsuki, T., Kajigaya, S., Ozawa, K., & Liu, J. M. (1999). SNX5, a new member of the sorting nexin family, binds to the Fanconi anemia complementation group A protein. *Biochem Biophys Res Commun*, 265(3), 630-635.  
doi:10.1006/bbrc.1999.1731

Otsuki, T., Nagashima, T., Komatsu, N., Kirito, K., Furukawa, Y., Kobayashi Si, S., . . . Ozawa, K. (2002). Phosphorylation of Fanconi anemia protein, FANCA, is regulated by Akt kinase. *Biochem Biophys Res Commun*, 291(3), 628-634.  
doi:10.1006/bbrc.2002.6504

Palmer, D. K., O'Day, K., Trong, H. L., Charbonneau, H., & Margolis, R. L. (1991). Purification of the centromere-specific protein CENP-A and

demonstration that it is a distinctive histone. *Proc Natl Acad Sci U S A*, 88(9), 3734-3738.

Palovcak, A., Liu, W., Yuan, F., & Zhang, Y. (2017). Maintenance of genome stability by Fanconi anemia proteins. *Cell Biosci*, 7, 8. doi:10.1186/s13578-016-0134-2

Park, I., Lee, H. O., Choi, E., Lee, Y. K., Kwon, M. S., Min, J., . . . Lee, H. (2013). Loss of BubR1 acetylation causes defects in spindle assembly checkpoint signaling and promotes tumor formation. *J Cell Biol*, 202(2), 295-309. doi:10.1083/jcb.201210099

Park, S. J., Ciccone, S. L., Beck, B. D., Hwang, B., Freie, B., Clapp, D. W., & Lee, S. H. (2004). Oxidative stress/damage induces multimerization and interaction of Fanconi anemia proteins. *J Biol Chem*, 279(29), 30053-30059. doi:10.1074/jbc.M403527200

Perera, D., Tilston, V., Hopwood, J. A., Barchi, M., Boot-Handford, R. P., & Taylor, S. S. (2007). Bub1 maintains centromeric cohesion by activation of the spindle checkpoint. *Dev Cell*, 13(4), 566-579. doi:10.1016/j.devcel.2007.08.008

Pichierri, P., Franchitto, A., & Rosselli, F. (2004). BLM and the FANC proteins collaborate in a common pathway in response to stalled replication forks. *EMBO J*, 23(15), 3154-3163. doi:10.1038/sj.emboj.7600277

Quentin, S., Cuccuini, W., Ceccaldi, R., Nibourel, O., Pondarre, C., Pages, M. P., . . . Soulier, J. (2011). Myelodysplasia and leukemia of Fanconi anemia are associated with a specific pattern of genomic abnormalities that includes cryptic



RUNX1/AML1 lesions. *Blood*, 117(15), e161-170. doi:10.1182/blood-2010-09-308726

Rahman, N., Seal, S., Thompson, D., Kelly, P., Renwick, A., Elliott, A., . . .

Collabo, B. C. S. (2007). PALB2, which encodes a BRCA2-interacting protein, is a breast cancer susceptibility gene. *Nat Genet*, 39(2), 165-167. doi:DOI 10.1038/ng1959

Reuter, T., Herterich, S., Bernhard, O., Hoehn, H., & Gross, H. J. (2000). Strong FANCA/FANCG but weak FANCA/FANCC interaction in the yeast 2-hybrid system. *Blood*, 95(2), 719-720.

Rieder, C. L., Cole, R. W., Khodjakov, A., & Sluder, G. (1995). The checkpoint delaying anaphase in response to chromosome monoorientation is mediated by an inhibitory signal produced by unattached kinetochores. *J Cell Biol*, 130(4), 941-948.

Risitano, A. M., Marotta, S., Calzone, R., Grimaldi, F., Zatterale, A., & Contributors, R. (2016). Twenty years of the Italian Fanconi Anemia Registry: where we stand and what remains to be learned. *Haematologica*, 101(3), 319-327. doi:10.3324/haematol.2015.133520

Rosenberg, P. S., Alter, B. P., & Ebell, W. (2008). Cancer risks in Fanconi anemia: findings from the German Fanconi Anemia Registry. *Haematologica*, 93(4), 511-517. doi:10.3324/haematol.12234

Rosenberg, P. S., Tamary, H., & Alter, B. P. (2011). How high are carrier frequencies of rare recessive syndromes? Contemporary estimates for Fanconi

Anemia in the United States and Israel. *American Journal of Medical Genetics Part A*, 155(8), 1877-1883.

Santaguida, S., & Musacchio, A. (2009). The life and miracles of kinetochores. *EMBO J*, 28(17), 2511-2531. doi:10.1038/emboj.2009.173

Sawyer, S. L., Tian, L., Kahkonen, M., Schwartzentruber, J., Kircher, M., University of Washington Centre for Mendelian, G., . . . Greenberg, R. A. (2015). Biallelic mutations in BRCA1 cause a new Fanconi anemia subtype. *Cancer Discov*, 5(2), 135-142. doi:10.1158/2159-8290.CD-14-1156

Schroeder, T. M., Tilgen, D., Kruger, J., & Vogel, F. (1976). Formal genetics of Fanconi's anemia. *Hum Genet*, 32(3), 257-288.

Schuler, M., Rupa, D. S., & Eastmond, D. A. (1997). A critical evaluation of centromeric labeling to distinguish micronuclei induced by chromosomal loss and breakage in vitro. *Mutat Res*, 392(1-2), 81-95.

Sdelci, S., Schutz, M., Pinyol, R., Bertran, M. T., Regue, L., Caelles, C., . . . Roig, J. (2012). Nek9 phosphorylation of NEDD1/GCP-WD contributes to Plk1 control of gamma-tubulin recruitment to the mitotic centrosome. *Curr Biol*, 22(16), 1516-1523. doi:10.1016/j.cub.2012.06.027

Seal, S., Thompson, D., Renwick, A., Elliott, A., Kelly, P., Barfoot, R., . . . Rahman, N. (2006). Truncating mutations in the Fanconi anemia J gene BRIP1 are low-penetrance breast cancer susceptibility alleles. *Nat Genet*, 38(11), 1239-1241. doi:10.1038/ng1902

- Shen, Y., Lee, Y. H., Panneerselvam, J., Zhang, J., Loo, L. W., & Fei, P. (2015). Mutated Fanconi anemia pathway in non-Fanconi anemia cancers. *Oncotarget*, 6(24), 20396-20403. doi:10.18632/oncotarget.4056
- Shepperd, L. A., Meadows, J. C., Sochaj, A. M., Lancaster, T. C., Zou, J., Buttrick, G. J., . . . Millar, J. B. (2012). Phosphodependent recruitment of Bub1 and Bub3 to Spc7/KNL1 by Mph1 kinase maintains the spindle checkpoint. *Current Biology*, 22(10), 891-899.
- Shimamura, A., & Alter, B. P. (2010). Pathophysiology and management of inherited bone marrow failure syndromes. *Blood Rev*, 24(3), 101-122. doi:10.1016/j.blre.2010.03.002
- Sigoillot, F. D., Lyman, S., Huckins, J. F., Adamson, B., Chung, E., Quattrochi, B., & King, R. W. (2012). A bioinformatics method identifies prominent off-targeted transcripts in RNAi screens. *Nat Methods*, 9(4), 363-366. doi:10.1038/nmeth.1898
- Solomon, P. J., Margaret, P., Rajendran, R., Ramalingam, R., Menezes, G. A., Shirley, A. S., . . . Seo, S. H. (2015). A case report and literature review of Fanconi Anemia (FA) diagnosed by genetic testing. *Ital J Pediatr*, 41, 38. doi:10.1186/s13052-015-0142-6
- Staser, K., Shew, M. A., Michels, E. G., Mwanthi, M. M., Yang, F.-C., Clapp, D. W., & Park, S.-J. (2013). A Pak1-PP2A-ERM signaling axis mediates F-actin rearrangement and degranulation in mast cells. *Exp Hematol*, 41(1), 56-66. e52.

Sudakin, V., Chan, G. K. T., & Yen, T. J. (2001). Checkpoint inhibition of the APC/C in HeLa cells is mediated by a complex of BUBR1, BUB3, CDC20, and MAD2. *Journal of Cell Biology*, 154(5), 925-936. doi:DOI 10.1083/jcb.200102093

Sudakin, V., Ganoth, D., Dahan, A., Heller, H., Hershko, J., Luca, F., . . .

Hershko, A. (1995). The cyclosome, a large complex containing cyclin-selective ubiquitin ligase activity, targets cyclins for destruction at the end of mitosis. *Mol Biol Cell*, 6(2), 185-197.

Sumara, I., Gimenez-Abian, J. F., Gerlich, D., Hirota, T., Kraft, C., de la Torre, C., . . . Peters, J. M. (2004). Roles of polo-like kinase 1 in the assembly of functional mitotic spindles. *Curr Biol*, 14(19), 1712-1722. doi:10.1016/j.cub.2004.09.049

Tang, Z., Shu, H., Oncel, D., Chen, S., & Yu, H. (2004). Phosphorylation of Cdc20 by Bub1 provides a catalytic mechanism for APC/C inhibition by the spindle checkpoint. *Mol Cell*, 16(3), 387-397. doi:10.1016/j.molcel.2004.09.031

Taniguchi, T., & Dandrea, A. D. (2002). Molecular pathogenesis of fanconi anemia. *Int J Hematol*, 75(2), 123-128.

Taniguchi, T., Tischkowitz, M., Ameziane, N., Hodgson, S. V., Mathew, C. G., Joenje, H., . . . D'Andrea, A. D. (2003). Disruption of the Fanconi anemia-BRCA pathway in cisplatin-sensitive ovarian tumors. *Nat Med*, 9(5), 568-574.

doi:10.1038/nm852

Thomashevski, A., High, A. A., Drozd, M., Shabanowitz, J., Hunt, D. F., Grant, P. A., & Kupfer, G. M. (2004). The Fanconi anemia core complex forms four complexes of different sizes in different subcellular compartments. *J Biol Chem*, 279(25), 26201-26209. doi:10.1074/jbc.M400091200

Tischkowitz, M., Ameziane, N., Waisfisz, Q., De Winter, J. P., Harris, R., Taniguchi, T., . . . Joenje, H. (2003). Bi-allelic silencing of the Fanconi anaemia gene FANCF in acute myeloid leukaemia. *Br J Haematol*, *123*(3), 469-471.

Tischkowitz, M. D., Morgan, N. V., Grimwade, D., Eddy, C., Ball, S., Vorechovsky, I., . . . Mathew, C. G. (2004). Deletion and reduced expression of the Fanconi anemia FANCA gene in sporadic acute myeloid leukemia. *Leukemia*, *18*(3), 420-425. doi:10.1038/sj.leu.2403280

Torres, K., & Horwitz, S. B. (1998). Mechanisms of Taxol-induced cell death are concentration dependent. *Cancer Res*, *58*(16), 3620-3626.

van der Groep, P., Hoelzel, M., Buerger, H., Joenje, H., de Winter, J. P., & van Diest, P. J. (2008). Loss of expression of FANCD2 protein in sporadic and hereditary breast cancer. *Breast Cancer Res Treat*, *107*(1), 41-47. doi:10.1007/s10549-007-9534-7

van der Heijden, M. S., Brody, J. R., Dezentje, D. A., Gallmeier, E., Cunningham, S. C., Swartz, M. J., . . . Kern, S. E. (2005). In vivo therapeutic responses contingent on Fanconi anemia/BRCA2 status of the tumor. *Clin Cancer Res*, *11*(20), 7508-7515. doi:10.1158/1078-0432.CCR-05-1048

van der Heijden, M. S., Yeo, C. J., Hruban, R. H., & Kern, S. E. (2003). Fanconi anemia gene mutations in young-onset pancreatic cancer. *Cancer Research*, *63*(10), 2585-2588.

Vigneron, S., Prieto, S., Bernis, C., Labbe, J. C., Castro, A., & Lorca, T. (2004). Kinetochores localization of spindle checkpoint proteins: who controls whom? *Mol Biol Cell*, *15*(10), 4584-4596. doi:10.1091/mbc.E04-01-0051

- Vinciguerra, P., Godinho, S. A., Parmar, K., Pellman, D., & D'Andrea, A. D. (2010). Cytokinesis failure occurs in Fanconi anemia pathway-deficient murine and human bone marrow hematopoietic cells. *J Clin Invest*, *120*(11), 3834-3842. doi:10.1172/JCI43391
- Voulgaridou, G. P., Anastopoulos, I., Franco, R., Panayiotidis, M. I., & Pappa, A. (2011). DNA damage induced by endogenous aldehydes: current state of knowledge. *Mutat Res*, *711*(1-2), 13-27. doi:10.1016/j.mrfmmm.2011.03.006
- Wang, X., & Dai, W. (2006). BRCA2 in mitotic exit: a new role in regulating genomic stability. *Future Oncol*, *2*(1), 43-46. doi:10.2217/14796694.2.1.43
- Wang, Z., Li, M., Lu, S., Zhang, Y., & Wang, H. (2006). Promoter hypermethylation of FANCF plays an important role in the occurrence of ovarian cancer through disrupting Fanconi anemia-BRCA pathway. *Cancer Biol Ther*, *5*(3), 256-260.
- Wei, M., Xu, J., Dignam, J., Nanda, R., Sveen, L., Fackenthal, J., . . . Olopade, O. I. (2008). Estrogen receptor alpha, BRCA1, and FANCF promoter methylation occur in distinct subsets of sporadic breast cancers. *Breast Cancer Res Treat*, *111*(1), 113-120. doi:10.1007/s10549-007-9766-6
- Willingale-Theune, J., Schweiger, M., Hirsch-Kauffmann, M., Meek, A. E., Paulin-Levasseur, M., & Traub, P. (1989). Ultrastructure of Fanconi anemia fibroblasts. *Journal of Cell Science*, *93* ( Pt 4), 651-665.
- Wiseman, H., & Halliwell, B. (1996). Damage to DNA by reactive oxygen and nitrogen species: role in inflammatory disease and progression to cancer. *Biochem J*, *313* ( Pt 1), 17-29.

Wong, J. C., Alon, N., McKerlie, C., Huang, J. R., Meyn, M. S., & Buchwald, M. (2003). Targeted disruption of exons 1 to 6 of the Fanconi Anemia group A gene leads to growth retardation, strain-specific microphthalmia, meiotic defects and primordial germ cell hypoplasia. *Hum Mol Genet*, *12*(16), 2063-2076.

Woo, H. I., Kim, H. J., Lee, S. H., Yoo, K. H., Koo, H. H., & Kim, S. H. (2011). Acute myeloid leukemia with complex hypodiploidy and loss of heterozygosity of 17p in a boy with Fanconi anemia. *Ann Clin Lab Sci*, *41*(1), 66-70.

Woods, C. M., Zhu, J., McQueney, P. A., Bollag, D., & Lazarides, E. (1995). Taxol-induced mitotic block triggers rapid onset of a p53-independent apoptotic pathway. *Mol Med*, *1*(5), 506-526.

Xie, Y., de Winter, J. P., Waisfisz, Q., Nieuwint, A. W., Scheper, R. J., Arwert, F., . . . Joenje, H. (2000). Aberrant Fanconi anaemia protein profiles in acute myeloid leukaemia cells. *Br J Haematol*, *111*(4), 1057-1064.

Young, N., & Alter, B. (1994). Clinical features of Fanconi's anemia. *Aplastic Anemia Acquired and Inherited. Philadelphia, PA: Saunders*, 275-309.

Zakrzewski, S., & Sperling, K. (1980). Genetic heterogeneity of Fanconi's anemia demonstrated by somatic cell hybrids. *Hum Genet*, *56*(1), 81-84.

Zhang, C. Z., Leibowitz, M. L., & Pellman, D. (2013). Chromothripsis and beyond: rapid genome evolution from complex chromosomal rearrangements. *Genes Dev*, *27*(23), 2513-2530. doi:10.1101/gad.229559.113

Zhang, C. Z., Spektor, A., Cornils, H., Francis, J. M., Jackson, E. K., Liu, S., . . . Pellman, D. (2015). Chromothripsis from DNA damage in micronuclei. *Nature*, *522*(7555), 179-184. doi:10.1038/nature14493

Zhang, J., Wang, X., Lin, C. J., Couch, F. J., & Fei, P. (2006). Altered expression of FANCL confers mitomycin C sensitivity in Calu-6 lung cancer cells. *Cancer Biol Ther*, 5(12), 1632-1636.

Zimmerman, W. C., Sillibourne, J., Rosa, J., & Doxsey, S. J. (2004). Mitosis-specific anchoring of gamma tubulin complexes by pericentrin controls spindle organization and mitotic entry. *Mol Biol Cell*, 15(8), 3642-3657.

doi:10.1091/mbc.E03-11-0796

Zou, J., Tian, F., Li, J., Pickner, W., Long, M., Rezvani, K., . . . Zhang, D. (2013). FancJ regulates interstrand crosslinker induced centrosome amplification through the activation of polo-like kinase 1. *Biol Open*, 2(10), 1022-1031.

doi:10.1242/bio.20135801

Zou, J., Zhang, D., Qin, G., Chen, X., Wang, H., & Zhang, D. (2014). BRCA1 and FancJ cooperatively promote interstrand crosslinker induced centrosome amplification through the activation of polo-like kinase 1. *Cell Cycle*, 13(23),

3685-3697. doi:10.4161/15384101.2014.964973

Zunino, A., Degan, P., Vigo, T., & Abbondandolo, A. (2001). Hydrogen peroxide: effects on DNA, chromosomes, cell cycle and apoptosis induction in Fanconi's anemia cell lines. *Mutagenesis*, 16(3), 283-288.



## CURRICULUM VITAE

Zahi Abdul Sater

### **Education:**

Biochemistry and Molecular Biology, Ph.D. 2012-2017

*Indiana University*

Biochemistry and Molecular Genetics, M.Sc. 2008-2010

*American University of Beirut (AUB)*

Professional Management, Diploma 2009-2010

*Haigazian University*

Biology, B.Sc. 2005-2008

*Haigazian University*

## **Professional Experience:**

Ph.D. candidate

2012-2017

*Indiana University*

- Performed high-throughput kinome screen to investigate synthetic lethality relationships between Fanconi Anemia (FA) genes and mitotic kinases.
- Teased out the signaling networks underlying the protective role of the FA pathway against genomic instability.

Research assistant

2010-2012

*American University of Beirut*

- Co-authored a review article about research output in the Arab world.
- Designed organizational charts for various AUBMC external medical affairs (EMA) projects.
- Managed a 4-month long project for developing a database for 5,400+ expatriate Lebanese physicians.

## **Awards and honors**

- Research featured on bitplane website, 2017
- Member of the American Society of Hematology, 2016
- Abstract achievement award - ASH conference, 2016

- Travel grant - ASH conference, 2016
- Cover page featured image - Experimental Hematology journal, December 2015 edition
- Graduate assistanship - AUB, 2010-2012
- Dean's honor list - Haigazian University, 2008

## **Publications**

- **Abdul-sater Z**, Sharma S, Potchanant ES, He Y. 2017. FANCA maintains the spindle assembly checkpoint through regulation of BUBR1 acetylation in mitosis. In preparation
- **Abdul-Sater Z**, Cerabona D, Potchanant ES, Sun Z, Enzor R, et al. 2015. FANCA safeguards interphase and mitosis during hematopoiesis in vivo. Exp Hematol. 2015 Dec
- **Abdul-Sater Z**, Yehya A, Beresian J, Salem E, Kamar A, et al. 2012. Two heterozygous mutations in NFATC1 in a patient with Tricuspid Atresia. PLoS One. 2012
- Potchanant ES, Cerabona D, **Abdul-sater Z** et al. 2016. INPP5E preserves genomic stability through regulation of mitosis. Mol Cell Biol. 2016 Dec
- Kwon, J. J., Nabinger, S. C., Vega, Z., Sahu, S. S., Alluri, R. K., **Abdul-Sater, Z** et al. 2015. Pathophysiological role of microRNA-29 in pancreatic cancer stroma. Sci Rep. 2015 Jun
- Farhat T, **Abdul-Sater Z**, Obeid M, Arabi M, Diab K, et al. 2013. Research in

congenital heart disease: a comparative bibliometric analysis between developing and developed countries. *Pediatr Cardiol.* 2013 Feb

### **Conferences attended**

- FANCA Fine-Tunes Chromosome Segregation By Controlling BUBR1K250 Acetylation at the Kinetochores. 2016. Oral presentation at American Society of Hematology (ASH) conference. San Diego, USA
- FANCA Controls Mitotic Phosphosignaling Networks To Ensure Genome Stability During Cell Division. 2015. Poster presentation at Cancer research day at IUSM. Indianapolis, USA
- Two heterozygous mutations in NFATC1 in a patient with Tricuspid Atresia. 2012. Poster presentation at Weinstein conference, Chicago, USA
- Characterization of novel mutations in the NFATc1 gene. 2010. Poster presentation at AUB research day. Beirut, Lebanon